Strategy for speedy field diagnosis and control of avian influenza viruses (AIV) outbreak at the point of contact/care (POC)

RS Maremagae

orcid.org/0000-0002-7632-3602

Thesis accepted in fulfilment of the requirements for the degree *Doctor of Philosophy in Microbiology* at the North-West University

Promoter:	Prof. CC Bezuidenhout
Co-promoter:	Dr P Lebea
Co-promoter:	Prof MA Jarvis

Graduation August 2021

24914428

DECLARATION

I, Ramaesela Sharon Maremagae, declare that this thesis is my own, unaided work. It is submitted for the Degree of Philosophy in Microbiology at the North-West University, Potchefstroom campus. It has not been submitted before for any degree or examination at any other university.

Ramaesela Sharon Maremagae Date

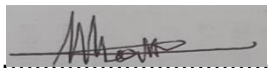

..... 09/06/2021 .....

ACKNOWLEDGEMENTS

First and foremost, I would like to extend my sincere gratitude to my supervisors, Dr Phiyani Lebea (Council of Scientific and Industrial Research) and Professor Carlos Bezuidenhout (North-West University, Potchefstroom Campus) for believing in me. There is no doubt that this PhD would not have come to fruition had it not been for your support. Dr Lebea, thank you so much for your invaluable advice, assistance, patience, and direction throughout this PhD journey. Despite your busy schedule, you always set time aside to help me, and for that I shall forever be grateful. Prof. Bezuidenhout, thank you for always availing yourself whenever I needed your help and for ensuring that things at the university are running smoothly. It was a real honour being your student. Thank you.

A heartfelt word of thanks also goes to my loving parents, Mr Ramagodi Alpheus Molepo and Mrs Merium Mapula Molepo, for always putting my education first. I am where I am today because of your teamwork as my parents. I love you and may God continue to bless you. Papa, thank you for instilling your love for biology in me. The enthusiasm you showed whenever you taught me biology made me fall in love with the subject. Thank you for leading me into my dream career. Mma, thank you for your unconditional love and for always standing by me. Whenever I was about to give up, you reminded me that I had done it before and I could do it again, and that just pulled me up.

I owe my deepest gratitude to my husband, my pillar of strength, the love of my life, Mr Lefa Arnold Maremagae. Thank you for your undying support and motivation which kept me going throughout this challenging journey. If it had not been for your love, tolerance and for lending an ear whenever I needed it, I would not have accomplished this PhD. I love you so much.

In addition, I would like to thank my parents-in-law, Mr Michael Maremagae and Mrs Gladys Maremagae, for your unconditional love, support, and prayers. Words are not sufficient to express my gratitude. I love you both and ask that God may bless you.

To my fellow colleagues: Thank you for always lending a helping hand, for always listening to me, for your encouragement, and for always managing to make me smile even after my experiments had failed several times. You are the best.

My gratitude is also extended to the Council of Scientific and Industrial Research (CSIR) for the financial support that made this PhD study possible.

Finally, I would like to thank God for giving me strength when I had none left, and for giving me more rewards than I actually worked for.

Philippians 4:13

“I can do everything through Christ who gives me strength.”

Deuteronomy 30:9

“God will prosper you abundantly in all the work of your hands.”

ABSTRACT

Avian influenza (AI) is an infectious viral disease in birds caused by a type A influenza virus of the family Orthomyxoviridae. These viral outbreaks usually cause significant economic losses to the poultry industry. Conventional strategies for AI detection and control using vaccination both start by growing the viruses and isolating them in embryonated chicken eggs. This entire process takes 6 to 8 months from viral detection to the release of the vaccine for that particular strain. A rapid and cost effective diagnostic method for the early detection of AI viruses, as well as a more effective vaccine that can be produced quickly, are urgently needed as tools for AI outbreak management. Therefore, the aim of this study was to develop a strategy for the point-of-care (POC) detection of AI and to develop a vaccine that is not only effective in the treatment of such outbreaks, but can also be produced quickly enough to manage AI viruses before they spread and cause an outbreak.

Loop-mediated isothermal amplification (LAMP), which is a rapid nucleic acid amplification assay that takes 30 to 60 minutes, was used for POC diagnosis of the AI viruses. Three LAMP assays were designed − one for the detection of general AI strains and the other two for the specific detection of the H5 and H7 AI subtypes. The device used to make the detection of these viruses at the POC possible was the Axxin T16 isothermal instrument. This device is ideal for POC assays as it is portable, the results can be detected in real time, and it operates on rechargeable batteries. Using the designed LAMP assays, the identification of the AI samples that were tested was successfully achieved within 30 minutes at the POC without having to transport the samples to a laboratory.

The Adenovirus vectors are known as suitable recombinant vaccine vectors because they are capable of infecting a wide variety of cell types, can grow to high titres *in vitro,* and cannot integrate in the host genome. Due to these features, the Adenovirus was used in this study to design a safe and effective vaccine that can be produced quickly. However, policies of the Department of Agriculture, Land Reform and Rural Development (DALRRD) formerly known as the Department of Agriculture, Forestry and Fisheries (DAFF) prohibit vaccination against AI as conventional vaccines previously interfered with surveillance programmes that did not allow any differentiation between infected and non-infected poultry that had been vaccinated using diffierentiation of infected and vaccinated animal (DIVA) strategies. To prove that the strategy proposed by this study will address the challenges that conventional AI vaccines pose, the Newcastle disease virus (NCDV) was used as a target virus in the design of the Adenovirus vector-based vaccine. The vaccine was designed by inserting the Matrix gene of the NCDV into the Adenovirus vector. The functionality and propagation of the recombinant Adenovirus were

performed in 293T human embryonic kidney (HEK) cells. This was followed by testing the recombinant Adenovirus *in vitro* in chicken embryo fibroblasts (CEFs) that were prepared in-house. The results demonstrated the successful expression of the recombinant Adenovirus in the CEFs, which suggests that the vaccine design strategy that was developed in this study may be successful for future application as the vaccine showed the desired expression *in vitro*. These results also suggest that the same strategy may be used for the design of Adenovirus-based vaccines against AI and any other viral diseases in chickens. Even more noteworthy is that the current strategy takes only 5 weeks from viral detection to vaccine production, while the conventional strategy takes up to 6 or 8 months for the entire process to be completed. However, despite these exciting results, clinical trials using live chickens will have to be conducted in future studies to check how safe and effective these vaccines are. This strategy may even be efficacious in solving the COVID-19 crisis that the world is currently facing.

Keywords: Avian influenza, Adenovirus, chicken embryo fibroblasts, loop-mediated isothermal amplification, point-of-care, polymerase chain reaction, vaccine

TABLE OF CONTENTS

DECLARATION ..... **I**

ACKNOWLEDGEMENTS ..... **II**

ABSTRACT ..... **IV**

TABLE OF CONTENTS ..... **VI**

LIST OF TABLES ..... **XIII**

LIST OF FIGURES ..... **XIV**

ABBREVIATIONS ..... **XVIII**

CHAPTER 1 INTRODUCTION AND BACKGROUND TO THE STUDY **1**

1.1 Introduction **1**

1.2 Methods for Detecting Avian Influenza **1**

1.3 Controlling the Spread of AI **2**

1.4 Main Aims of the Study **3**

1.5 Main Challenges in Addressing the Aims of the Study **3**

1.6 Conclusion **4**

CHAPTER 2 LITERATURE REVIEW **5**

2.1 Introduction **5**

2.2 Influenza A Viruses: Structure, Genome and Proteins **5**

2.2.1 Classification and nomenclature of influenza A viruses 6

2.2.2 Avian influenza pathogenicity 6

2.2.3 The avian influenza virus infection cycle 7

2.3 Clinical Signs of Avian Influenza in Birds/Poultry **9**

2.3.1 Influenza A virus variation 10

2.3.2 Epidemiology of AI 12

2.4 Avian influenza control and management strategies 13

2.4.1 Biosecurity 14

2.4.2 Diagnostics and surveillance 14

2.4.3 Vaccination 15

2.4.4 Elimination of the AI virus in infected poultry 17

2.4.4.1 Controlled marketing and recovering of flocks 17

2.4.4.2 Stamping out 17

2.4.4.3 Euthanasia 18

2.4.4.4 Incineration 18

2.4.4.5 Composting 18

2.4.5 Education 18

2.5 Current Avian Influenza Control Strategies 19

2.5.1 The point-of-care diagnosis of AI using loop-mediated isothermal amplification 19

2.5.1.1 The principles of LAMP 19

2.5.1.2 The mechanism of LAMP 20

2.5.2 Recombinant vaccination using the Adenovirus vectors 22

2.5.2.1 Structure, genome, and proteins of the Adenovirus 22

2.5.2.2 Adenovirus vectors in vaccination 24

2.5.2.3 Lambda (λ) homologous recombination 25

2.6 Problem Statement 27

2.7 Hypothesis 29

2.8 Aims and Objectives 30

2.8.1 Aims 30

2.8.2 Objectives 30

CHAPTER 3 MATERIALS AND METHODS 31

3.1 Introduction 31

3.2 Workflow 33

3.3 Point-of-care (POC) Diagnosis of Avian Influenza (AI) Using Loop-Mediated Isothermal Amplification (LAMP) 33

3.3.1 Primer design 33

3.3.2 Confirming the status of the viruses 33

3.3.3 Testing the functionality of the LAMP primers 35

3.4 Development and optimisation of the LAMP method 35

3.4.1 Testing of the avian influenza RNA samples using the Matrix specific LAMP detection assay 35

3.4.2 Selecting the best template starting material for the LAMP assay 36

3.4.3 Verification of LAMP assay non-detected samples using the OIE approved AI detection method 37

3.4.4 LAMP vs PCR sensitivity 38

3.4.5 The application of LAMP at the POC using the T16 Axxin isothermal Instrument 38

3.5 Adenovirus vector-based vaccine development for avian influenza 40

3.5.1 Fertilised egg incubation 40

3.5.2 Technical CEF preparation 40

3.5.3 Assessing the expression of the non-replicative Adenovirus vector (pAd/CMV/V5-GW/lacZ control plasmid) (Life Technologies, K4930-00) in chicken embryo fibroblasts 42

3.5.3.1 Amplification of the Adenovirus vector pAd/CMV/V5-GW/lacZ control plasmid in 293T cells 42

3.5.3.2 Extraction of the Adenovirus DNA from the supernatant 43

3.5.3.3 Confirmation of the presence of the Adenovirus DNA in the crude virus supernatant using PCR 44

3.5.4 Whole protein extraction from the cell pellet 44

3.5.4.1 Adenovirus vector expression assessment through western blot analysis 44

3.5.4.2 Adenovirus vector expression assessment in chicken embryo fibroblasts and Vero cells using western blot analysis 45

3.6 Development of a Non-Replicative, Recombinant Adenovirus (rAd) (pAd/PL-DEST™) for the Expression of the Gene of Choice 45

3.6.1 Newcastle disease virus (NCDV) Matrix gene primer design 45

3.6.2 NCDV nucleotide confirmation using OIE approved NCDV detection PCR primers 48

3.6.2.1 Testing the designed PCR primers on the NCDV cDNAs 48

3.6.2.2 Vectors used for creating an expression clone (Adenovirus vector expressing the NCDV Matrix gene) 49

3.6.2.3 Primer design for cloning the Matrix gene derived from PCR into the pENTR™/D-TOPO vector 50

3.6.2.4 Cloning and transformation 51

3.6.2.5 Creating the Adenoviral expression clone/recombinant Adenovirus 52

3.6.3 293T cell transfection with the recombinant Adenovirus 54

3.6.4 Next generation sequencing (NGS) for the recombinant Adenovirus vector to confirm the Matrix inserted in the vector 55

3.6.5 Assessing the RNA expression of the designed recombinant Adenovirus in 293T cells 56

3.6.6 Assessing the DNA expression of the recombinant Adenovirus in chicken embryo fibroblasts (CEFs) 57

3.6.7 Mass spectrometry (MS) protein expression analysis 58

3.6.7.1 Protein extraction from the recombinant Adenovirus crude lysate 58

3.6.7.2 Protein extraction from CEFs 59

3.6.7.3 Mass spectrometry (MS) protein expression analysis of the recombinant Adenovirus in CEFs 59

CHAPTER 4 POINT-OF-CARE (POC) DIAGNOSIS FOR AI USING LAMP: RESULTS AND DISCUSSIONS 61

4.1 Sequence Alignment of AI Viruses 61

4.2 Testing the functionality of the LAMP primers 63

4.2.1 Development and optimisation of the LAMP method 64

4.2.1.1 Samples used for LAMP optimisation 64

4.2.1.2 Viral RNA concentrations 65

4.2.2 Detected viral RNA from samples (Table 4.1) using the Matrix specific LAMP detection assay 66

4.2.3 cDNA synthesised with Matrix specific primers is the best template for obtaining optimum LAMP results 67

4.2.4 Concentrations of the cDNA synthesised for all samples using the Matrix specific primers 69

4.2.5 AI detection by targeting the Matrix gene 70

4.2.6 The H5 subtype specific detection 73

4.2.7 The H7 subtype specific detection 75

4.2.8 Summary of the RT-LAMP results 77

4.2.9 LAMP vs PCR sensitivity 79

4.3 POC RT-LAMP for AI detection using the Axxin T16 isothermal instrument 81

CHAPTER 5 EXPRESSION OF NON-REPLICABLE ADENOVIRUS VECTORS IN 293T, CHICKEN EMBRYO FIBROBLASTS, AND VERO CELLS: RESULTS AND DISCUSSION 84

5.1 Introduction 84

5.2 Preparation of Chicken Embryo Fibroblasts 85

5.2.1 Egg development stages 85

5.2.2 Chicken embryo fibroblasts viewed under the microscope 87

5.2.3 Amplified Adenovirus: crude virus using PCR 88

5.3 Expressions of the Adenovirus Protein 89

5.3.1 Expression of the Adenovirus (pAD /CMV/V5-GW/lacZ control plasmid) protein in 293T cells 89

5.3.2 Expression of the Adenovirus (pAD /CMV/V5-GW/lacZ control plasmid) protein in 293T, chicken embryo fibroblasts and Vero cells using western blot analysis 90

CHAPTER 6 RESULTS AND DISCUSSION: EXPRESSION OF NON-REPLICATIVE, RECOMBINANT ADENOVIRUS VECTOR EXPRESSING THE NCDV MATRIX GENE IN CHICKEN EMBRYO FIBROBLASTS 93

6.1 Introduction 93

6.2 Authentication of the NCDV Samples for Desired Gene Selection before Cloning 93

6.3 Primary Cloning of the Gene of Interest as a Step in Devising a Vaccine Model 97

6.4 Secondary NCDV Matrix Gene Cloning through Homologous Recombination into pAD/CMV/V5-DEST™ 98

6.5 Recombinant Virus Vaccine Confirmation and Authentication 99

6.5.1 Propagation of the Adenovirus vector pAD/CMV/V5-DEST™ expressing the NCDV Matrix gene 100

6.5.2 Next generation sequencing (NGS) for the Adenovirus vector pAD/CMV/V5-DEST™ expressing the NCDV Matrix gene 102

6.5.3 Assessing the RNA expression of the recombinant Adenovirus in 293T cells . 104

6.6 Assessing the Functionality of the Recombinant Adenovirus Expressing the NCDV Matrix in Chicken Embryo Fibroblasts (CEFs) 106

6.6.1 RNA analysis of the recombinant Adenovirus vector by PCR 106

6.6.2 Protein analysis of the recombinant Adenovirus vector by mass spectrometry (MS) 107

CHAPTER 7 GENERAL DISCUSSION, CONCLUSION AND RECOMMENDATIONS FOR FUTURE STUDIES 113

7.1 Introduction 113

7.2 Loop-Mediated Isothermal Amplification (LAMP) 113

7.3 Developing a Vaccine against NCDV 114

7.4 Recommendations for Future Studies 116

7.5 Conclusion 117

REFERENCES 118

LIST OF TABLES

Table 3.1: ISZVe AI viruses used to test the B3/F3 and F2/B2 LAMP primers using the PCR method 34

Table 3.2: PCR cycling programme used for the reaction in section 3.3.2 34

Table 3.3: Avian Influenza viral samples and a Newcastle viral sample used to validate the LAMP detection assay 36

Table 3.4: Ten primer sets for the specific detection of the Matrix gene (Figure 3.6). These primers were designed using the NCBI 3 and Blast databases 45

Table 3.5: PCR primer sets used to detect the largest NCDV gene Matrix fragment using H3090/11 and H3343/11 NCDV cDNA..... 49

Table 3.6: PCR primers (section 3.6.1) and cloning primers designed by modifying the PCR primers 51

Table 3.7: PCR thermo cycling steps for the confirmation of the recombinant Adenovirus..... 54

Table 4.1: RNA concentrations quantified using the Qubit® 2.0 Fluorometer (Life Technologies, Singapore) and Qubit® RNA high sensitivity kit (Life Technologies, USA) 65

Table 4.2: cDNA concentrations quantified using the Qubit® 2.0 Fluorometer (Life Technologies, Singapore) and Qubit® double stranded DNA (dsDNA) high sensitivity kit (Life Technologies, USA) 70

Table 4.3: Summary of the RT-LAMP assays for the detection of avian influenza viruses (Matrix gene, H5 and H7 detection) 78

Table 6.1: NCDV Matrix protein identification in the recombinant Adenovirus and the CEFs infected with the recombinant Adenovirus 112

LIST OF FIGURES

Figure 2.1: Structure of the influenza A virus showing the three main viral transmembrane proteins and the segments contained within the M1 Matrix 5

Figure 2.2: Structure of the influenza A virus and its life cycle beginning with attachment to the host cell and ending with the release of the progeny virions 9

Figure 2.3: Clinical signs of AI in chickens 10

Figure 2.4: Diagrammatic representation of a pig as a mixing vessel for influenza A viruses 11

Figure 2.5: The distribution patterns of LPAI and HPAI in bird populations from 2010-2016 13

Figure 2.6: Schematic representation of a loop-mediated isothermal amplification reaction 22

Figure 2.7: Schematic representation of the Adenovirus showing the major capsid and the core proteins 23

Figure 2.8: Adenovirus genome organisation 24

Figure 2.9: The integration of the bacteriophage Lambda (λ) genome into the *Escherichia coli* (*E.coli*) chromosome 26

Figure 2.10: The LR recombination reaction using the Gateway® cloning system (Life Technologies Ltd, California) 27

Figure 2.11: Conventional strategy and workflow for avian influenza outbreak management and vaccine production 29

Figure 3.1: Workflow showing the protocols that were followed in this study for avian influenza detection and prevention 32

Figure 3.2: The Axxin T16 isothermal instrument with 16 positions for loading tubes with samples and a touch result screen for real-time monitoring 39

Figure 3.3: Illustration of the test operator conducting tests in the field using the Axxin T16 LAMP device connected to a mobile phone via Wifi 39

Figure 3.4: Preparation of chicken embryo fibroblasts (CEFs) from an 11-day-old chicken embryo 41

Figure 3.5: Adenovirus vector (pAd/CMV/V5-GW/lacZ control plasmid) (Life Technologies, K4930-00) used in this study 43

Figure 3.6: The NCDV Matrix gene sequenced in-house using the Ion PGM system (Thermo Scientific) for next generation sequencing 46

Figure 3.7: Maps of the two vectors. A: pENTR™/D-TOPO (Figure 3.7A) was a donor vector and B: pAd/CMV/V5-DEST™ (Figure 3.7B) functioned as an expression vector 50

Figure 3.8: TOPO® cloning site for pENTRTM/D-TOPO® 51

Figure 3.9: An LR recombination reaction between a pENTR™/D-TOPO entry clone and the pAd/CMV/V5-DEST™ destination vector to create an expression clone and a by-product 53

Figure 4.1: Sequence alignment of the conserved Matrix gene regions of the South African avian influenza viruses aligned using the MUSCLE multiple sequence alignment (influenza research database). 62

Figure 4.2: Sequence alignment of the conserved hemagglutinin (HA) gene of the H5 subtypes of the South African avian influenza viruses aligned using the MUSCLE multiple sequence alignment (influenza research database) 62

Figure 4.3: Sequence alignment of the conserved hemagglutinin (HA) gene of the H7 subtypes of the South African avian influenza viruses aligned using the MUSCLE multiple sequence alignment (influenza research database) 63

Figure 4.4: Image of 1% Agarose gel electrophoresis showing PCR products of the tested LAMP primers 64

Figure 4.5: LAMP screening of Avian influenza using RNA as a template 66

Figure 4.6: H5N1 inactivated antigen: ANHUI/1/2005 (H5N1) IBCDC - RG-6 07/290 (sample 1) processed in different ways to improve the sensitivity of LAMP 67

Figure 4.7: H5N1 inactivated antigen: A/Cambodia/R040505/2007 (H5N1) NIBRG-88 (Sample 2) processed in different ways to improve the sensitivity of LAMP 68

Figure 4.8: H5N1 A/mallard/Italy/3401/05 (sample 3) processed in different ways to improve the sensitivity of LAMP 69

Figure 4.9: Screening of Avian influenza viruses using LAMP 72

Figure 4.10: Testing the specificity of the H5 detection assay 74

Figure 4.11: Testing the specificity of the H7 detection assay 76

Figure 4.12: Verification of the RT-LAMP non-detected samples (12-H7N9, 20-H6N8 and 21-H5N1) as avian influenza or not, using the OIE approved RT-PCR detection method for avian influenza 79

Figure 4.13: The sensitivity of LAMP in comparison to real-time PCR 81

Figure 4.14: POC validation of the Axxin T16 isothermal instrument 83

Figure 5.1: Chicken embryo development in a fertilised egg from day 1 to day 11 86

Figure 5.2: An 11-day-old chicken embryo 87

Figure 5.3: Passage three of chicken embryo fibroblasts at different confluence points 88

Figure 5.4: Test for the presence of Adenovirus produced in 293T cells 89

Figure 5.5: SDS-PAGE gel of protein extracted from 293T cells infected with Adenovirus vector 90

Figure 5.6: SDS-PAGE gel of protein extracted from various cell lines, infected and uninfected with Adenovirus vector (pAd/CMV/V5-GW/lacZ) 92

Figure 6.1: PCR products for NCDV samples (H3090/11 and H3343/11) 94

Figure 6.2: PCR products of the NCDV Matrix gene of the H3090/11 and H3343/11 samples using 6 different designed primer sets 96

Figure 6.3: Purified PCR product of a NCDV H3090/11 amplified using set 5 of the Matrix specific gene 96

Figure 6.4: PCR products of the Matrix gene with the added overhangs/blunt end PCR products using the designed cloning primers 97

Figure 6.5: PCR products of the NCDV Matrix gene cloned into the pENTR™/D-TOPO® vector 98

Figure 6.6: Image depicting 1% agarose gel electrophoresis of the PCR products of the NCDV Matrix gene 99

Figure 6.7: Images of 1% agarose gel electrophoresis..... 101

Figure 6.8: Part of a sequence of the pAD/CMV/V5-DESTTM vector expressing the NCDV Matrix gene 103

Figure 6.9: Part of a sequence of the pAd/CMV/V5-GW/lacZ control vector showing the position of the V5 epitope..... 104

Figure 6.10: Amplification curves, melting curves, cq Table and 1% agarose gel electrophoresois showing RT-PCR products of the recombinant Adenovirus containing the NCDV Matrix gene expressed in 293T cells..... 105

Figure 6.11: Image of 1% agarose gel electrophoresis showing the expression of the Adenovirus with an inserted NCDV Matrix gene in CEFs 107

Figure 6.12: The NCDV Matrix protein sequence which was cloned in the Adenovirus vector (pAD/CMV/V5-DEST™)..... 108

Figure 6.13: Mass spectrometry-based detection of the Matrix gene in recombinant Adenovirus purified stock 110

Figure 6.14: Mass spectrometry-based detection of the Matrix gene in the CEFs infected with the recombinant Adenovirus 111

Figure 7.1: Timeline for avian influenza detection and vaccine production as developed in the current study 116

ABBREVIATIONS

Adv: Adenovirus

AI: Avian influenza

APMV-1: Avian paramyxovirus type 1

Att: Attachment

attB: Bacterial attachment

attL: Attachment on the left site

attP: Bacteriophage attachment

attR: Attachment on the right

BIP: Backward inner primer

BLP: Backward loop primer

B3: Backward outer primer

Bp: Basepair

cDNA: Complementary deoxyribonucleic acid

CEFs: Chicken embryo fibroblasts

CO_2: Carbon dioxide

CPE: Cytopathic effect

Cq: Quantification cycle

DAFF: Department of Agriculture, Forestry and Fisheries

DALRRD: Department of Agriculture, Land Reform and Rural Development

DIVA: Differentiation between infected and vaccinated

DMEM: Dulbeco's modified eagle medium

DNA: Deoxyribonucleic acid

dNTPs: Deoxyribonucleotide triphosphates

dsDNA: Double stranded DNA

DTT: Dithiothreitol

***E.coli*:** *Escherichia coli*

FBS: Fetal bovine serum

FIP: Forward inner primer

FLP: Forward loop primer

FPV: Fowl pox virus

F3: Forward outer primer

HA: Hemagglutinin

HEK: Human embryonic kidney

HPAI: Highly pathogenic avian influenza

HVT: Herpesvirus of turkeys

IAA: Iodoacetamide

IgG-HRP: Immunoglobulin G horseradish peroxidase

Int: Integrase

ITRs: Inverted terminal repeats

ISPs: Ion sphere particles

Kb: Kilobase

LAMP : Loop-mediated isothermal amplification

LB: Luria bertani

LPAI: Low pathogenic avian influenza

MDCK: Madin darbi canine kidney cells

mRNA: Messenger ribonucleic acid

MS: Mass spectrometry

M1: Matrix 1

M2: Matrix 2

NA: Neuraminidase

NASBA: Nucleic acid sequence based amplification

NCBI: National Centre for Biotechnology Information

NCDV: Newcastle disease virus

NE: Nuclear export protein

NGS: Next generation sequencing

NP: Nucleoprotein

NS2: Non-structural protein 2

OIE: (Historical acronym for) World Organization for Animal Health

PA: Polymerase acidic protein

PBS: Phosphate buffered saline

PBST: Phosphate buffered saline -Tween 20

PB1: Polymerase basic protein 1

PB1-F2: Polymerase basic protein 1-F2

PB2: Polymerase basic protein 2

PCR: Polymerase chain reaction

POC: Point-of-care

PGM: Personal genome machine

RNA: Ribonucleic acid

RNP: Ribonucleoprotein

Rpm: Revolutions per minute

RT-LAMP: Real-time loop-mediated isothermal amplification

RT-PCR: Real-time polymerase chain reaction

rtRT-PCR: Real-time reverse transcriptace polymerase chain reaction

SDS-PAGE: Sodium dodecyl sulfate polyacrylamide gel electrophoresis

UV: Ultraviolet

Vrna: Viral Ribonucleic acid

vRNPs: Viral ribonucleoproteins

Xis: Excision

CHAPTER 1

INTRODUCTION AND BACKGROUND TO THE STUDY

1.1 Introduction

Avian influenza (AI), commonly known as bird flu, is a highly contagious disease that affects the respiratory, digestive, and nervous systems of many species of birds (Peiris *et al.*, 2007; The Poultry Site, 2017; Shi *et al.*, 2019; Scott *et al.*, 2020). This disease is caused by a virus belonging to the influenza A genus. Depending on its virulence, AI can lead to systemic infections resulting in high mortality due to highly pathogenic avian influenza (HPAI) viruses or mild to no symptoms caused by low pathogenic avian influenza (LPAI) viruses (Alexander, 2000; OIE, 2009; Gonzales *et al.*, 2017; Li *et al.*, 2018, Charlton, 2018; Scott *et al.*, 2020; Amanollahi *et al.*, 2020; Nishiyama *et al.*, 2020). Several outbreaks of AI in poultry led to culling of millions of birds which resulted in serious economic losses in the poultry industry worldwide (Alexander *et al.*, 2006; FAO, 2011; de Villiers, 2017; Charlton, 2018; Baron *et al.*, 2018; Chatziprodromidou *et al.*, 2018; Kim *et al.*, 2019; Scott *et al.*, 2020; Song *et al.*, 2020; Almayahi *et al.*, 2020). These outbreaks emphasise the urgent need for a diagnostic tool that will facilitate the early detection of AI viruses. Moreover, a more reliable method to prevent the infection and spread of these viruses is also urgently required. The combination of early disease detection and the prevention of new infections through effective vaccines could be an effective method to mitigate animal disease spread and hence minimise losses in the poultry industry.

1.2 Methods for Detecting AI

Classical methods for detecting and identifying AI viruses involve growing the viruses and subsequently isolating them in embryonated chicken eggs. However, this method is time consuming and laborious as it requires between 5 to 10 days for the process to be completed, even when performed by trained staff using special laboratory instruments (Kilic *et al.*, 2020). Molecular techniques such as real-time reverse transcriptase PCR (rtRT-PCR) and nucleic acid sequencing have also been used for the detection of these viruses (Lee and Suarez, 2004; Ng *et al.*, 2005; Payungporn *et al.,* 2006; Liu *et al.*, 2018; Zhang *et al.*, 2018; Shi *et al.*, 2019; Kim *et al.*, 2019). Although these molecular techniques are more sensitive, specific, and faster than the 'egg-based' method for the detection of AI viruses, these methods are still cumbersome in that they require specialised training, are expensive, and sometimes sequencing takes as long as two days to complete and release the required answers. Moreover, transportation of samples from the point-of-care (POC) to the laboratory is needed in both the classical and molecular detection

methods, which further increases the turnaround time for the diagnosis results (Shi *et al.*, 2019). The requirement for cold chain storage further complicates sample stability and adds to the overall costs of sample analysis. The best approach would thus be to develop a POC diagnostic method for use at the sampling area in order to provide results in the shortest time possible (preferably within minutes), thus allowing quick decision-making which is usually dependent on the issuing of field sample analysis results. One of the major challenges with POC assay development is that, depending on the design of the primers and the nucleic acid extraction method, these protocols are prone to low sensitivity and hence present the possibility of false negatives (Woolcock and Cardona, 2005; Chua *et al.*, 2007; Ma *et al.*, 2014; Yu *et al.*, 2017; Sharma *et al.*, 2018; Kim *et al.*, 2019).

1.3 Controlling the Spread of AI

To manage the spread of an AI outbreak by early detection and identification of AI viruses, it is also critical to be able to have a strategy for the control of these viruses. One of the main tools that has been used in the control and management of AI outbreaks is vaccination, but this method is largely dependent on the policies and legislations of the country within which the outbreak occurred. In South Africa, for example, vaccination for AI is only allowed using the non-virulent H6N2 viral strain (Rauff *et al*, 2016).

It is also commonly known that conventional vaccine production is time consuming and may not be suitable for disease control during an active outbreak situation. It usually takes 6 to 8 months from identifying the viruses to the release of the vaccine when using conventional methods (GAO, 2000). On the other hand, Adenovirus vector-based vaccines can be produced in a shorter time and have also been shown to allow differentiation between infected and vaccinated animals (DIVA) (Capua *et al.*, 2003; Toro and Tang, 2009; Baron *et al.*, 2018), which is a feature that conventional vaccines do not have. The DIVA strategy is the only strategy that allows infected animals to be differentiated from vaccinated animals.

In summary, a vaccine containing the same hemagglutinin but a different neuraminidase/no neuraminidase as the field virus is used. Antibodies for the neuraminidase antigen of the field virus will be detected while the same antibodies will not be detected in vaccinated animals that are not infected with the field virus (Capua and Alexander, 2004; Capua *et al.*, 2004; Suarez, 2012; Suarez and Partin-Jackwood, 2017). Currently, in terms of the diagnosis and control of AI viruses using vaccination, it is clear that a better strategy with improved turnaround times is urgently needed for the early detection, control, and management of avian influenza outbreaks.

1.4 Main Aims of the Study

The aim of this study was thus to develop a quicker strategy for viral disease outbreak management in poultry, with specific focus on POC detection and prevention of the spread of AI viruses. It was envisaged that this could be achieved by designing and developing an Adenovirus vector-based vaccine for the control of AI infections in poultry. To achieve this aim, a POC method known as loop-mediated isothermal amplification (LAMP) was developed for the detection of AI viruses. The resultant detection protocol involves the simple detection of all serotypes of AI while also determining whether the offending AI pathogen is of a high or low pathogenic strain. The high pathogenic strains were defined as all strains belonging to the H5 and H7 varieties. The detailed design, which included an investigation into the sensitivity, specificity, and robustness of this method, was tested and validated as discussed in Chapter 3 of this thesis. In brief, the results showed that using the LAMP detection assay it is possible not only to identify AI viruses, but also to determine which variety of the highly pathogenic AI strain is circulating within a certain area. All this could be done in less than two hours. The results supporting this finding, as well as the validated process, are presented in Chapter 4.

The findings highlight that, once the viruses have been identified, it is necessary to have a quick vaccine design and production strategy for the control and management of the spread of these viruses. To address these requirements, an Adenovirus vector-based vaccine targeting AI genes was developed. The vector-based vaccine that was designed was tested using chicken embryo fibroblasts that had been generated in-house. A detailed description of the methods that were followed is presented in Chapter 3. In Chapter 6, an assessment of the levels of protein expression of the gene of interest is presented. In essence, it was found that the Adenovirus vector was expressed in CEFs, hence this was deemed a suitable medium to carry the targeted AI genes of interest. By extension, it may be argued that the vector can be used as a cargo for any gene of interest in chickens, and possibly in other poultry as well.

1.5 Main Challenges in Addressing the Aims of the Study

The DALRRD is the responsible wing of government for all animal reportable and notifiable diseases. One of its policies determines that no vaccination of poultry in the Republic of South Africa other than for the H6N2 strain is allowed. This is because animals that are vaccinated with conventional vaccines usually test seropositive for AI, and this therefore disrupts AI surveillance which is critical for the declaration of poultry farms to be free from AI. Instead, eradicating the virus by means of culling is the preferred method because it has had the highest success rate in eliminating AI incursions.

As an alternative to the original objective, which was to design a full strategy for AI management and control, an Adenovirus vector expressing the Matrix gene of the closely related virus (Newcastle disease virus, or NCDV) was designed as proof of concept that any gene, including the Matrix gene of AI, can be inserted in the Adenovirus vector and be successfully expressed in CEFs. It was argued that, if this were possible, it would mean that one could potentially use an Adenovirus based vaccine against AI. To investigate this hypothesis, the Newcastle Matrix gene was selected. The Newcastle disease, just like AI, is a disease that affects poultry (Doyle, 1935; Capua and Alexander, 2001; Alsahami *et al.*, 2018; Belgrad *et al.*, 2018, Bello *et al.*, 2018). Moreover, its genetic structure closely resembles that of AI.

1.6 Conclusion

The design and seed production of the Adenovirus-based vaccine could be achieved in approximately 10 days from the day of AI virus identification. This quick turnaround time of the vaccination design, in conjunction with the POC diagnostic method that was developed, was found to ensure a quick turnaround time of approximately 15 to 30 days to detect, design, and propagate virus seed stock and also possibly start a smaller batch of vaccine stock. Even with subsequent vaccine finishing steps such as filtration, formulation, filling, packaging, and labelling, this vaccine formulation will arguably drastically reduce the amount of time required to move from detection to vaccination and will thus improve the management of the AI virus outbreaks.

It is an exciting possibility that the strategy referred to above can be adapted to ensure a quick turnaround time for vaccine development combined with POC diagnosis, even for other diseases caused by viruses such as the current Coronavirus (COVID-19).

CHAPTER 2

LITERATURE REVIEW

2.1 Introduction

This Chapter introduces the study by shedding light on the biology of the Influenza A viruses, with a specific focus on the avian influenza viruses. The traditional and current control strategies for these viruses are also discussed in detail in this Chapter. The problem statement is presented, followed by the hypothesis and the aims and objectives of the study.

2.2 Influenza A Viruses: Structure, Genome and Proteins

Influenza A viruses are pleomorphic, enveloped viruses belonging to the family of Orthomyxoviridae (Chatziprodromidou *et al.*, 2018; Amanollahi *et al.*, 2020; Almayahi *et al.*, 2020). Their viral envelope is made up of a lipid bilayer which consists of three viral transmembrane proteins, namely: Hemagglutinin (HA), Neuraminidase (NA), and Matrix 2 (M2), as shown in Figure 2.1. HA is the most abundant of the three proteins at approximately 80 percent, followed by NA at 17 percent and M2 with only 16-20 molecules per virion. Situated just below the viral lipid is the Matrix 1 (M1) protein.

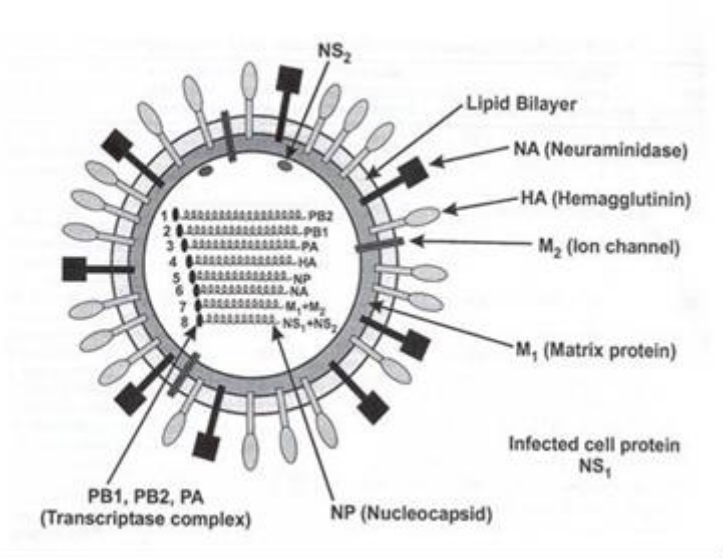

Figure 2.1: Structure of the influenza A virus showing the three main viral transmembrane proteins and the segments contained within the M1 Matrix (CSB, 2011)

The influenza A virus has a segmented genome, consisting of eight single-stranded, negative RNA molecules (Koutsakos *et al.*, 2019; Scott *et al.*, 2020) that range in size from 890 to 2341 nucleotides. The genome arrangement is illustrated in Figure 2.1. The genes encode 11 viral proteins: hemagglutinin (HA), neuraminidase (NA), matrix 1 (M1), matrix 2 (M2), nucleoprotein (NP), non-structural protein 2/nuclear export protein (NS2/NE), polymerase acidic protein (PA), polymerase basic protein 1 (PB1), polymerase basic protein 2 (PB2), and polymerase basic protein 1-F2 (PB1-F2) (Webster *et al.*, 1992; Alexander, 2006; Palese and Shaw, 2007; Bourret, 2018; Klemm *et al.*, 2018; Pham *et al.*, 2018).

The RNA segments are contained within the M1 Matrix in association with the nucleoprotein and three viral polymerase subunits (PA, PB1, and PB2) which, together, form the ribonucleoprotein (RNP) complex involved in RNA replication and transcription.

2.2.1 Classification and nomenclature of influenza A viruses

Influenza A viruses are classified into subtypes based on their antigenic differences of the surface glycoproteins, HA and NA (Shi *et al.*, 2019; Koutsakos *et al.*, 2019; Song *et al.*, 2020). Of these, 18 HA (H1-H18) and 11 NA (N1-N11) subtypes have been identified to date (Durães-Carvalho and Salemi, 2018; Shi *et al.*, 2019; Amanollahi *et al.*, 2020; Song *et al.*, 2020). Different combinations of HA and NA antigens are used to make up the subtypes of influenza A, for example (H1N1, H7N7) (Song *et al.*, 2020). New influenza A strains are conventionally named on the basis of the type of virus, the host of origin (excluding human), the geographic region from which the strain was isolated, the strain number, year of identification, and the HA and NA antigen subtypes (e.g., A/Duck/Vietnam/11/04 (H5N1).

2.2.2 Avian influenza pathogenicity

AI, also known as bird flu, is a highly contagious disease that affects the respiratory, digestive, and nervous systems of various bird species (Grillo *et al.*, 2015; Shi *et al.*, 2019; Scott *et al.*, 2020). AI viruses belong to the influenza A genus of the Orthomyxoviridae family (Lamb and Krug, 1996; Lamb and Krug, 2001; Shabat *et al.*, 2010; Ferhadian *et al.*, 2018, Shi *et al.*, 2019; Amanollahi *et al.*, 2020; Almayahi *et al.*, 2020). These viruses are divided into two groups, namely the highly pathogenic avian influenza virus (HPAI) and the low pathogenic avian influenza (LPAI) virus based on their virulence differences (Sutton, 2018; Amanollahi *et al.*, 2020). HPAI viruses mostly belong to the H5 and H7 subtypes and infection with these viruses usually results in high mortality in poultry species (Chatziprodromidou *et al.*, 2018; Tahir *et al.*, 2020). LPAI viruses, on the other hand, can produce mild to no symptoms within a susceptible poultry species (Rebel *et*

al., 2011; Gonzales *et al.*, 2017; Li *et al.*, 2018; Peng *et al.*, 2018). The HPAI H5N1 was first detected in Southern China in 1996 and spread to birds across Asia, Europe, and Africa (FAO, 2011; Shi *et al.*, 2019), causing major losses in poultry species through either direct infection or preventive culling in affected areas (Alexander *et al.*, 2006). In South Africa, the first AI outbreak occurred in 2004 due to a HPAI H5N2 virus isolated from ostriches on a farm in the Eastern Cape Province. It was accordingly designated as A/Ostrich/S.Africa/2004 (H5N2) (Olivier, 2006). Although most AI viruses do not infect humans, some (particularly H5, H7 and H9) have been reported to have crossed the species barrier and infected and killed mammals, including humans (Guo *et al.*, 1999; Lin *et al.*, 2000; Guo *et al.*, 2001; Lupiani and Reddy, 2009; Gao *et al.*, 2018; Kwok-Yung, 2018; Xue-Cheng *et al.*, 2018; Chatziprodromidou *et al.*, 2018; Shi *et al.*, 2019; Koutsakos *et al.*, 2019; Almayahi *et al.*, 2020; Tahir *et al.*, 2020).

2.2.3 The avian influenza virus infection cycle

Wild aquatic birds such as ducks, geese, gulls, and shorebirds are carriers of various influenza A subtypes (Krauss *et al.*, 2004; Widjaja, 2004; Grillo *et al.*, 2015; Kim *et al.*, 2019; Scott *et al.*, 2020). Although all bird species are thought to be susceptible to influenza A viruses, some domestic poultry species such as chickens, turkeys, and guinea fowl are known to be highly vulnerable to such infections. In susceptible birds, AI is transmitted in a number of ways, including contact with contaminated nasal, salivary or faecal material from infected birds (CDC, 2017). Indirect transmission via virus contaminated water and formites has also been reported (Webster and Govorkova, 2014).

The virus attaches to the host cell through interactions between its HA glycoprotein and sialic acid receptors found on the host cell's membrane, as shown in Figure 2.2 (Samji, 2009; Webster and Govorkova, 2014). Two major linkages are found between sialic acids and the carbohydrates they are bound to in glycoproteins. These linkages are known as the α-2, 3, and α-2, 6. Human influenza A viruses preferentially bind to the α-2, 6 linkages which predominate in human tracheal epithelial cells, whereas those in avian targets recognise the α-2, 3 linkages, which are more common in avian gut epithelium. Sialic acids with terminal α-2, 3 linkages are also found in human respiratory epithelium. However, they are found in less abundance than those found in the α-2, 6 linkages (Couceiro *et al.*, 1993; Matrosovich *et al.*, 2004; Samji, 2009). Humans can therefore be infected by avian influenza viruses, although they are less virulent in humans than when they are infected with the human strains. On the other hand, viruses from swine can recognise both linkages (Skehel and Wiley, 2000), thus making swine a good mixing vessel for both avian and human influenza viruses (Webster and Govorkova, 2014).

Upon attachment to the host cell, the virus is internalised by endocytosis. The acidic pH of the endosome triggers a conformational change in the HA which exposes a fusion peptide that mediates the merging of the viral envelope with the endosomal membrane (Bouvier and Palese, 2008; Samji, 2009). The endosomal pH also opens up the M2 ion channel, thus allowing the hydrogen ions to be pumped into the virus particle. This allows the viral RNPs (vRNPs) to be released into the host cell's cytoplasm (Martin and Helenius, 1991; Stegmann, 2000; Sieczkarski and Whittaker, 2005; Samji, 2009). The vRNPs are transported through the nuclear pore into the nucleus.

Once in the nucleus, the viral polymerase complex, comprising of PB1, PB2 and PA polymerases, initiates the viral mRNA synthesis in a process referred to as 'cap snatching' (Krug, 1981; Lamb and Krug, 2001; Samji, 2009). During this process, PB2 binds to the 5' cap of the host pre-mRNAs, and the endonuclease domain in the PA subunit cleaves off the 5' end of the host mRNA about 10-13 nucleotides downstream from the 5' end and uses this as a primer for viral mRNA synthesis. The viral mRNAs are then transported into the cytoplasm where they are translated into viral proteins. The surface proteins (HA, M2, and NA) are processed and glycosylated in the endoplasmic reticulum and golgi apparatus respectively, followed by transportation to the cell membrane. The newly synthesised polymerase proteins − NP, M1, MS1 and NS2 − are transported into the nucleus. Once in the nucleus, the NS1 protein interferes with the host's innate defence mechanisms by suppressing the synthesis of antiviral cytokines and proteins, thus allowing continuous virus replication (Hay *et al.*, 1982; Shapiro and Krug, 1988; Hale *et al.*, 2008). To produce more viral RNAs (vRNAs) that are needed to assemble new virions, the viral polymerase complex and NP catalyse the replication of a complementary RNA (cRNA) strand from vRNA, followed by the synthesis of new copies of vRNA. The newly made vRNAs are then used as templates for secondary mRNA synthesis. Later in the life cycle, the NS1 protein splices the M and NS mRNAs, thus leading to the formation of M2 and NS2 mRNAs, respectively. Viral mRNAs are then transported into the cytoplasm for the synthesis of the structural proteins. The polymerase complex, MP, M1, and the NS2 proteins are then transported in the nucleus, which is where the assembly of vRNP complexes occurs. The newly formed vRNPs, associated with the NP and the polymerase complex proteins, are exported from the nucleus. This process is made possible by the M1-NS2 complex that is bound to the vRNPs (Portela *et al.*, 1999; Akarsu *et al.*, 2003; Cros and Palese, 2003; Boulo *et al.*, 2007). This complex is directed to the plasma membrane that has been previously modified with the viral membrane protein HA, NA, and M2 (Palese and Shaw, 2007). The progeny virions assemble and bud at the plasma membrane. The HA proteins continue to attach the virions to the sialic acid on the cell surface even after budding has been completed. The sialidase activity of the NA protein cleaves the terminal sialic acid residues from the surface glycoproteins, thus releasing the progeny virions from the host cell

(Palese *et al.*, 1974; Samji, 2009). Once the progeny virions have been released, the host cell dies either from cytolytic or apoptotic mechanisms (Takizawa *et al.*, 1993).

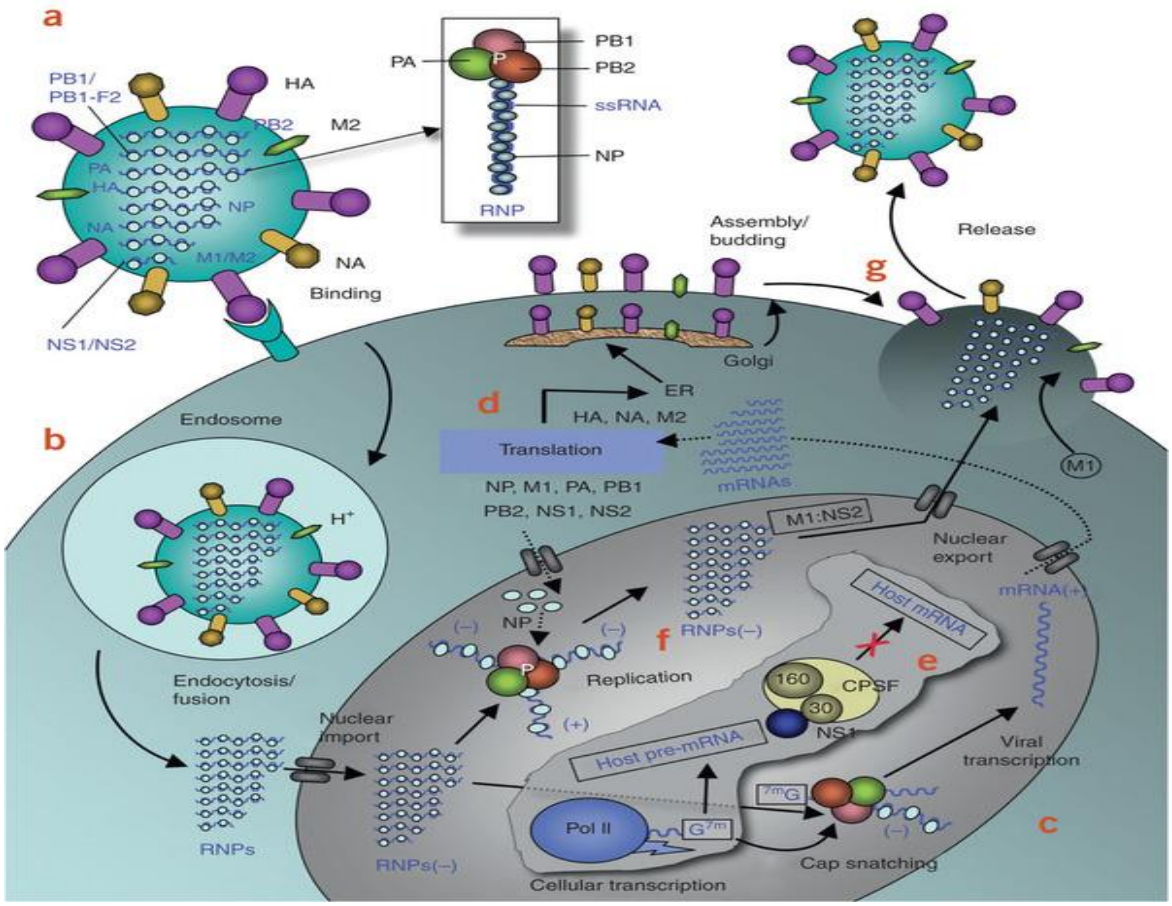

Figure 2.2: Structure of the influenza A virus and its life cycle beginning with attachment to the host cell and ending with the release of the progeny virions (Das *et al.*, 2010).

2.3 Clinical Signs of Avian Influenza in Birds/Poultry

LPAI virus symptoms in birds may be seen only as ruffled feathers, reduced egg production, or mild effects on the respiratory system (Chatziprodromidou *et al.*, 2018). HPAI also affects the respiratory tract while multiple organ and tissue invasion occurs, thus resulting in major internal haemorrhaging. Other clinical signs that are visible in birds infected with HPAI, such as H5N1, include quietness, serious depression, and a sudden drop in egg production. Most eggs are also soft-shelled if not shell-less, and there is also swelling of the skin under the eyes, coughing, sneezing, diarrhoea, and mortality (OIE, 2017a; Chatziprodromidou *et al.*, 2018). Some of these clinical signs are shown in Figure 2.3 (A-F) below.

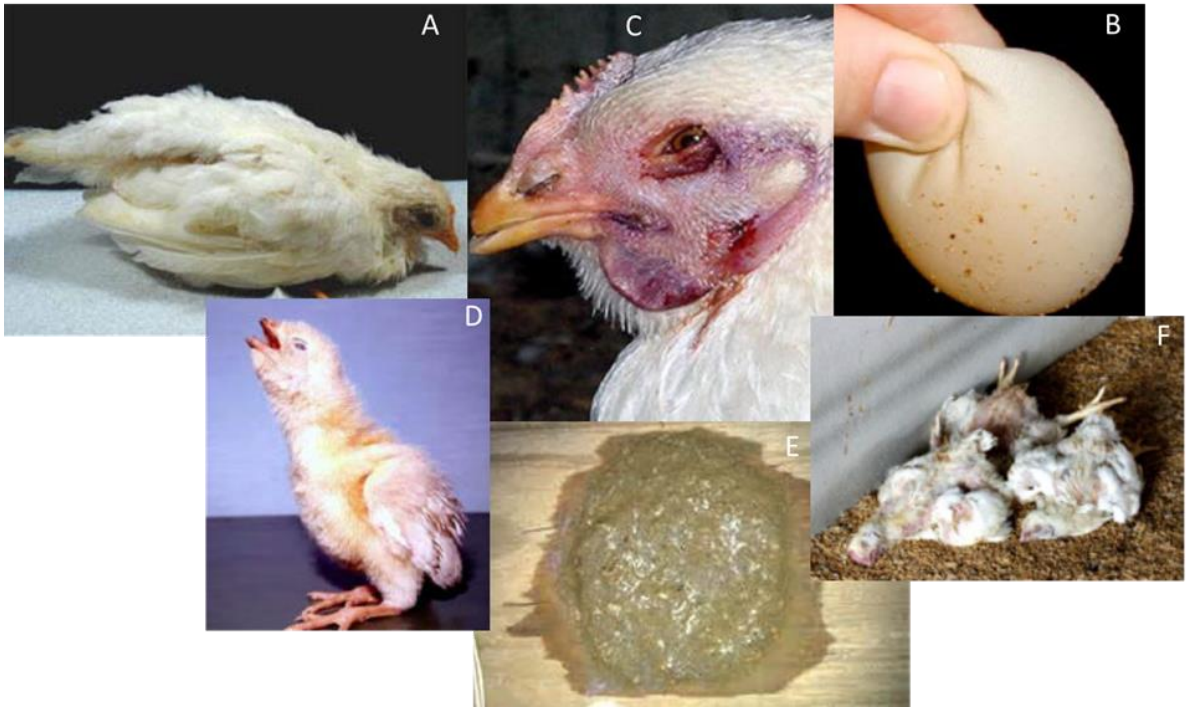

Figure 2.3: Clinical signs of AI in chickens (Darre, 2015). A: Quietness and depression in an AI infected chicken. B: A soft-shelled egg laid by an AI infected chicken. C: Swelling of the skin under the eye of an AI infected chicken. D: Chicken coughing due to AI infection. E: Chicken diarrhoea caused by AI infection. F: Mortality of chickens infected with HPAI.

2.3.1 Influenza A virus variation

Throughout the influenza A replication cycle, a high mutation rate of 7.3×10^{-5} per nucleotide base per cycle of replication occurs which is equivalent to one nucleotide exchange per genome (Drake, 1993). This error rate occurs as a result of lack of proofreading from the viral RNA polymerase and is the main reason why influenza A viruses are continuously changing (Webster and Govorkova, 2014). These changes can take place in two different ways referred to as antigenic drift and antigenic shift (Robertson, 1987; Weldemariam, 2016; Song *et al.*, 2020). In influenza A viruses, an antigenic drift is a small, gradual change of the surface proteins hemagglutinin and neuraminidase caused by point mutations (Pu *et al.*, 2015; Sanjuán and Domingo-Calap, 2016; Sobel *et al.*, 2017; Song *et al.*, 2020, Scott *et al.*, 2020). This leads to the formation of new virus strains that are unrecognisable by the antibodies of the pre-existing host immune system. This explains why humans or animals can be infected with influenza A viruses several times. Previous studies on poultry revealed that a LPAI, that had circulated in wild birds for a number of months, underwent antigenic drift, thus resulting in the formation of an HPAI virus (Ito *et al.*, 2001; Zhang *et al.*, 2013; Ke *et al.*, 2017; Zhu *et al.*, 2018; Scott *et al.*, 2020). This phenomenon is one of the important reasons for global surveillance in order to monitor the

changes of influenza A virus strains and to know which strain should be targeted by the influenza vaccine produced annually (Webster and Govorkova, 2014; Weldemariam, 2016).

Antigenic shift, on the other hand, is the process by which two or more different strains of a virus combine to form a new subtype with a combination of the hemagglutinin and neuraminidase of the two or more original viral strains (Li *et al.*, 2004; Webster and Govorkova, 2014). As already mentioned in section 2.2.3, pigs/swine are known to be susceptible to both human and avian type influenza viruses, which is why they are also referred to as 'the mixing vessel' for genetic re-assortment (Ma *et al.*, 2009; Neumann *et al.*, 2009). This is illustrated in Figure 2.4. An antigenic shift can also occur through a direct introduction of a strain without re-assortment from animals to humans, as is also shown in Figure 2.4 below (Cox and Subbarao, 2000).

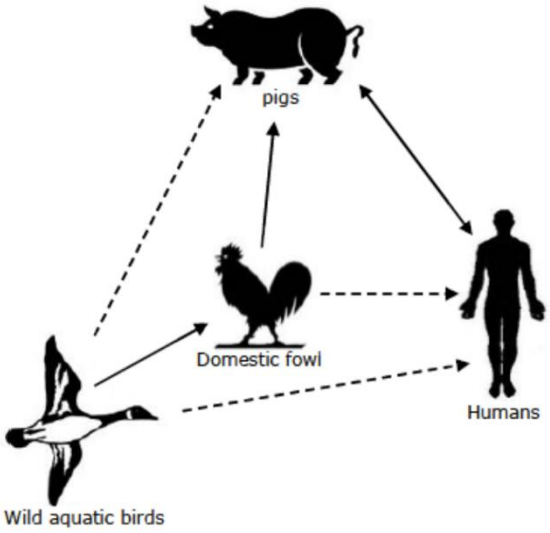

Figure 2.4: Diagrammatic representation of a pig as a mixing vessel for influenza A viruses. This diagram shows AI viruses being transmitted from a natural wildlife reservoir to the domestic fowl and from the domestic fowl to the pig. The phenomenon of human and AI A viruses that infect pigs where re-assortment occurs between avian, swine and human influenza A viruses is also shown. The diagram also illustrates that human can be infected by influenza A viruses from pigs. Solid lines show frequent and/or confirmed transmissions, while dotted lines show possible and/or occasional transmissions (Ma, 2009).

2.3.2 Epidemiology of AI

Avian influenza viruses are divided into two groups based on the severity of the disease they cause, namely HPAI and low LPAI (Sutton, 2018; Amanollahi *et al.*, 2020). The HPAI viruses, some of which are formed by mutations in LPAI viruses after being introduced into poultry, are associated with systemic infections that often result in high mortality and morbidity (Swayne and Halvorson, 2003; Gonzales *et al.*, 2017; Li *et al.*, 2018; Peng *et al.*, 2018; Scott *et al.*, 2020). It is known that LPAI viruses cause mild or no symptoms in birds (Horimoto and Kawaoka, 2001; Alexander, 2006; Gonzales *et al.*, 2017; Li *et al.*, 2018; Peng *et al.*, 2018). To date, only viruses of the H5 and H7 subtypes have been shown to cause HPAI, but not all H5 and H7 viruses are highly pathogenic. Moreover, H7 and H5 are the only subtypes that are notifiable to the World Organization for Animal Health (OIE) (Senne *et al.*, 2006; Chatziprodromidou *et al.*, 2018; Tahir *et al.*, 2020).

The primary introduction of AI into poultry is usually due to wild bird activities, such as the behaviour of waterfowl (Scott *et al.*, 2018a; Scott *et al.*, 2020). However, in previous outbreaks the main risk factors in the spread of HPAI were the illegal trade in infected poultry and poultry products and the unintended mechanical passing on of the virus through human movement by travellers and refugees (Alexander, 2006). For more in-depth information, an investigation into global avian influenza outbreaks from 2010-2016 was conducted. In this investigation ~82.5% of the subtypes comprised HPAI, while 9.7% was due to LPAI (Figure 2.5) (Chatziprodromidou *et al.*, 2018). Although most outbreaks were due to both LPAI and HPAI of the H5 and H7 subtypes, outbreaks due to the LPAI H9N2 viruses were also reported (Alexander, 2006). In South Africa, the first reported case of HPAI occurred in 2004. This was due to the HPAI subtype H5N2 and led to the culling of 30 000 ostriches on 15 farms (Alexander, 2006).

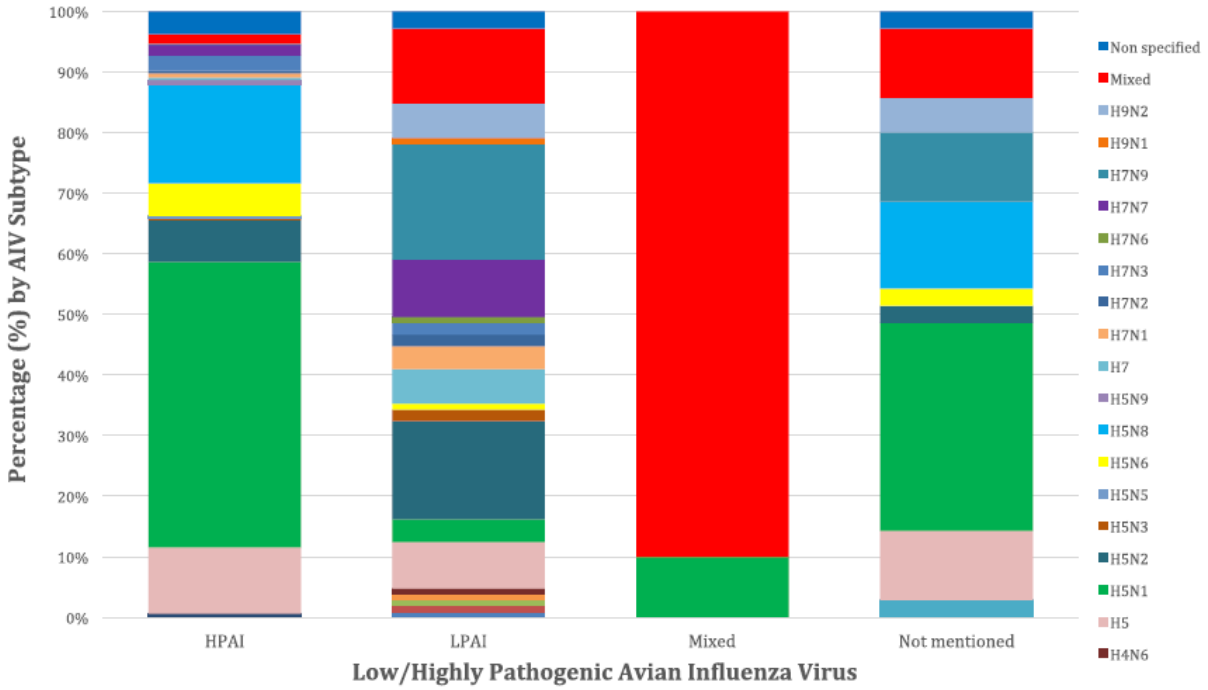

Figure 2.5: The distribution patterns of LPAI and HPAI in bird populations from 2010-2016 (Chatziprodromidou *et al.*, 2018)

2.4 Avian Influenza Control and Management Strategies

Poultry and its products are a major source of human food and protein as a nutrient, thus keeping poultry free from avian influenza is critical in order to continue international trading in poultry and its products (Alexander, 1997; Charlton, 2018). In South Africa, ostrich farming is highly dependent on the export of leather, feathers, and fresh ostrich meat products to trade partners in Europe, Japan, and the United States of America (USA) (South African Ostrich Business Chamber, 2011). The main production systems and processing facilities of ostrich in South Africa are located in the Klein Karoo region in the Western Cape, which is home to 70-80% of the South African ostrich industry (Olivier, 2006). In 2011, the export of ostrich meat from South Africa was suspended after the detection of the H5N2 avian influenza virus amongst a few ostriches in the Western Cape (South African Ostrich Business Chamber, 2011; Business Day Live, 2012). By the year 2012, ostrich meat contributed about 62% of income for the ostrich industry in South Africa, but the 2011-2012 outbreak cost the ostrich industry an estimated R1 billion (R108 million per month). Heartbreakingly, about 41 000 birds were culled in this period (South African Ostrich Business Chamber, 2011; Business Day Live, 2012). Just recently, over 2 million birds died in the Western Cape Province due to a new avian influenza outbreak (de Villiers, 2017).

These data confirm that, in the poultry industry, prevention, control, and eradication of virus infections are the three major goals for dealing with AI outbreaks. Five main strategies are known to achieve these goals, namely biosecurity, diagnostics and surveillance, vaccination, elimination of AI infected poultry, and education (Akey, 2003).

2.4.1 Biosecurity

Biosecurity is the use of management procedures to prevent either the introduction of AI in a poultry farm or the escape of the AI viruses to a new area. This can be achieved in various ways such as movement restrictions of AI contaminated equipment and sterilising clothing and shoes (Scott *et al.*, 2018b; Scott *et al.*, 2020). Movement prevention of AI infected poultry or their by-products and preventing exposure of poultry to wild birds are also ways of preventing the spread of AI (Scott *et al.*, 2018b; Scott *et al.*, 2020). For instance, between 1978 and 2000 poultry farmers in Minnesota in the USA experienced 108 cases of AI outbreaks as various AI strains were transmitted from migratory ducks to turkeys (Halvorson, 2002).

Farm quarantine is another way of practising proper biosecurity (Hamilton *et al.*, 2009; Glass *et al.*, 2019; Scott *et al.*, 2020). Poultry farms should also preferably be located in low density geographical areas in order to decrease or prevent farm-to-farm AI transmissions (Capua and Marangon, 2003). However, such restrictions are not only practised in terms of animal related diseases. For instance, in light of the current COVID-19 pandemic, most countries worldwide have introduced human social distancing, robust disease tracking systems, quarantine facilities, and education about this viral disease as vital tools to reduce infections (Kilic *et al.*, 2020; Al-Rohaimi and Al-Otaibi, 2020).

2.4.2 Diagnostics and surveillance

The rate at which a disease is eradicated is highly dependent on how fast that particular disease is detected (Afzal, 2020). High mortality among a poultry flock can be a sign that there is an HPAI virus circulating on a poultry farm, therefore a reliable diagnosis is required to identify the disease or virus (Swayne and Halvorson, 2003). Previously, the diagnosis of AI was achieved by isolating the virus in embryonated chicken eggs, followed by identification using antigen testing (Okamatsu *et al.*, 2016; Kim *et al.*, 2019). However, this process is slow as it takes 1-3 weeks to finalise the results, and it is also highly labour intensive (Swayne *et al.*, 2008; Vemula *et al.*, 2016; Kim *et al.*, 2019). For this reason, two alternatives to virus isolation and identification were developed. These methods are the direct detection of type A influenza virus antigens and the amplification and detection of AI virus genes (Akey, 2003; Yu *et al.*, 2017; Liu *et al.*, 2018; Zhang *et al.*, 2018). In

previous studies, the antigen-ELISA displayed 100% specificity and 79% sensitivity for detecting AI virus from outbreak samples in poultry (Akey, 2003). However, in other studies on the antigen-ELISA during the Virginia H7N2 LPAI outbreak, false positive results were obtained on a few farms (Ding *et al.*, 2011; Ping *et al.*, 2015).

Despite the fact that the antigen-ELISA had been used as an effective field-screening test, a rapid, more sensitive and specific diagnostic test was urgently required for AI. A laboratory based, one-step, real-time reverse-transcriptase polymerase chain reaction (RRT-PCR) assay for the detection of AI viruses in field specimens was then developed and validated (Spackman *et al.*, 2002; Liu *et al.*, 2018; Zhang *et al.*, 2018). It took less than 3 hours to obtain real-time results from these assays. Although this method is currently used to address some issues such as time and specificity, its main drawback is that these assays are laboratory based. It would thus be ideal if these assays could be adapted for POC usage. Other assays that are currently used include nucleic acid sequence-based amplification (NASBA), real-time RT-PCR, and multiplex RT-PCR assay (Choi *et al.*, 2002; Collins *et al.*, 2003; Ellis *et al.*, 2002; Playford *et al.*, 2002; Okamatsu *et al.*, 2016; Liu *et al.*, 2018; Zhang *et al.*, 2018; Shi *et al.*, 2019; Kim *et al.*, 2019). A major drawback of most of these methods, however, is that they require expensive reagents and specialised instruments that may not be readily available in diagnostic laboratories in developing and underdeveloped countries (Kilic *et al.*, 2020). This is the same struggle that the world is currently facing with the COVID-19 pandemic. In this regard, RT-PCR was the first method developed for the detection of COVID-19 (Kilic *et al.*, 2020; Corman *et al.*, 2020; Afzal, 2020; Park *et al.*, 2020; Shen *et al.*, 2020). As experienced with the detection of other viral diseases using RT-PCR, using this technique to detect COVID-19 is also costly and slow in delivery. A single RT-PCR kit may cost roughly $100 USD, while setting up a suitable laboratory may cost more than $15 000 USD. Moreover, the turnaround time when using RT-PCR is more than 24 hours (Afzal, 2020; Sheridan, 2020; Ramdas *et al.*, 2020). Moreover, in addition to these drawbacks, some studies have reported a high proportion of false negative results of RT-PCR diagnosis for COVID-19 (Huang *et al.*, 2020; To *et al.*, 2020; Afzal, 2020; Chen *et al.*, 2020; Liu *et al.*, 2020).

2.4.3 Vaccination

Vaccines are known for the induction of protective immunity against a disease-causing pathogen without causing the disease (Swayne and Kapczynsk, 2008; Zepp, 2010; Al-Rohaimi and Al-Otaibi, 2020). The main aim of a vaccine is to cause a long-term immunological memory which, when reactivated, can respond quickly and efficaciously to curb the actual disease (Esser *et al.*, 2003; Moser and Leo, 2010, Amanollahi *et al.*, 2020). The mechanism of vaccine protection occurs through the production of neutralising antibodies (Wilson-Welder *et al.*, 2009). Vaccination

thus protects the recipient against clinical signs and mortality, decreases virus shedding, increases infection resistance, and protects against a wide range of viruses within similar subtypes (Swayne and Suares, 2000; Swayne, 2003; Capua *et al.*, 2004).

Conventionally inactivated, oil adjuvanted, whole virus vaccines are commonly used against AIV and account for 95.5% of AIV vaccinations in the poultry industry (Swayne *et al.*, 2011; Lone *et al.*, 2017). The major drawback of these types of vaccines is the existence of a large number of virus subtypes, which makes it difficult when choosing strains to produce influenza vaccines. Additionally, some strains do not grow to sufficiently high titre to produce potent vaccines (Lu *et al.*, 2005; Horimoto *et al.*, 2006; Donis, 2014; Milián and Kamen, 2015). Some vaccines are produced from isolates specifically involved in an epizootic, while others depend on vaccines produced from viruses that have the same hemagglutinin subtypes and the ability to yield high antigen concentrations (Bankwoski, 1985; Koutsakos *et al.*, 2019).

As an alternative, recombinant vaccines for AIV have been produced by inserting the AIV hemagglutinin (HA) gene into a live virus vector and using this recombinant virus to immunise poultry against AI (Swayne, 2004; Bublot *et al.*, 2010; Kapczynski, 2015; Suarez and Pantin-Jackwood, 2017). Recombinant live vector vaccines have various advantages, such as the ability to induce humoral, mucosal as well as cellular immunity. These vaccines can also be administered to young poultry, thus inducing early protection. Another advantage is that they allow differentiation between infected and vaccinated (DIVA) poultry (e.g., they only induce the production of the antibodies against the gene inserted in the virus vector, while infected poultry will produce antibodies of other proteins such as the Matrix protein) (Suarez and Pantin-Jackwood, 2017). However, recombinant live vector vaccines also have limitations, such as poor replication and only possessing partial protective immunity (if at all) in poultry that were previously exposed to, or were previously vaccinated with, the vector virus (Koutsakos *et al.*, 2019). Additionally, recombinant vector vaccines have a restricted host range, which means that they are only effective in certain poultry species and not in others. The only known exception is the herpesvirus (HVT) of turkeys, as it is not susceptible to maternal antibodies even though immunity is not induced for a long term (Li *et al.*, 2011; Rauw *et al.*, 2012; Kapczynski, 2015; Suarez and Pantin-Jackwood, 2017).

The use of recombinant vaccines is only allowed in countries in which they are licensed. For example, the fowl pox virus (FPV), HVT, and non-virulent avian Paramyxovirus type 1 (APMV-1) have all been licensed in certain countries and have been utilised as vectors for AIV vaccines in the field (Swayne, 2003; Qiao *et al.*, 2003; Bublot *et al.*, 2006; Qiao *et al.*, 2006; Zhigao, 2007; Chen, 2009; SarFati-Mizhari *et al.*, 2010; Bublot *et al.*, 2010; Suarez and Pantin-Jackwood, 2017).

Recombinant vaccines have been used to treat for instance *Salmonella enterica*, the Laryngotracheitis virus, and the Adenovirus, but none of these vaccines have been applied in the field due to the fact that they have not been licensed (Pavlova *et al.*, 2009; Park *et al*, 2009; Al-Rohaimi and Al-Otaibi, 2020; Porto *et al*, 2020).

2.4.4 Elimination of the AI virus in infected poultry

Currently, two systems are used for the elimination of the AI virus in infected poultry flocks. The two systems are controlled marketing of recovering or recovered flocks and the stamping-out of infected flocks (Charlton, 2018; Scott *et al.*, 2020). These methods are mainly used in countries such as South Africa where the vaccination of uninfected poultry is prohibited. The prohibition motives are based on the fact that one cannot prevent infection or virus shedding by vaccinated poultry. Therefore, the spread of the AI virus continues unabated and could lead to genetic shift which, in turn, could lead to re-assortment (see section 2.3.1). In such cases, the emergence of a highly pathogenic strain that has never been identified before is highly likely (Webster and Govorkova, 2014).

2.4.4.1 Controlled marketing and recovering of flocks

Historically, AIV infected turkey flocks were allowed to recover from infection and were marketed via routine processing (Halvorson, 2002). Recovering flocks are usually handled with more care than non-infected ones by disinfecting working areas. At times flocks show no symptoms until they get to the slaughterhouse, while in others the virus is detected early in an outbreak and they then recover from the AI infection. Such flocks continue to be marketed, especially in cases where there is limited landfill space for disposal (Akey, 2003; Halvorson, 2002). Another method of dealing with infected flocks is to use their meat for further processing and as pre-cooked products, especially because both the LPAI and HPAI viruses are thermally labile (Swayne and Halvorson, 2003).

2.4.4.2 Stamping out

The World Organization for Animal Health (OIE) defines the stamping-out process in the OIE terrestrial animal health code as “the killing of animals that are affected, suspected of being affected, and have been exposed to infection either by direct or indirect contact as a means of control and eradication strategy for animal diseases such as HPAI” (OIE, 2017b). Two processes are usually followed for the stamping out of infected flocks (Scott *et al.*, 2020), namely euthanasia (quick and painless killing of large numbers of poultry) and disposal of the carcasses at landfill

sites (Mohan and Gregory, 1990; The Poultry Site, 2007). These two methods seem to be the preferred methods for eliminating flocks that are acutely infected or have recovered from an acute HPAI virus.

2.4.4.3 Euthanasia

The most preferred method of euthanasia is the application of carbon dioxide (CO_2) gas. Individual birds are placed in a large, tightly closed container and euthanized by the addition of CO_2. This process takes less than 15 minutes once the CO_2 has been introduced (Mohan and Gregory, 1990; Akey, 2003; The Poultry Site, 2007).
The disposal of euthanized birds occurs by means of a variety of methods such as off-farm burial, incineration, and composting (de Villiers, 2017). The term off-farm burial is self-explanatory: the euthanized birds are buried in an isolated area away from farming activities. The use of off-farm burial will be reduced in future due to environmental regulations that prohibit ground water contamination and endangering the lives/health of the public (Akey, 2003).

2.4.4.4 Incineration

In simple terms, incineration is used to destroy unwanted objects by burning them. However, the use of incineration has been reduced due to complaints about smoke, the high cost for the maintenance of the incineration equipment and fuel used, as well as challenges associated with carcass transportation and ash disposal once the process has been completed (Akey, 2003; Stingone and Wing, 2011).

2.4.4.5 Composting

Dead birds are also dumped at a landfill site that has been approved for the purpose of composting. This method was used in the H7N2 LPAI Virginia outbreak, but a drawback was that the transportation of the carcasses became too costly as the primary location was a 3-hour drive away from the quarantine zone (Akey, 2003; Virginia Cooperative Extension, 2009; Flory and Peer, 2010).

2.4.5 Education

This is an important strategy for AI prevention, control, and eradication (Alders and Bagnol, 2007; FAO, 2007) and entails educating the people working in the poultry industry about the biology of AI viruses, how the viruses can be introduced and spread on farms or in batteries, and the

biosecurity methods that can be followed to prevent the introduction of the viruses onto farm. Education is also required to equip farm workers with knowledge on how to prevent the AI virus from leaving the farm and thus spreading to other farms (Alders and Bagnol, 2007; FAO, 2007). Education is necessary not only in terms of AI, but also to inform workers of other viral diseases. A recent study on the current COVID-19 pandemic showed that educating the public in terms of vigilance and sensitivity towards COVID-19 and taking appropriate precautionary measures to prevent infections played a huge role in managing COVID-19 globally (Hu *et al.*, 2020).

2.5 Current Avian Influenza Control Strategies

Traditional AI control strategies have not been a hundred percent efficient in AI eradication. The two main areas that will play an important role in ensuring that AI management moves towards disease eradication are POC detection of these viruses and concomitant vaccine matching strategies to target these viruses, specifically during local outbreaks. Movement control and selective marketing of infected birds and vaccinated fowls are also critical in ensuring no accidental spread of viruses occurs in naïve populations. Information about the two AI control strategies that are highlighted in the literature will be discussed. The mechanisms that are commonly used will be explained and evaluated to determine their applicability in the poultry industry and in future applications. These two strategies are the POC diagnosis of AI using the LAMP method, and second is the recombinant vaccine design and application using Adenovirus vectors. The theories that underpin the use of these strategies will be analysed in depth.

2.5.1 The point-of-care diagnosis of AI using LAMP

2.5.1.1 The principles of LAMP

LAMP is a relatively new nucleic acid amplification technique that can be used in a water bath at an isothermal range of 60-65°C. The technique does not require any expensive or specialised equipment (Shi *et al.*, 2019) and is simple to use, has high specificity and rapidity, and can be completed within 30-60 minutes (Notomi *et al.*, 2000; Tomlinson *et al.*, 2010; Bhat *et al.*, 2013, Camp and Nowotny, 2016; Maan *et al.*, 2016; Kim *et al.*, 2018; Zeng *et al.*, 2018; Shi *et al.*, 2019). The simplicity of this technique enables the investigator to detect pathogenic microorganisms in field conditions. Currently, LAMP has been used successfully for the detection of various viruses (Poon *et al.*, 2005; Ito *et al.*, 2006; Imai *et al.*, 2006; Imai *et al.*, 2007; Xu *et al.*, 2009; Kubo *et al.*, 2010; Song *et al.*, 2018; Lai *et al.*, 2018; Shi *et al.*, 2019). Various LAMP assays have been developed for COVID-19 detection (Afzal, 2020;Yan *et al.*, 2020; Yu *et al.*, 2020; Kilic *et al.*, 2020; Lu *et al.*, 2020; Zhang *et al.*, 2020; Zhu *et al.*, 2020) and the sensitivity of these assays were

shown to be similar to that of RT-PCR, but they had a quicker turnaround time of less than 1 hour (Kilic *et al.*, 2020). Amongst these LAMP assays, the Atila Biosystem's iAMP detection kit was approved by the FDA for emergency use due to its 100% sensitivity, low LoD of ~4 copies/µL, and a 1-hour sample-to-result time (Afzal, 2020; Atila Biosystems, 2020). LAMP is based on the auto-cycling strand displacement synthesis carried out in the presence of Bst DNA polymerase, dNTPS, specific primers, and a DNA template (Notomi *et al.*, 2000; Pumford *et al.*, 2020). This method uses a DNA polymerase with high strand displacement activity, a set of four primers (two inner and two outer primers), and it recognises six specific sequences on the target DNA (Notomi *et al.*, 2000; Nagamine *et al.*, 2002; Parida *et al.*, 2006; Pumford *et al.*, 2020). The use of four primers ensures high specificity for target amplification. The inner primers are differentiated into the forward inner primer (FIP) and the backward inner primer (BIP), each containing two sequences specific to the sense and antisense sequences of the target DNA. The design of the LAMP primers is based on the following distinct regions of the target DNA: the F3c, F2c and F1c at the 3' side and the B1, B2, and B3 at the 5' side. The FIP is made up of a complementary sequence of F1 (F1c) at the 5' end, a TTT spacer, and an F2 sequence at the 3' end that is complementary to the F2c sequence on the target DNA. The BIP contains a complementary sequence of B1 (B1c) at the 5' end, and a TTT spacer and a sequence of B2 at the 3' end, that is complementary to B2c on the target DNA. The backward outer primer (B3) is complementary to the B3c sequence of the target DNA while the forward outer primer (F3) sequence is complementary to the F3c sequence of the target DNA. LAMP requires two steps, namely the non-cyclic and the cyclic steps. In the initial steps of the LAMP reaction, all primers are used but later, during the cyclic reaction step, only the inner primers are used for strand displacement DNA synthesis (Notomi *et al.*, 2000; Mori *et al.*, 2001; Nagamine *et al.*, 2001; Nagamine *et al.*, 2002; Tomita *et al.*, 2008; Pumford *et al.*, 2020). These steps are diagrammatically illustrated in Figure 2.6.

2.5.1.2 The mechanism of LAMP

Non-cyclic step is when the FIP anneals to the F2c region in the target DNA, thus initiating complementary strand synthesis. The F3 outer primer anneals to the F3c region in the target DNA, outside of the FIP, forming a double stranded DNA which, together with the help of Bst DNA polymerase, releases the FIP-linked complementary strand as a single strand. Due to the complementary F1c and F1 regions, this released single strand forms a stem-loop structure at the 5' end. This stem-loop structure serves as a template for BIP-initiated DNA synthesis as well as B3-primed strand displacement DNA synthesis. The BIP anneals to the stem-loop structure and synthesizes a complementary strand. This is followed by the annealing of the B3 primer which, together with the activity of the Bst DNA polymerase, displaces and releases the single

stranded BIP-linked complementary strand. This strand forms a structure with stem-loops at each end which is converted into a stem-loop DNA by self-primed DNA synthesis. The stem-loop then serves as the starting structure for the LAMP cycling reaction (Notomi *et al.*, 2000; Mori *et al.*, 2001; Nagamine *et al.*, 2001; Nagamine *et al.*, 2002; Pumford *et al.*, 2020).

The cyclic step is when the FIP anneals to the single stranded region in the stem-loop DNA and initiates strand DNA synthesis that leads to the release of the strand synthesised previously. Due to the complementary B1c and B1 regions, the released single strand forms a stem-loop structure at the 3' end. Using self-structure as a template, DNA synthesis starts from the 3' end of the B1 region, thus releasing the FIP-linked complementary strand. Two products are formed from the above process: one is the complementary structure of the original stem-loop DNA (formed from the released single strand) and the other is the gap repaired stem-loop DNA with a stem elongated to twice as long and a loop at the opposite end. BIP anneals to the B2c region of the two products and initiates strand displacement DNA synthesis as well as the release of the BIP-linked complementary strand. These reactions continue which leads to an accumulation of 10^9 copies of the target DNA in less than 1 hour. The final products of LAMP are stem-loops with several inverted repeats of the target DNA and cauliflower-like structures with multiple loops (Notomi *et al.*, 2000; Mori *et al.*, 2001; Nagamine *et al.*, 2001; Nagamine *et al.*, 2002; Pumford *et al.*, 2020).

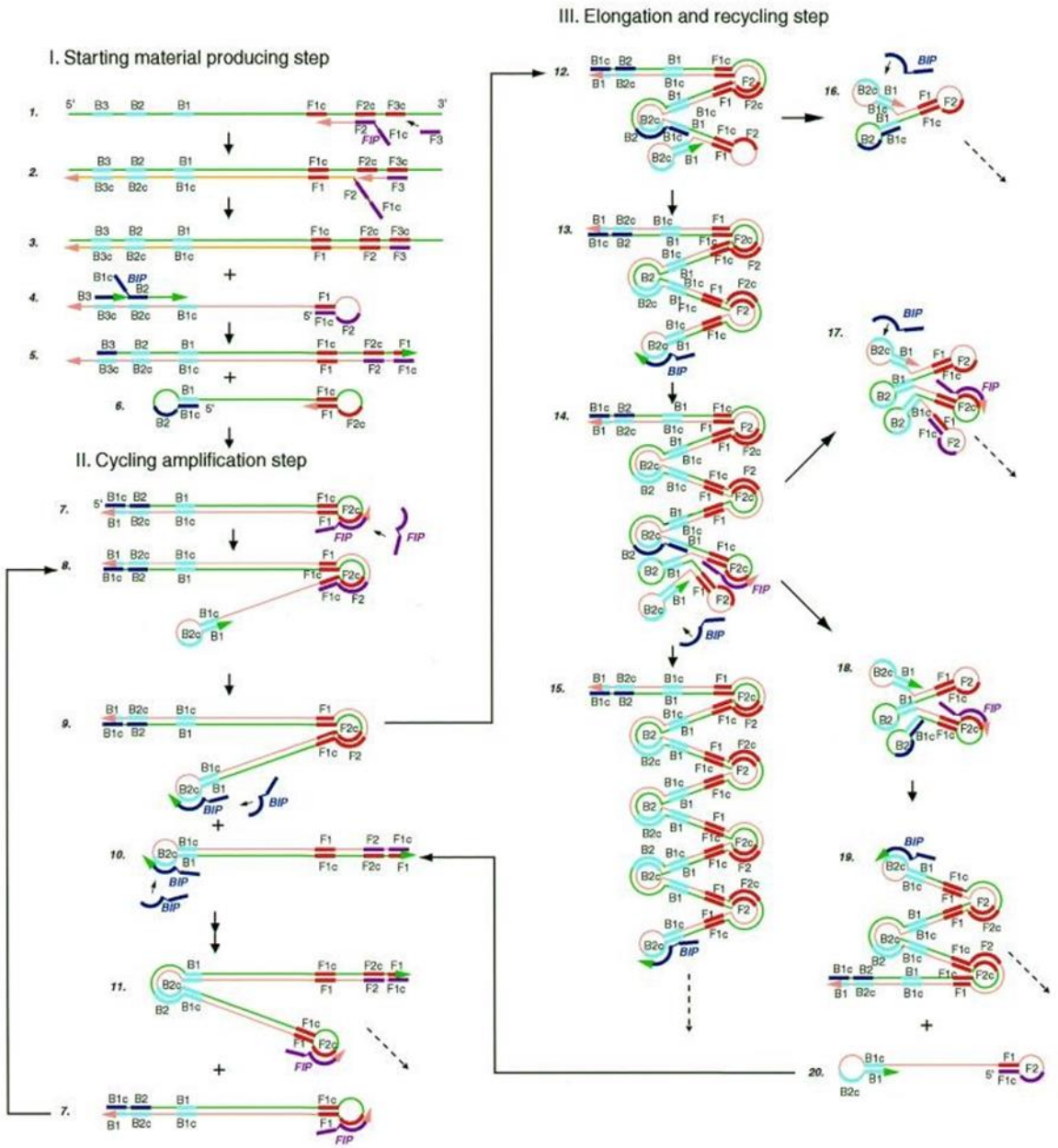

Figure 2.6: Schematic representation of a loop-mediated isothermal amplification reaction (Notomi *et al.*, 2000).

2.5.2 Recombinant vaccination using the Adenovirus vectors

2.5.2.1 Structure, genome, and proteins of the Adenovirus

Adenoviruses belong to the family Adenoviridae and range in size from ~70-100nm (Berk, 2007; Reddy and Nemerow, 2014; Lasswitz *et al.*, 2018; Porto *et al.*, 2020). These viruses have a broad host range and they have been identified in birds, reptiles, fish, and various species of vertebrates,

including humans (Wellehan *et al.*, 2004; Schrenzel *et al.*, 2005; Walker *et al.*, 2017). In humans they can cause infections that result in respiratory disease, conjunctivitis, and gastroenteritis (Kojaoghlanian, 2003; Vogels *et al.*, 2003; Terasako *et al.*, 2012; Lion, 2014; Saha *et al.*, 2014). The virion is made up of an iscosahedral protein capsid surrounding the genomic material of the virus. The capsid consists of three subunits which are the hexon, penton, and a fiber (Reddy *et al.*, 2010; Lasswits *et al.*, 2018; Ma and Guan, 2018; Porto *et al.*, 2020). The structure of the virus is shown in Figure 2.7. The hexon is the most abundant of the subunits while the penton and the fiber occur only at the vertices. The genome of the Adenovirus is linear, double stranded, and ~36Kb in size (Ma and Guan, 2018; Ismail *et al.*, 2018). As part of their life cycle, these viruses do not integrate into the host genome, but their genome remains as a linear episome in the nucleus of the host cell (Hillgenberg *et al.*, 2001; Lasswitz *et al.*, 2018).

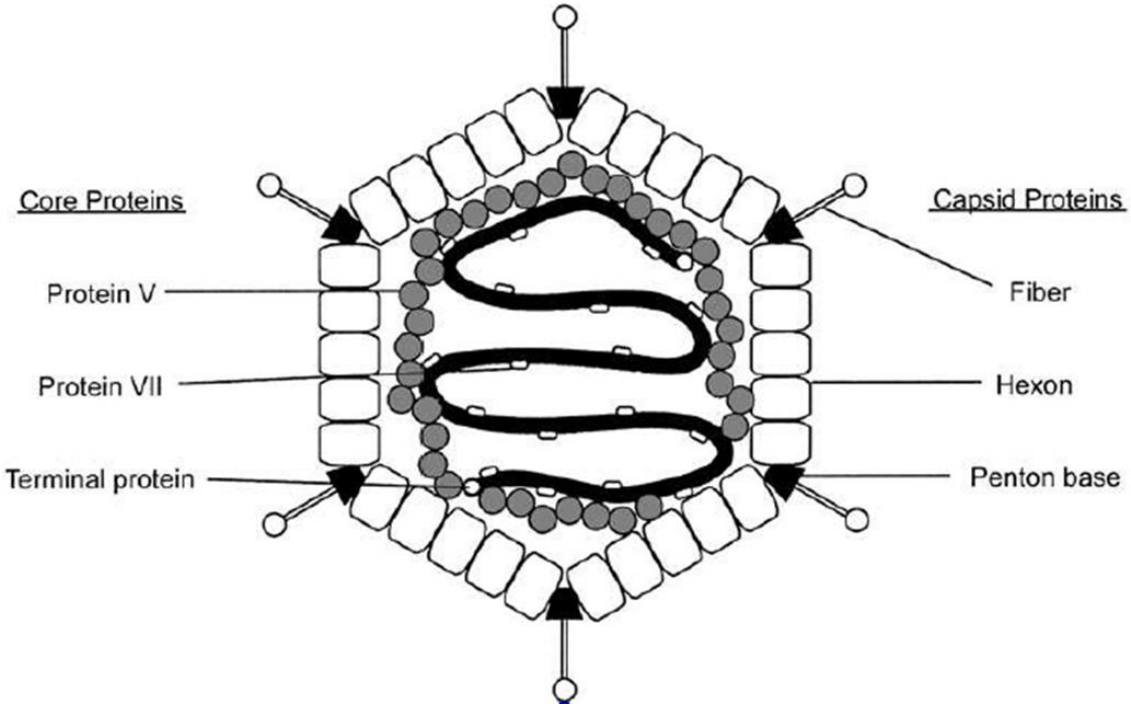

Figure 2.7: Schematic representation of the Adenovirus showing the major capsid and the core proteins (Shenk, 1996).

The linear genome is flanked by two inverted terminal repeat (ITR) sequences that serve as the origin of replication and eight units that are responsible for RNA polymerase II-mediated transcription, as shown in Figure 2.8. The viral genome consists of five early units (E1A, E1B, E2, E3, E4 and E5) (Branton, 1999; Saha *et al.*, 2014), two units with a delayed expression after the start of the replication of the virus (IX and Iva2), and one late unit (L) that is subdivided into L1-

L5 (Saha *et al.*, 2014; Ahi and Mittal, 2016). Each of these units has a role in the viral life cycle. The E1A unit, which is positioned next to the 5' ITR, gets transcribed first and is also responsible for the transcription activation of the other viral genes (Saha *et al.*, 2014). The E2 unit is also responsible for viral replication, while the E3 unit encodes an Adenovirus death protein polypeptide which promotes the death of the infected cells as well as the release of the virus particles. The E4 unit, on the other hand, is responsible for the nuclear export of the viral RNA (Tatsis and Ertl, 2004; Saha *et al.*, 2014). The virion stability is increased by the IX gene product, while the IVa2 protein is essential for the assembly of the Adenovirus and the viral DNA packaging (Ahi and Mittal, 2016). Finally, the products of the latter transcription units (L1-L5) are essential for the formation of the viral capsid (Rux and Burnett, 1999; Saha *et al.*, 2014).

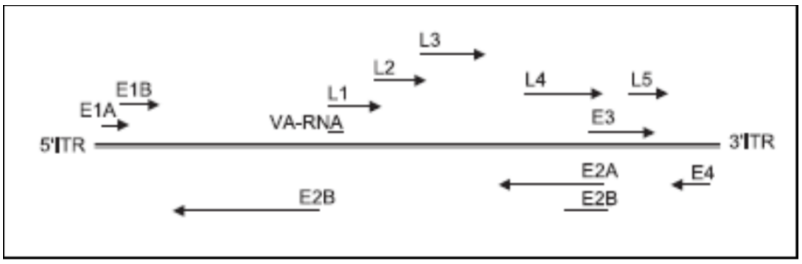

Figure 2.8: Adenovirus genome organisation. The different transcription units and the direction of transcription are shown (Tatsis and Ertl, 2004).

2.5.2.2 Adenovirus vectors in vaccination

Human adenoviruses ADVs have been demonstrated to be suitable recombinant vaccine vectors due to their ability to efficiently infect a wide variety of cell types. To grow to high titres *in vitro* they have high levels of transgene expression, and there is a lack of integration in the host genome as well as genetic stability (Robert-Guroff, 2007; Zhang *et al.*, 2017; Lasswitz *et al.*, 2018; Ma and Guan, 2018). More than 50 human Adenovirus serotypes have been identified, but most of the recombinant Adenoviral vectors are based on serotypes 2 (Ad2) and 5 (Ad5) (Schmitz *et al.*, 1983; Lasswitz *et al.*, 2018).

For vaccination purposes, most ADV vectors are deleted in the E1 or E3 regions and are replaced with antigenic gene targets (Gao *et al.*, 2006; Jones *et al.*, 2011; Silva *et al.*, 2016; Ma and Guan, 2018). Viral vectors with the deleted E1 gene are replication defective and such recombinant viral vectors with foreign genes inserted in the E1 region can only be produced in cells that are lined with constitutively expressed E1 proteins, such as human embryonic kidney (HEK) 293 cells (Graham *et al.*, 1977; Kamen and Henry, 2004; Silva *et al.*, 2010; Silva *et al.*, 2016; Ma and Guan, 2018) and PerC6 cells (Fallaux, 1998). Viral vectors with E3 deletion may affect these vectors'

interaction with the host's immune system. Reports have shown that these recombinant vectors induce both neutralizing antibodies and cell-mediated immunity in animals (Gao *et al.*, 2006; Hoelscher *et al.*, 2007; Jones *et al.*, 2011; Gabitzsch *et al.*, 2011). It is because of these characteristics that the Ad5-nCoV Adenovirus based vaccine against the COVID-19 disease is already undergoing clinical trials (Al-Rohaimi and Al-Otaibi, 2020). The E1-deleted Adenoviral vectors are usually constructed using the Lambda (λ) bacteriophage homologous recombination technology.

2.5.2.3 Lambda (λ) homologous recombination

Bacteriophages are viruses that infect bacteria. These viruses are the majority of viruses in general and they have also been shown to outnumber bacteria by approximately 10:1 (Hambly and Suttle, 2005). Once they have infected their host, most bacteriophages undergo the lytic life cycle where they take over the host's molecular machinery by rapid replication and dissemination (Fogg *et al.*, 2014). Under certain conditions, bacteriophages can integrate their genome into the host's genome and stay dormant until they are stimulated to enter the lytic life cycle (Ptashne, 2004). A classic example is the integration of the circular bacteriophage Lambda (λ) genome into the *Escherichia coli* (*E.coli*) chromosome (Campbell, 1962; Ptashne, 1992; Hartley *et al.*, 2000; Walhout *et al.*, 2000). First, the λ bacteriophage recognises a specific attachment (att) site such as the attB site found in the *E.coli* bacterial chromosome. The attB site recombines with the λ bacteriophage attachment site (attP), thus giving rise to an integrated prophage flanked by two hybrid sites, the attL (on the left site) and the attR (on the right site). This process is illustrated in Figure 2.9.

The integrated prophage is therefore made up of one site from the attB (bacteria) and the other site from the attP (phage). This reaction is catalysed by an integrase (Int) encoded by the λ bacteriophage. In some instances, a reverse reaction, in which attL and attR recombine to reform attB and attP, can occur. This reverse reaction is catalysed by the Int and Excision (Xis) proteins (Landy, 1989; Ptashne, 1992; Hartley *et al.*, 2000; Fogg *et al.*, 2014). This reaction is also shown in Figure 2.9.

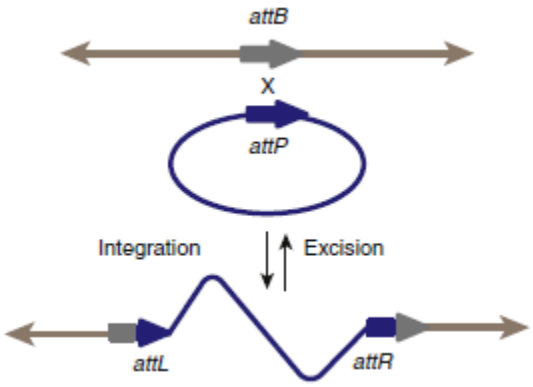

Figure 2.9: The integration of the bacteriophage Lambda (λ) genome into the *Escherichia coli* (*E.coli*) chromosome (Fogg *et al.*, 2014). Lambda (λ) genome is represented by a blue circle, while the *E.coli* is represented by a dark grey arrow.

The most widely used λ-based recombination system is the Gateway® cloning system (Life Technologies (Pty) Ltd, California). The Gateway® technology has two types of recombination strategies, namely the BP and the LR recombination strategies. For the purpose of this study, the focus was on the LR recombination reaction. Generally, to improve the LR recombination strategy, the wild type λ attL and attR recombination sites are modified. First, mutations are introduced to the core regions of the att sites in order to remove stop codons and to make sure that the recombination reactions are specific and also to restore the orientation as well as the reading frame. Secondly, a part of the attR is eliminated to ensure that the *in vitro* attL and attR reaction is not reversible. The LR recombination reaction is then catalysed by the LR CLONASE enzyme mix which is made up of the λ recombination proteins Int, Xis and the IHF protein which is encoded by the *E. coli*. The LR recombination starts when the recombination proteins cut the attL sites positioned on the left and right sites of the gene of interest in the entry clone. This is followed by the ligation of the gene to the compatible attR sites in the destination vector. The attL1 and attR1 or attL2 and attR2 recombine and thus produce a co-integrate. A second recombination is then performed using the co-integrate to produce two daughter molecules which have the same structure regardless of which pair of sites (attL1 and attR1 or attL2 and attR2) reacts first in forming the co-integration. The final product is the expression clone which is transformed in the *E. coli* cells. It is only the plasmids that do not contain the ccdB gene that form colonies on a selective media containing the antibiotic ampicillin. This process is illustrated in Figure 2.10.

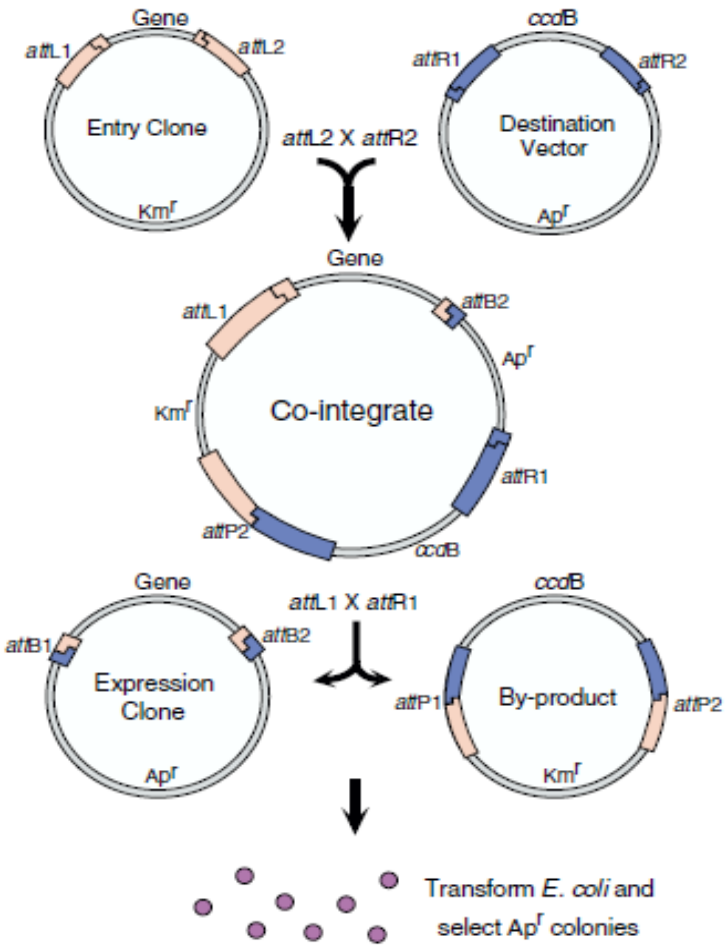

Figure 2.10: The LR recombination reaction using the Gateway® cloning system (Life Technologies Ltd, California)

2.6 Problem Statement

Poultry production has increasingly been recognised as one of the solutions for problems such as malnutrition, food insecurity, low income, and poverty (Pitt *et al.*, 2003; Gawande *et al.*, 2007; Fasina *et al.*, 2007; Dei *et al.*, 2009). However, HPAI virus outbreaks usually cause significant economic losses to the poultry industry worldwide, and this impacts hunger alleviation (Alexander *et al.*, 2006; FAO, 2011; Li *et al.*, 2018; Charlton, 2018; Chatziprodromidou *et al.*, 2018; Kim *et al.*, 2019; Scott *et al.*, 2020; Song *et al.*, 2020; Almayahi *et al.*, 2020). Certain types of HPAI viruses are known to cause human pandemics (Lin *et al.*, 2000; Fouchier *et al.*, 2004; Hirst *et al.*, 2004; Chen *et al.*, 2013; Bomfanti *et al.*, 2014; Gao *et al.*, 2018; Kwok-Yung, 2018; Xue-Cheng *et al.*, 2018; Chatziprodromidou et al., 2018; Shi *et al.*, 2019; Koutsakos *et al.*, 2019; Almayahi *et al.*, 2020; Tahir *et al.*, 2020). Conventional methods for HPAI virus detection and characterisation involve virus isolation in embryonated chicken eggs and molecular techniques such as real-time

reverse transcriptase PCR (rtRT-PCR) (Lee and Suarez, 2004; Ng *et al.*, 2005; Payungporn *et al.*, 2006; Liu *et al.*, 2018; Zhang *et al.*, 2018; Shi *et al.,* 2019; Kim *et al.*, 2019) and nucleic acid sequencing, as illustrated in Figure 2.11. HPAI virus isolation and characterisation usually take a minimum of 5 days when performed by an experienced technician, while the resultant virus identification can be performed within 1-2 days. These extended time periods that are required to isolate and characterise the virus result in delays in the control and management of AI virus outbreaks. A rapid and cost-effective diagnostic protocol for the early detection of these viruses is thus urgently needed for outbreak management. The best approach for this would be to develop a point-of-contact diagnostic method that can detect viruses in the environment where these viruses exist rather than collecting and transporting samples to a central laboratory. However, available POC methods have low sensitivity and often give false negative results (Woolcock and Cardona, 2005; Chua *et al.*, 2007; Yu *et al.*, 2017; Sharma *et al.*, 2018).

OIE is an organisation that is responsible for fighting animal diseases at a global scale by reporting detected animal diseases and spreading suitable information to other countries that should then take appropriate preventative action (OIE, 2003). The OIE thus categorises HPAI viruses as part of List A diseases. List A diseases are transmissible and have the potential for very serious and rapid spread (OIE, 2017c; Chatziprodromidou *et al.*, 2018; Tahir *et al.*, 2020). HPAI viruses are also categorised as List A diseases because they are associated with systemic infections that often result in high mortality and morbidity (Swayne and Halvorson, 2003).This means that the only accepted control measure for such diseases is the ‘stamping out’ procedure accompanied by strict restrictions in the movement of poultry, personnel, and other activities within a quarantined area (Capua and Marangon, 2003; Akey, 2003; Capua and Marangon, 2006; Scott *et al.*, 2020). In areas with high poultry density, however, these strict control procedures may not be enough or applicable to prevent the virus from spreading (Pavade *et al*, 2011).

Vaccination has been successfully used previously as an additional tool in the control of AI outbreaks (Webster and Govorkova, 2014). The DALRRD, which is responsible for animal disease control and management in South Africa, has a policy of no avian influenza vaccination (DAFF, 2017). Stamping out infected poultry has always been the preferred method for the control and eradication of this disease. The reasoning behind this is that AI vaccinated animals with standard vaccines test seropositive, and this interferes with the surveillance required to declare a region AI free (Webster and Govorkova, 2014). As a disease that is A listed by the OIE, HPAI outbreaks cause serious economic losses not only because the animals die or are culled, but also because countries may then place an export/import ban on any poultry products. Another challenge linked to AI vaccination using standard methods is that it takes as long as 6 to 8 months from the identification of the viral strain to the release of the vaccine when using the simplified

workflow as illustrated in Figure 2.11 (GAO, 2000; Webster and Govorkova, 2014). Adenovirus vector-based vaccines have been shown to allow differentiation between infected and vaccinated animals, referred to as 'DIVA' (Capua *et al*, 2003; Toro and Tang, 2009; Baron *et al.*, 2018), and it has been argued that they can significantly speed up vaccine production in comparison to egg-based methods. Considering the scenario described above, it is evident that an efficient strategy with better turnaround times is required to control and manage avian influenza outbreaks and other similar viral outbreaks in livestock and poultry.

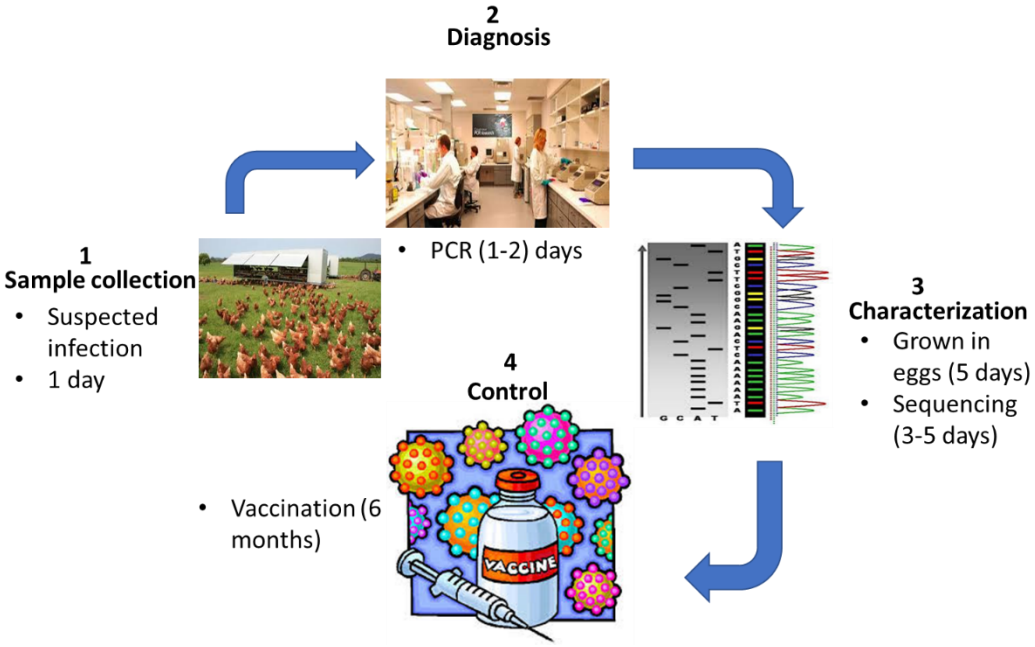

Figure 2.11: Conventional strategy and workflow for avian influenza outbreak management and vaccine production

2.7 Hypothesis

Adenovirus vector-based vaccines, in combination with LAMP as a point-of-care diagnostic tool, can be used as drivers of a speedy model to arrest the spread of AI or other contagious livestock/poultry diseases caused by viruses.

2.8 Aims and Objectives

2.8.1 Aims

The aim of this study was two-fold:

1. The first aim of the study was to develop a reverse transcriptase real-time LAMP (RT-LAMP) assay for the detection of AI viruses at the POC.

2. Secondly, the study aimed to develop a non-replicative Adenovirus vector-based vaccine for the control of AI.

2.8.2 Objectives

The objectives of this study were to address the following two distinct phases:

Phase I: Proof of concept study focusing on the functionality of the LAMP assay in a laboratory setting, with the following specific objectives:

- Design of primers specific for the detection of AI viruses H5 and H7 subtypes.
- Assessment of the appropriate starting template material for determination of specificity of AI LAMP, specifically Influenza A, H5 and H7 subtypes.
- Determination of LAMP sensitivity compared to the gold standard for molecular detection real-time PCR.

Phase II: The validation of the T16, a custom-engineered, portable, isothermal device designed by Axxin (Pty) Ltd for the amplification and detection of AI in the field/POC.

A proof-of-concept study would also be conducted to determine whether the Adenovirus-based vaccine can be expressed *in vitro* in CEFs, with the specific objectives being:

- Preparation of fibroblasts from a chicken embryo.
- Propagation of the Adenovirus vector (pAd/CMV/V5-GW/lacZ control plasmid) in 293T cells.
- Assessment of the expression of the non-replicative Adenovirus vector (pAd/CMV/V5-GW/lacZ control plasmid) in CEFs using western blot analysis.
- Creating the Adenoviral expression clone containing the gene of interest by performing an LR recombination using the attL-containing entry clone and the attR-containing pAd/CMV/V5-DEST^{TM}.
- Assessing the expression of the designed recombinant Adenovirus vector in CEFs.

CHAPTER 3

MATERIALS AND METHODS

3.1 Introduction

Successful eradication of animal diseases requires the best detection method in combination with the application of an effective vaccine that can protect susceptible animals within the affected region. This chapter details the protocols that were developed and designed as the potential workflow to manage and control contagious, virus-caused animal diseases using AI as an example. The methods developed are meant to fit within a specific single workflow, ranging from pathogen detection, vaccine design, a vaccine production method development, to *in vitro* vaccine functionality testing. The detection protocols are detailed in sections 3.3 and 3.4, while the vaccine development and testing methods are described in sections 3.5, 3.6, and 3.7. The workflow diagram (Figure 3.1) below is a summary of the proposed protocols that should be followed to manage and control AI. According to the DALRRD vaccination against avian influenza is prohibited in South Africa. The reasons for this are that it is often impossible to differentiate between vaccinated and infected birds and that non-infected vaccinated birds always test AI positive. If this policy did not exist, an Adenovirus vector-based vaccine expressing the AI Matrix gene would have been developed and tested *in vitro* for functionality according to the initial plan. However, to abide by this law, an alternative recombinant Adenovirus vector expressing the Newcastle disease virus (NCDV) Matrix gene was developed and tested *in vitro* for functionality. The NCDV was chosen as this virus is closely related to AI, infects poultry just like AI does, and also causes similar symptoms to those caused by AI in poultry (Miller and Torchetti, 2014; Shekaili *et al.*, 2015; Bertran *et al.*, 2017). The NCDV vaccine was thus used as proof of concept that the same method can be used to develop avian influenza vaccines and that they also work in a similar way. Because Adenovirus-based vaccines allow differentiation of infected animals from vaccinated ones (Capua *et al.*, 2003; Toro and Tang, 2009; Baron *et al.*, 2018), which is a feature that AI vaccines in the market currently do not have, successful results in this study might encourage DALRRD to amend the policy and allow vaccination against AI. This will undeniably ensure a quicker turnaround time for the control of AI.

3.2 Workflow

Figure 3.1 is a diagrammatic presentation of the workflow plan that was devised in order to follow the correct protocol.

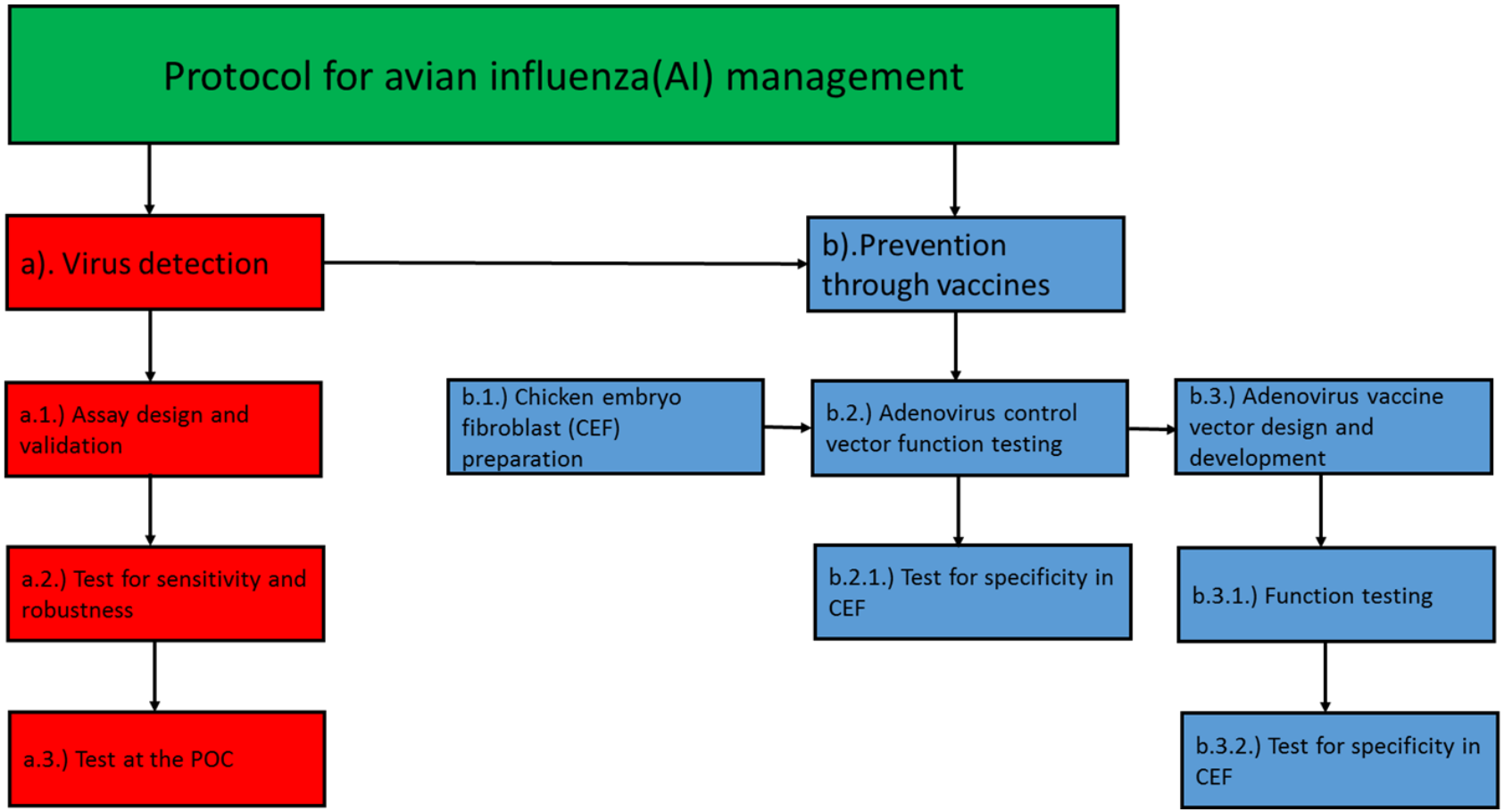

Figure 3.1: Workflow showing the protocol that was followed in this study for AI detection and its possible prevention

3.3 Point-of-care (POC) Diagnosis of Avian Influenza (AI) Using Loop-Mediated Isothermal Amplification (LAMP).

The protocols of methods summarised in Figure 3.1 are presented in detail in the following sections.

3.3.1 Primer design

LAMP primers were designed specifically for the detection of a highly conserved region of the Matrix gene across all the AI viruses for specific detection of HPAI. The specific HPAIs in this case were the H5 and H7 serotypes. To achieve specific detection for the Matrix gene across AI serotypes, sets of primers were designed on conserved sequence regions. The conserved sequences were selected by sequence comparison and alignment of 27 Matrix genes: 12 for H5 subtypes and 5 for H7 subtypes from South African AI viruses retrieved from the Influenza Research Database (http:www.fludb.org/). Due to large sequence variations within the Matrix genes across the serotypes, for each serotype the region that exhibited conserved regions after alignment across various serotypes was uploaded into the LAMP primer explorer (http:primerexplorer/jp/e/). Primer sets for the LAMP, comprising of two inner primers, a forward inner primer (FIP), a backward inner primer (BIP), two outer primers (F3 and B3), and two loop primers (FL and BL) were designed accordingly. Non-specific primers were checked by using the BLAST program (http://blast/ncbi.nlm.nih/gov/blast.cgi). The primer sets that showed minor non-specificities were chosen. The primers were then chemically synthesised through Integrated DNA technologies (IDT) contract services. The chosen primers were then tested for specificity and functionality using PCR methodology. The samples used for this purpose are listed in Table 3.1 below.

3.3.2 Confirming the status of the viruses

The viruses listed in Table 3.1 were purchased from Dr G. Gittoli of the Instituto Zooprofilattico Sperimantale delle Venezie (IZSV) in Italy in a lyophilized deactivated antigen form. The samples were dissolved in 500µL Phosphate-buffered saline (PBS) (Lonza, Belgium). Viral RNA was extracted using the QIAamp® viral RNA mini kit (QIAGEN Ltd, Valencia, CA, USA) according to the manufacturer's instructions. Briefly, the 140µL aliquot of each sample was incubated with the QIAGEN lysis buffer and carrier RNA for 10 minutes at room temperature.

The lysates were each applied to a QIAamp mini column, washed twice with the wash buffers, and eluted in 60µL QIAGEN elution buffer. The RNA was quantified using the Qubit® 2.0

Fluorometer (Life Technologies, Singapore) and Qubit™ high sensitivity kit (Life Technologies, USA).

Table 3.1: ISZVe AI viruses used to test the B3/F3 and F2/B2 LAMP primers using the PCR method

Sample	Lab-Labelling
HP-H5N2 (11060333C)	A
LP-H5N2 (12060229)	B
LP-H7N1(12080123A)	C

The cDNA for each sample was synthesised using the Transcriptor strand cDNA synthesis kit (Roche Applied Science, Mannheim, Germany) according to the manufacturer's instructions. Briefly, total RNA, 60µM of the provided random hexamer primer, nuclease free water, 1 x Transcriptor reverse transcriptase reaction buffer, 20U of protector RNASE inhibitor, 1mM of each deoxynucleotide mix, and 10U of Transcriptor reverse transcriptase were mixed in a reaction tube per sample to make a final volume of 20µL. The reaction tubes were incubated at 25°C for 10 min, 55°C for 30 min, and 85°C for 5 min using the BIO-RAD T100 thermocycler (BIO-RAD, USA). The cDNA was stored at -20°C for longer storage.

As an initial step, the three Italian AI viruses listed in Table 3.1 were tested to confirm whether they were avian or not using the OIE approved AI PCR detection primers. The 20µL PCR mixture was prepared by mixing 10µL of the 2x BIO-RAD SYBR green master mix, 0.8µM of the forward primer (5'-AGATGAGTCTTCTAACCGAGGTCG-3'), 0.8µM of the reverse primer (5'-TGCAAAAACATCTTCAAGTCTCTG-3'), and 4.4µL of the nuclease free water. Table 3.2 below shows the PCR cycling programme that was followed for this PCR.

Table 3.2: PCR cycling programme used for the reaction in section 3.3.2.

Steps	Temperature	Time (seconds)	Cycles
Activation	95ºC	30s	1
Denaturation	95ºC	5s	45
Annealing	53ºC	10s	
Extension	60ºC	10s	

3.3.3 Testing the functionality of the LAMP primers

Different sets of the LAMP primers were generated as discussed in section 3.3.1. In order to check whether the designed LAMP primers would work in the LAMP assay, these primers were tested using the same PCR mixture and the PCR cycling programme a described in section 3.3.2. Annealing occurred at a low temperature of 53ºC because the LAMP primers were not necessarily perfect primers for PCR. However, the PCR cycling was used to control for complementarity rather than full fidelity or specificity. The only changes made were the sets of primers used. The sets that were used are as follows: Set 1A: forward primer (F2) and backward primer (B2). Set 2A: forward primer for segment 7 (F2) and backward primer for segment 7 (B2). Set 1B: forward primer (F3) and backward primer (B3). Set 2B: forward primer for segment 7 (F3) and backward primer for segment 7 (B3). The primer sets that showed minor or non-specificities were selected for use in the LAMP assays.

3.4 Development and optimisation of the LAMP method

3.4.1 Testing of the avian influenza RNA samples using the Matrix specific LAMP detection assay

The viruses listed in Table 3.3 were donated by Dr M. Iqbal from the Pirbright World Reference Laboratory in the UK while some were purchased through Dr G. Gittoli from the Instituto Zooprofilattico Sperimantale delle Venezie in Italy in a lyophilized deactivated antigen form. The samples were processed, and RNA was extracted following the same methods described in section 3.3.2.

Table 3.3: Avian Influenza viral samples and a Newcastle viral sample used to validate the LAMP detection assay

SAMPLE	Numbering
H5N1 inactivated antigen: ANHUI/1/2005 (H5N1) IBCDC - RG-6 07/290	1
H5N1 inactivated antigen: A/Cambodia/R040505/2007 (H5N1) NIBRG-88	2
H5N1 A/mallard/Italy/3401/05	3
H5N1 A/turkey/Turkey/1/05	4
H5N2 A/turkey/Italy/80	5
H5N2 A/turkey/Italy/1258/V05	6
H5N3 A/duck/Italy/775/04	7
H5N9 A/chicken/Italy/22A/98	9
H6N8 A/turkey/Italy/4776-52/2015	10
H7N1 inactivated antigen: AV98/00 984v00/OST/ITALY P2	11
H7N9 inactivated antigen: A/Anhui/1/2013 (H7N9) (NIBRG-268)	12
H7N1 A/turkey/Italy/1067/99	13
H7N1 A/starling/Africa/983/79	14
H7N3 A/turkey/Italy/9289/02	15
H7N4 A/mallard/Italy/4810-79/04	16
H7N7 A/macaw/England/626/80	17
H8N4 A/turkey/Ontario/6118/68	18
H9N2 A/mallard/Italy73817-34/05	19
A/Turkey/Canada H6N8 NOV84	20
A/Chick/Scotland/59 H5N1 A/S 7/89	21
NCDV	22

The Matrix gene-specific LAMP was carried out in a 25µL reaction mixture containing 1.6µM of FIP and 1.6µM of BIP, 0.8µM of FL and 0.8µM of BL, 0.2µM of F3 and 0.2µM of B3, 400µM of dNTP (Thermo Scientific, EU, Lithuania), 1x LAMP buffer (Lucigen, Middleton, WI), 8U of BST DNA polymerase (Lucigen, Middleton, WI), 40U of reverse transcriptase k (Roche Applied Science, Mannheim, Germany), 0.8M betaine (Sigma, England), RNA template, and nuclease free water (Ambion, USA). The reaction was incubated at 65°C for 30 min in the Roche light cycler. To confirm amplification, 10µL of the LAMP products was resolved on a 1% agarose (Whitehead Scientific (Pty) Ltd, USA) gel electrophoresis stained with ethidium bromide.

3.4.2 Selecting the best template starting material for the LAMP assay

To determine the best template for virus detection using LAMP, the RNA templates were compared with two cDNA templates synthesised in two different ways. The two different cDNAs were synthesised using the three virus samples indicated as sample 1, sample 2 and sample 3 in Table 3.3 and the Transcriptor strand cDNA synthesis kit following the same method as described in section 3.3.2. The first template cDNA was synthesised using 60µM random

hexamer primer while the second template cDNA was synthesised using 60µM of F3 and B3 LAMP primers. The actual method of synthesis was as described in section 3.3.2.

For testing purposes, three different starting materials were utilised, namely RNA, random hexamer cDNA, and specific F3/B3 cDNA which were respectively aliquoted in equivalent molar concentrations. LAMP was carried out in a total of 25µL reaction mixture containing FIP and BIP (1.6µM each), FL and BL (0.8µM each), F3 and B3 (0.2µM each), and 400µM of dNTP (Thermo Scientific, EU, Lithuania), 1x LAMP buffer (Lucigen, Middleton, WI), 8U of BST DNA polymerase (Lucigen, Middleton, WI), 40U of reverse transcriptase k (Roche Applied Science, Mannheim, Germany), 0.8M betaine (Sigma, England), RNA or Random primer cDNA or F3 and B3 cDNA as templates, 2µL of 1:1000 SYBR® green (Invitrogen, USA), and nuclease free water (Ambion, USA). The reaction was incubated at 65°C for 30min in the ROCHE lightCycler® 96 (Thermofisher, USA). The results were viewed using the standard Roche lightCycler software by plotting fluorescence against the number of cycles at excitation wavelength 430nm and emission fluorescence intensity at 560nm. To confirm real-time amplification graphs, 10µL of the LAMP products was resolved on a 1% agarose (Whitehead Scientific (Pty) Ltd, USA) gel electrophoresis. The best template in terms of the quality of results and in improving the LAMP sensitivity was the cDNA synthesised with the F3 and B3 primers. All the LAMP assays that were performed after this experiment were conducted using cDNA synthesised with the F3 and B3 primers as a template. To test all the AI samples (see Table 3.3) using the best template, the LAMP assays specific for the Matrix gene H5 and H7 subtypes were performed following the same method as described in section 3.4.1.

3.4.3 Verification of LAMP assay non-detected samples using the OIE approved AI detection method

None of the three LAMP assays could detect the AI viruses in samples 12, 20 and 21 (Table 3.3). Therefore, the OIE approved AI RT-PCR detection method was used to verify if these samples were false negatives or genuine non-avian influenza specimens. These three samples were tested together with sample 1 as a positive control (Table 3.3). The RT-PCR mixture contained 10µL of the ROCHE probe master (ROCHE Applied Science, Mannheim, Germany), 0.8µM of the forward primer (5'-AGATGAGTCTTCTAACCGAGGTCG-3'), 0.8µM of the reverse primer (TGCAAAAACATCTTCAAGTCTCTG-3'), and the Taqman probe (5, -/56-FAM/TCAGGCCCCCTCAAAGCCGA/36-TAMSp/-3'). Four microlitres of cDNA and 3.6µL of nuclease free water (Ambion, USA) were also added to the mixture. The thermocycling program using the ROCHE lightCycler® 96 (Thermofisher, USA) was as follows: Pre-incubation was done

at 95°C for 600s, followed by 45 cycles at 95°C for 10s, and at 54°C for 45s. The cooling cycle was then done for 30s at 37ºC.

3.4.4 LAMP vs PCR sensitivity

The results of this part of the experiment are shown in a.2 (Figure 3.1) of the overall workflow of protocols that were used in this study. To determine the sensitivity of the RT-LAMP assay, sample 4 (Table 3.3) was randomly chosen. To proceed, 10-fold serial dilutions of the cDNA of this sample were prepared using nuclease free water (Ambion, USA). Each dilution was tested using both LAMP and RT-PCR by detecting the Matrix gene. All dilutions were tested in duplicate for confirmation of results. The LAMP assay was performed following the same method as described in section 3.4.1.

The RT-PCR mixture contained 10µL of 1x SsoFast Evagreen® supermix master mix (BIO-RAD, Hercules, CA), 0.8µM of B3 and 0.8µM of F3, LAMP primers that can also be used as two Forward and Reverse conventional primers for PCR, 4µL of cDNA, and 3.6µL of nuclease free water (Ambion, USA).

The thermocycling program using the BIO-RAD T100 thermocycler (BIO-RAD, USA) was as follows: Pre-incubation was done at 95°C for 30s, followed by 45 cycles at 95°C for 10s, at 53°C for 10s, and at 60°C for 40s.

3.4.5 The application of LAMP at the POC using the T16 Axxin isothermal Instrument

The overall design of the POC assay system included validation of the Axxin T16 isothermal instrument (Axxin (Pty) Ltd) (Figure 3.2). This part of the protocol workflow of the study (Figure 3.1) is shown in section a.3. This instrument is affordable, portable, uses rechargeable batteries and thus consumes little power, is sensitive, and can read three fluorescent signals simultaneously for real-time detection. These features make it ideal for POC diagnosis of AI viruses.

Figure 3.2: The Axxin T16 isothermal instrument with 16 positions for loading tubes with samples and a touch result screen for real-time monitoring

The LAMP assays were tested and validated in the laboratory using the T16 instrument in field conditions. The LAMP device has a Wifi functionality which pairs it with a mobile phone whenever a POC test is being conducted. The mobile phone is also connected to a server in the laboratory where data of all the tests that are being conducted in the field are saved and analysed by the laboratory analyst (see Figure 3.3).

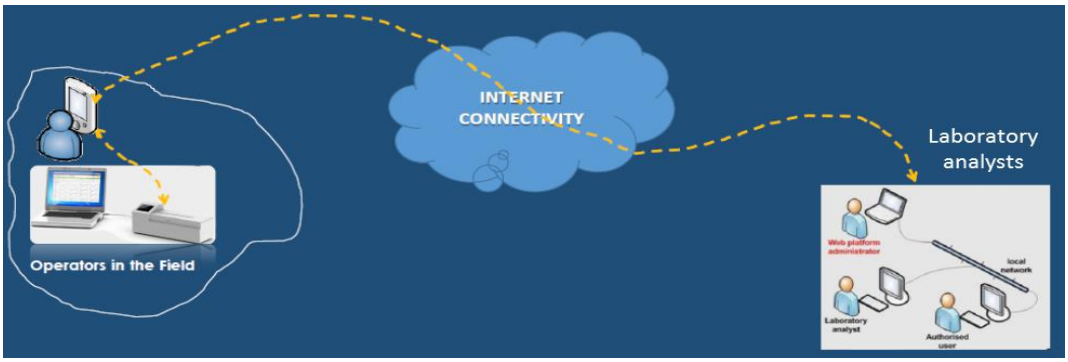

Figure 3.3: Illustration of the test operator conducting tests in the field using the Axxin T16 LAMP device connected to a mobile phone via Wifi

3.5 Adenovirus vector-based vaccine development for avian influenza

This section describes the preparation of chicken embryo fibroblasts (CEF). The aim of the investigations that is described in this section is summarised in b.1 in the protocol workflow (Figure 3.1).

3.5.1 Fertilised egg incubation

All the experimental protocols involving the egg embryo were approved by the Research Ethics Committee of the Council for Scientific and Industrial Research (CSIR) (Approval number: 73/2013).

A freshly laid fertilised egg was sterilised using 70% ethanol and incubated for 11 days at 37ºC in a humid incubator. The egg was turned at least twice daily. The embryonic development was followed by daily candling the egg using a torchlight.

3.5.2 Technical CEF preparation

All solutions for this experiment were pre-warmed in a 37ºC water bath to preserve the normal functioning of the embryo fibroblasts. The egg was candled, checked for abnormalities, and sterilised using 70% ethanol. It was then placed on a rack with the pointed end facing downwards. The wide end of the egg was cracked open and the shell removed as shown in Figure 3.4, step 1. The egg contents were poured into a sterile petri-dish that contained PBS (Lonza, 17-516F) as shown in Figure 3.4, step 2. Figure 3.4, step 3 shows the stage when the embryo was separated from the egg contents and transferred into another sterile petri-dish containing PBS, followed by removal of the embryo head with an incision close to the body as well as complete removal of the limbs. The body of the embryo was placed into another sterile petri-dish with 20mL PBS (Figure 3.4, step 4). The body was minced using a blade and scissors (Figure 3.4, steps 5 and 6). The minced embryo body was transferred into a 50mL glass beaker containing a magnetic stirrer bar in PBS solution and the 50mL beaker was subsequently placed on a 37ºC heating block. The contents was mixed slowly at 40 rpm for 5 min to avoid shearing the newly released embryogenic contents. The supernatant containing cell debris was discarded, and 20mL PBS was added to the pellet and mixed for 5 min on a heating block set at 40 rpm at 37ºC. The supernatant was decanted and 20mL Trypsin-EDTA (Gibco, 25200-072) was added to the pellet to digest the cell membranes and therefore release individual cells.

The resulting mixture was mixed at 40 rpm for 25 min at 37ºC (Figure 3.4, step 7). The supernatant was mixed with 20mL Dulbecco's Modified Eagle Medium (DMEM) (Lonza, BE12-614F)

containing 10% foetal bovine serum (FBS) (Gibco, 10100147) and 0.05 mg Gentamicin (Lonza, 17-519Z). This preparation was centrifuged at 1106xg for 10 min. Such a mixture is referred to as full medium. The supernatant was discarded, and the pellet was resuspended in full media and finally transferred to a tissue culture flask. The cells were then incubated at 37ºC in a 5% CO_2 incubator with set humidity. After 24 hours, the original full medium was removed, the cells were rinsed with PBS, and fresh full medium was added. The cells were left to divide, and by the third passage, images of the cells were taken under an OLYMPUS (BX53) microscope using a phase contrast at 10x magnification.

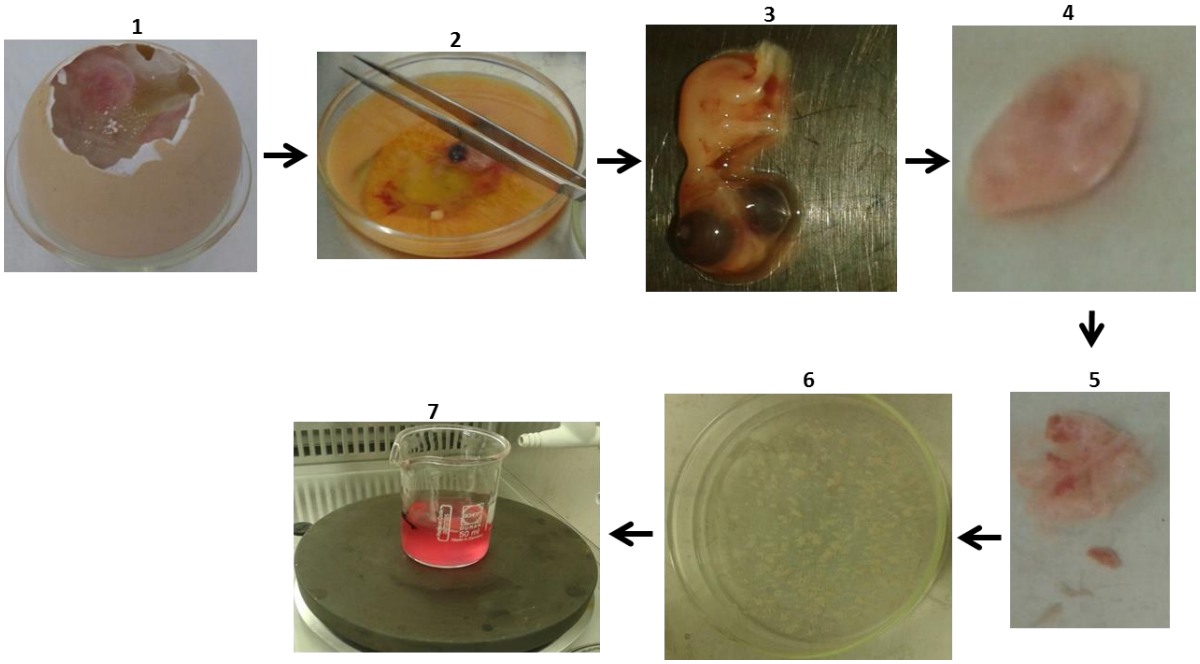

Figure 3.4: Preparation of chicken embryo fibroblasts (CEFs) from an 11-day-old chicken embryo. 3.4.1: The egg is cracked open. 3.4.2: The egg contents poured into a sterile glass petri-dish. 3.4.3: The PBS rinsed embryo transferred into a sterile glass petri-dish with PBS. 3.4.4: The body of the embryo with the head and limbs removed. 3.4.5: The embryo body minced with scissors and a blade in PBS. 3.4.6: The embryo body completely minced. 3.4.7: The minced embryo body digestion in Trypsin-EDTA.

3.5.3 Assessing the expression of the non-replicative Adenovirus vector (pAd/CMV/V5-GW/lacZ control plasmid) (Life Technologies, K4930-00) in chicken embryo fibroblasts

3.5.3.1 Amplification of the Adenovirus vector pAd/CMV/V5-GW/lacZ control plasmid in 293T cells

The Life Technologies replication deficient Adenoviral vector pAd/CMV/V5-GW/lacZ control plasmid (Figure 3.5) that was used in this part of the study was a gift from colleagues at Plymouth University, UK. About 1 x 10^6 293T cells were seeded per well in a six-well plate with 2mL DMEM supplemented with 10% FBS and 0.05mg Gentamicin. Once the cells were approximately 60-70% confluent, the spent medium was removed. The cells were rinsed three times with PBS, and then 100µL of the Adenoviral vector stock was mixed with 0.5mL DMEM containing 10% FBS. This mixture was added to the cells and incubated at 37ºC in a 5% CO_2 incubator for 1-2 hours before adding another 1.5mL of DMEM containing 10% FBS to allow attachment to the plate surface. The viral medium was removed and replaced with fresh medium after incubation for 24 hours. Once a complete cytopathic effect (CPE) characterised by rounding off of cells accompanied by cell detachment from plate surface had been reached, both the medium and the cells were collected into a 15mL conical tube and centrifuged in a table-top centrifuge at 1106xg for 15 min at room temperature. The supernatant containing the viral particles was transferred to cryovials in 1mL aliquots and stored at -80ºC. The cell pellets were subsequently used for the assessment of protein expression.

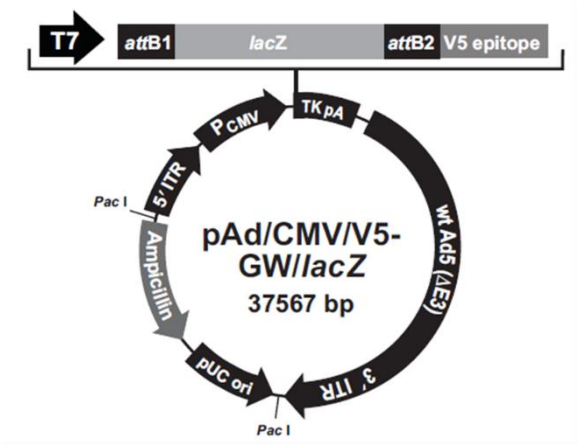

Figure 3.5: Adenovirus vector (pAd/CMV/V5-GW/lacZ control plasmid) (Life Technologies, K4930-00) used in this study. This vector was first amplified in 293T cells before expressing infecting chicken embryo fibroblasts and Vero cells. Human Ad5 sequences (wt 1-458; includes 5' L-ITR and packaging signal): 1-458, pAd forward priming site: bases 361-384, CMV promoter: bases 728-1315, T7 promoter/priming site: bases 1359-1378, *att*R1 site bases: 1407-1531, *cc*dB gene: bases 1960-2265 (C), Chloramphenicol resistance gene (Cm^R): bases 2607-3266 (C), *att*R2 site: bases 3547-3671, V5 epitope: bases 3697-3738, TK polyadenylation signal: bases 3765-4036, human Ad5 sequence(wt 3513-35935; E3 region deleted, includes 3' R-ITR): bases 4056-34604, pAd reverse priming site: bases 4059-4082, pUC origin: bases 34781-35442 (C), Ampicillin (*bla*) resistance gene: bases 35568-36428 (C), *bla* promoter: bases 36429-36527 (C), *Pac* I restriction sites: bases 34610 and 36684, (C) = complementary strand.

3.5.3.2 Extraction of the Adenovirus DNA from the supernatant

The Adenovirus DNA was extracted from the supernatant that had been prepared as described in section 3.5.3.1. The extraction was done using the PureLink® viral RNA/DNA kit (Life Technologies, 12280-050) according to the manufacturer's instructions. Briefly, 200µL of the supernatant was lysed in a lysis buffer containing 25µL proteinase K and 5.6µg carrier RNA. This was mixed by vortexing for 15 s and incubated at 56ºC for 15 min. Exactly 250µL of 100% ethanol was added to the lysate and mixed by vortexing for 15 s to precipitate the exposed nucleic acids after lysis. The lysate was incubated for 5 min at room temperature. This was followed by centrifugation using the viral spin column at 6800xg for 1 min. The column was rinsed twice with 500µL wash buffer and the DNA eluted in 20µL sterile RNase free water. The DNA was stored at -80ºC.

3.5.3.3 Confirmation of the presence of the Adenovirus DNA in the crude virus supernatant using PCR

This test was done using the KAPA HIFI hotstart ready mix PCR kit (KAPA BIOSYSTEMS, KK2601) according to the manufacturer's instructions. The PCR mixture contained 12.5µL of 2x KAPA HIFI hotstart ready mix, 0.6µM each of forward (5'-TAATACGACTCACTATAGGG-3') and reverse (5'-ACCGAGGAGAGGGTTAGGGAT-3') primers, and 11µL of DNA. The thermocycling program was performed using the Roche LightCycler® 96 as follows: Pre-incubation at 95°C for 180 s, followed by 25 cycles at 98°C for 20 s (denaturation), at 47°C for 15 s (annealing), and at 72°C for 15 s (extension). Lastly, the final extension step was performed at 72ºC for 60 s. Then 10µL of the PCR products was resolved using 1% agarose (Whitehead Scientific (Pty) Ltd, USA) gel electrophoresis to confirm the presence of amplification product.

3.5.4 Whole protein extraction from the cell pellet

About 430µL of lysis buffer consisting of 1M Tris, 0.5M EDTA, 1M KCL, 0.5% Triton x 100 and 1 x protease inhibitor in distilled water was added to the 293T cells infected with the Adenovirus vector and to 293T non-infected cells that were to act as the control. The cells were rotated at 45 rpm for 25 min at room temperature. This was followed by centrifugation at 10 285xg for 10 min at 4ºC. The supernatant was taken and centrifuged at 15 641xg for 10 min at 4ºC. The supernatant contained whole cell protein that was stored at -70ºC until it was required for western blot analysis.

3.5.4.1 Adenovirus vector expression assessment using western blot analysis

For this part of the experiments, protein concentrations were not determined, but different volumes of the protein (10µL, 5µL, 2µL, and 1µL) of the Adenovirus infected 293T cell protein and 5µL of the non-infected 293T cell protein were separated by SDS-PAGE on Bolt™ 4-12% Bis-Tris Plus gels (Life Technologies, MAN0006862). Protein solution was transferred to an Immun-Blot® PVDF membrane (BIO-RAD, 162-0174) in a 1x Bolt™ MES running buffer (Life Technologies, B002) for 1 hour at a constant voltage of 100V, using the BIO-RAD mini trans-blot system. The membrane was rinsed three times with PBS.

To block non-specific proteins, the membrane was incubated for 5 hours in 5% non-fat dry milk (BIO-RAD blotting-grade blocker, 170-6404) in PBS containing 0.1% Tween-20 (Sigma, P9416-100ML) (PBST). The membrane was rinsed three times with PBST and incubated overnight at 4ºC with mouse anti-V5 (AbD Serotec ®, USA) at 1:2000 in 5% milk PBST for the detection of the

V5 epitope expressed in the Adenovirus pAD /CMV/V5-GW/lacZ. After three times (5 min each) rinsing in PBST, the membrane was incubated with 1:2000 goat anti-mouse IgG-HRP (Santa Cruz Biotechnology, Inc, sc-2031) in 5% milk PBST for 1 hour at room temperature. The signal was revealed by chemiluminescence using clarity™ western ECL substrate (BIO-RAD, 170-5061). The membrane was then exposed to UV-light, and images were taken using the Gel Doc™ XR + documentation system (BIO-RAD, 1708195).

3.5.4.2 Adenovirus vector expression assessment in chicken embryo fibroblasts and Vero cells using western blot analysis

This investigation was conducted to test the specificity of the Adenovirus control vector in chicken embryo fibroblasts. The process is illustrated in section b.2.1 of the protocol workflow (Figure 3.1). Both the chicken embryo fibroblasts and Vero cells were seeded at a concentration of 1 x 10^6 cells per well in a 6-well plate with 2mL DMEM containing 10% FBS and 0.05mg Gentamicin. Once the cells were approximately 60-70% confluent, the spent medium was removed. The cells were then rinsed three times with 2mL PBS. Exactly 200µL of the Adenovirus amplified stock was mixed with 2mL of DMEM containing 10% FBS. The same virus mixture was added to each well of the chicken embryo fibroblasts and the Vero cells. Each of these cells had a control well which was non-treated. After 5 days of incubation, the spent medium was removed, the cells were rinsed three times with ice-cold PBS, scraped off the wells in a final volume of 1mL PBS, and transferred into a sterile Eppendorf tube. The cells were centrifuged at 1145xg for 2 min using the bench top mini centrifuge to pellet the cells. The supernatant was discarded and whole protein was extracted from the cell pellet using the same method as described in section 3.5.4. Protein concentration was determined using the Qubit® 2.0 Fluorometer and Qubit™ protein assay kit (Life Technologies, USA). Western blot analysis of all samples was performed according to the method described in section 3.5.4.1.

3.6 Development of a Non-Replicative, Recombinant Adenovirus (rAd) (pAd/PL-DEST™) for the Expression of the Gene of Choice

Sections 3.6 is shown in the protocol overview workflow (Figure 3.1, b.3).

3.6.1 Newcastle disease virus (NCDV) Matrix gene primer design

The NCDV Matrix gene was sequenced in-house using the next generation sequencer, Ion PGM system (Thermo Scientific). The NCDV (3090/11) sample used for sequencing was a gift from our collaborators at Rainbow Farms (Pty) Ltd. The 1095 base pairs Matrix gene shown in Figure 3.6

was used to design primers specific for this gene using the NCBI 3 and Blast (https://www.ncbi.nlm.nlh.gov/tools/primer-blast). Ten (10) primer sets were generated. These sets are shown in Table 3.4 below. Primer pairs were specific to the input template as no other targets were found in the selected database. A set that amplified the longest fragment was selected for downstream experiments.

```
ATGGACTCATCTAGGACAATTGGGCTGTACTTTGATTCTGCCCATTCTTCTAGCAACCTG
TTAGCATTTCCGATCGTCCTACAAGACACAGGAGATGGGAAGAAGCAAATCGCCCCGCAA
TATAGGATCCAGCGCCTTGACTTGTGGACTGATAGTAAGGAAGACTCAGTATTCATCACC
ACCTATGGATTCATCTTTCAAGTTGGGAATGAAGAAGCCACTGTCGGCATTATCGATGAT
AAACCCAAGCGCGAGTTACTTTCCGCTGCGATGCTCTGCCTAGGAAGCGTCCCAAATACC
GGAGACCTTATTGAGCTGGCAAGGGCCTGTCTCACTATGATGGTCACATGCAAGAAGAGT
GCAACTAATACTGAGAGAATGGTTTTCTCAGTAGTGCAGGCACCCCAAGTGCTGCAAAGC
TGTAGGGTTGTGGCAAACAAATACTCATCAGTGAATGCAGTCAAGCACGTGAAAGCGCCA
GAGAAGATCCCCGGGAGTGGAACCCTAGAATACAAGGTGAACTTTGTCTCCTTGACTGTG
GTACCGAAGAAGGATGTCTACAAGATCCCAGCTGCAGTATTGAAGATTTCTGGCTCGAGT
CTGTACAATCTTGCGCTCAATGTCACTATTAATGTGGAGGTAGACCCGAGGAGTCCTTTG
GTTAAATCTCTGTCTAAGTCTGACAGCGGATACTATGCTAACCTCTTCTTGCATATTGGA
CTTATGACCACCGTAGATAGGAAGGGGAAGAAAGTGACATTTGACAAGCTGGAAAAGAAA
ATAAGGAGCCTTGATCTATCTGTCGGGCTCAGTGATGTGCTCGGGCCTTCCGTGTTGGTA
AAAGCAAGAGGTGCACGGACTAAGCTTTTGGCACCTTTCTTCTCTAGCAGTGGGACAGCC
TGCTATCCCATAGCAAATGCTTCTCCTCAGGTGGCCAAGATACTCTGGAGTCAAACCGCG
TGCCTGCGGAGCGTTAAAATCATTATCCAAGCAGGTACCCAACGCGCTGTCGCAGTGACC
GCTGACCACGAGGTTACCTCTACTAAGCTGGAGAAGGGGCACACCCTTGCCAAATACAAT
CCTTTTAAGAAATAA
```

Figure 3.6: The NCDV Matrix gene sequenced in-house using the Ion PGM system (Thermo Scientific) for next generation sequencing. The 1096 base pairs gene was used to design primers to be used for the amplification of this gene.

Table 3.4: Ten primer sets for the specific detection of the Matrix gene (Figure 3.6). These primers were designed using the NCBI 3 and Blast databases.

		Sequence (5'->3')	Template strand	Length	Start	Stop	Tm	GC%	Self Complementarity	Self 3' complementarity
Primer Pair 1	Forward Primer (MF1A)	CAAGCGCGAGTTACTTTCCG	Plus	20	246	265	59.91	55	5	2
	Reverse primer (MR1A)	GCTTAGTCCGTGCACCTCTT	Minus	20	865	846	60.04	55	6	0
	Product length	620								
Primer Pair 2	Forward Primer (MF2A)	GCCTAGGAAGCGTCCCAAAT	Plus	20	278	297	60.11	55	6	2
	Reverse primer (MR2A)	AAGCTTAGTCCGTGCACCTC	Minus	20	867	848	60.04	55	6	0
	Product length	590								
				20	285	304	60.11	55	4	0
Primer Pair 3	Forward Primer (MF3A)	AAGCGTCCCAAATACCGGAG	Plus	20	491	472	60.11	55	4	0
	Reverse primer (MR3A)	GGGATCTTCTCTGGCGCTTT	Minus							
	Product length	207								
Primer Pair 4	Forward Primer (MF4A)	AAAGCGCCAGAGAAGATCCC	Plus	20	472	491	60.11	55	4	1
	Reverse primer (MR4A)	GCCAAAAGCTTAGTCCGTGC	Minus	20	872	853	60.11	55	6	2
	Product length	401								
Primer Pair 5	Forward Primer (MF5A)	AAGAGGTGCACGGACTAAGC	Plus	20	846	865	60.04	55	6	2
	Reverse primer (MR5)	GTATTTGGCAAGGGTGTGCC	Minus	20	1077	1058	59.75	55	5	3
	Product length	232								
Primer Pair 6	Forward Primer (MF6A)	GCACGGACTAAGCTTTTGGC	Plus	20	853	872	60.11	55	6	2
	Reverse primer (MR6)	GATTTTAACGCTCCGCAGGC	Minus	20	981	962	60.25	55	4	2
	Product length	129								
Primer Pair 7	Forward Primer (MF7A)	CGTCCCAAATACCGGAGACC	Plus	20	288	307	60.18	60	4	1
	Reverse primer (MR7A)	CAACCCTACAGCTTTGCAGC	Minus	20	430	411	59.76	55	4	3
	Product length	143								
Primer Pair 8	Forward Primer (MF8A)	ATAGGATCCAGCGCCTTGAC	Plus	20	122	141	59.61	55	6	2
	Reverse primer (MR8A)	CGCGCTTGGGTTTATCATCG	Minus	20	253	234	60.04	55	4	2
	Product length	132								
Primer Pair 9	Forward Primer (MF9A)	AGCTGTAGGGTTGTGGCAAA	Plus	20	418	437	59.82	50	4	3
	Reverse primer (MR9A)	TTAGTCCGTGCACCTCTTGC	Minus	20	863	844	60.32	55	6	2
	Product length	446								
Primer Pair 10	Forward Primer (MF10A)	GTTACTTTCCGCTGCGATGC	Plus	20	255	274	60.25	55	5	2
	Reverse primer (MR10A)	GTTTGCCACAACCCTACAGC	Minus	20	438	419	59.69	55	5	2
	Product length	184								

3.6.2 NCDV nucleotide confirmation using OIE approved NCDV detection PCR primers

Both the NCDV H3090/11 and H3343/11 samples were a gift from our collaborators at Rainbow Farms (Pty) Ltd. The viral RNA was extracted from these samples using the QIAamp® viral RNA mini kit as described in section 3.3.2. cDNA was synthesised using the same method as described in section 3.3.2. To confirm the sequencing results that the H3090/11 and H3343/11 were indeed NCDVs, these samples were tested using the KAPA HIFI hotstart ready mix PCR kit as described in section 3.5.3.3. The forward (5'-TCCGGAGGATACAAGGGT-3') and reverse (5'-AGCTGTTGCAACCCCAAG-3') primers were used instead of primers used in section 3.5.3.3. The annealing temperature was 60ºC.

3.6.2.1 Testing the designed PCR primers on the NCDV cDNAs

Using the KAPA HIFI hotstart ready mix PCR kit, amplification was conducted using different NCDV Matrix gene primer sets designed for the detection of the same gene (see Table 3.5). The aim was to get a set that would amplify the largest PCR fragment for subsequently cloning in the donor vector, which was the pENTR^{TM} directional TOPO vector (Life Technologies, K2400-20). The PCR was made up of 12.5µL of 2 x KAPA HIFI hotstart ready mix (KAPA BIOSYSTEMS, KK2601) for fast and high-fidelity PCR for long fragment amplification and for amplification of DNA fragments for cloning, 0.6µM of each forward and reverse primer sets in Table 3.5 and 11µL of cDNA were also added to the reaction. The thermocycling program using the ROCHE lightCycler® was as follows: Pre-incubation at 95ºC for 180 s, 25 cycles at 98ºC denaturation for 20 s, annealing for 15 s at 57ºC, and extension for 15 s at 72ºC. This was followed by a final extension at 72ºC for 60 s. The PCR products were resolved on a 1% agarose (Whitehead Scientific (Pty) Ltd, USA) gel electrophoresis for amplification confirmation. The largest PCR fragment amplified was cut out of the agarose gel under a UV light and cleaned using the GeneJET gel extraction kit (Thermoscientific, #K0691). The cleaned PCR products were stored at -20ºC.

Table 3.5: PCR primer sets used to detect the largest NCDV gene Matrix fragment using H3090/11 and H3343/11 NCDV cDNA

Primer Sets	Forward and Reverse Primers
Set 1	MF1A and MR1A
Set 2	MF1A and MR5
Set 3	MF1A and MR6
Set 4	MF8A and MR1A
Set 5	MF8A and MR5
Set 6	MF8A and MR6

3.6.2.2 Vectors used for creating an expression clone (Adenovirus vector expressing the NCDV Matrix gene)

The vector illustrated in Figure 3.7, pENTR™/D-TOPO (Life Technologies, K2400-20) (Figure 3.7A), which was a donor vector, and the pAd/CMV/V5-DEST™ (Life Technologies, V493-20) (Figure 3.7B), which functioned as an expression vector, were used to create an expression clone to express the NCDV Matrix gene. This is what was used as a vector vaccine that was tested for functionality in 293T cells.

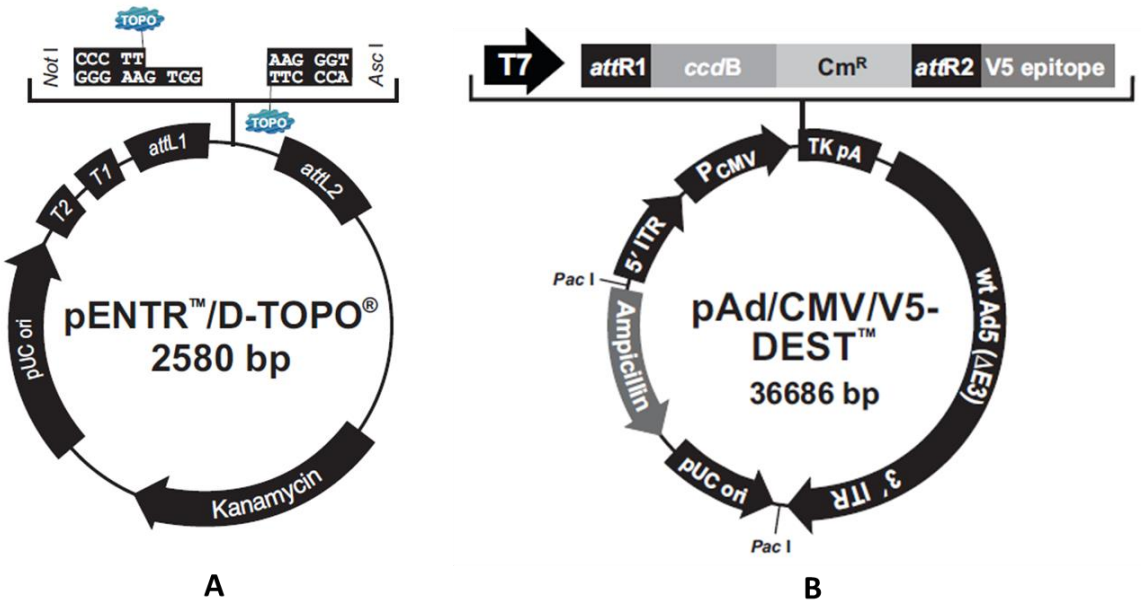

Figure 3.7: Maps of the two vectors. A: pENTR™/D-TOPO (Figure 3.7A) was a donor vector and B: pAd/CMV/V5-DEST™ (Figure 3.7B) functioned as an expression vector.

3.6.2.3 Primer design for cloning the Matrix gene derived from PCR into the pENTR™/D-TOPO vector

The PCR primers that were designed as discussed in section 3.6.1 were modified in order to make them ideal for directional cloning. For directional cloning to be successful, the CACC sequence was added at the 5' end of the forward primer (Table 3.6) in order for this sequence to pair with the overhang sequence, GTGG in the pENTR™/D-TOPO vector. This is illustrated in Figure 3.8. For proper initiation of translation in mammalian cells, the ATG initiation codon was also included with the forward primer (Table 3.6). No changes were made to the reverse primer. To produce a blunt-end PCR product, the KAPA HIFI hotstart ready mix PCR kit was used. The PCR mixture was made up of the following: 12.5µL of 2 x KAPA HIFI hotstart ready mix, 0.6µM of forward (5'- CACCATGTATAGGATCCAGCGCCTTGAC-3') and 0.6µM of reverse (5'-GTATTTGGCAAGGGTGTGCC-3') primers, and 11µL of the gel cleaned PCR product prepared (as discussed in section 3.5.3.3) in order to add the over-hangs to the PCR products. The thermocycling program using the ROCHE lightCycler® was set as follows: Preincubation at 95ºC for 180 s, 25 cycles of denaturation for 20 s at 98ºC, annealing for 15 s at 57ºC, and extension for 15 s at 72ºC. This was followed by a final extension at 72ºC for 60 s. The PCR products were run on 1% agarose (Whitehead Scientific (Pty) Ltd, USA) gel electrophoresis to confirm amplification. The PCR products with the overhangs were cut out from the gel and cleaned using

the GeneJET gel extraction kit according to the manufacturer's instructions. The cleaned PCR products were stored at -20ºC for later cloning into the pENTR™/D-TOPO® vector.

Table 3.6: PCR primers (section 3.6.1) and cloning primers designed by modifying the PCR primers

Primers	PCR	Cloning
Forward primer	ATAGGATCCAGCGCCTTGAC	CACCATGTATAGGATCCAGCGCCTTGAC
Reverse primer	GTATTTGGCAAGGGTGTGCC	GTATTTGGCAAGGGTGTGCC

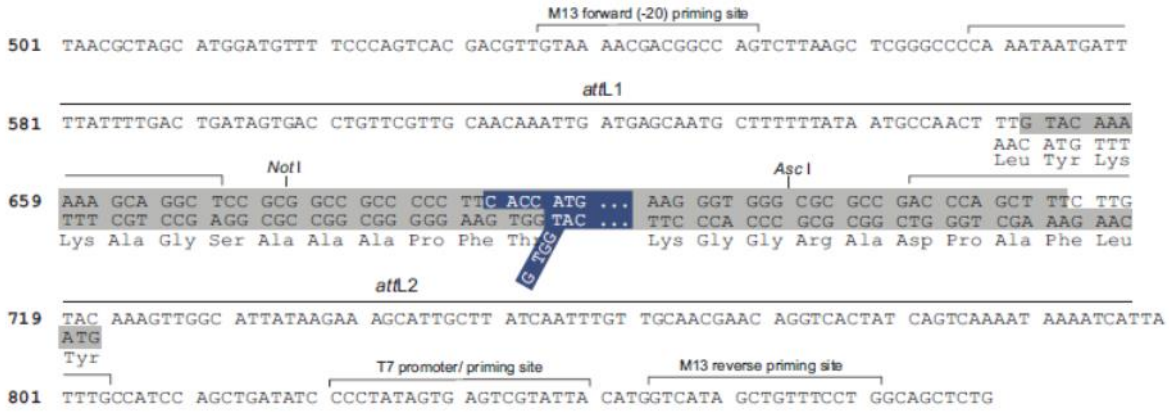

Figure 3.8: TOPO® cloning site for pENTRTM/D-TOPO®. This figure shows how to design suitable PCR primers to clone the PCR product into the pENTR™/D-TOPO®. The shaded region corresponds to the DNA sequence that was transferred from the entry clone to the destination vector (pAd/PL-DEST™) following LR recombination.

3.6.2.4 Cloning and transformation

The pENTR™ directional TOPO® cloning kit was used to set up the TOPO™ cloning reaction. Briefly, 4µL of the cleaned blunt-end PCR products (PCR products with the overhangs) and 1µL of the TOPO® vector were gently mixed in an Eppendorf tube and incubated for 5 min at room temperature. Two µL of the TOPO® cloning reaction was added into a 50µL vial of one Shot® TOP10 chemically competent *E.coli* and mixed gently. This mixture was incubated on ice for 30 min, followed by heat-shocking the cells for exactly 30 s at 42ºC and immediately transferring the tubes to ice. About 250µL of room temperature S.O.C medium (Life Technologies, K2400-20) was added to the mixture. The vial was closed tightly and shaken horizontally at 200 rpm for 1 hour in a 37ºC incubator. Two hundred (200) µL of the transformation mixture was spread on a

pre-warmed Luria-Bertani (LB) plate consisting of 1L distilled water, 32g of LB agar (Invitrogen, 22700-25), and 50µg/mL kanamycin to select the positively transformed *E.coli*. The plates were then incubated overnight at 37ºC.

Five (5) colonies were chosen and cultured overnight in LB medium containing 10g of tryptone, while 10g sodium chloride and 5g yeast extract were dissolved in 1L distilled water at pH 7. The medium was supplemented with 100µg/mL Kanamycin. The plasmid DNA was extracted using the PureLink™ HQ mini plasmid purification kit (Invitrogen, K2100-01) according to the manufacturer's instructions.

Briefly, 3mL of the *E.coli* cells from an overnight culture was centrifuged in a table-top centrifuge at 1,500xg for 15 min. The supernatant was discarded, and the pellet completely resuspended in 240µL of a resuspension solution with RNASe A. To this solution, 240µL of the lysis buffer was added and mixed gently by inverting the tubes 8 times. This mixture was incubated for 5 min at room temperature, followed by an addition of 340µL of a neutralising/binding buffer. The lysate was then mixed gently by inverting the tube 8 times and centrifuging the contents for 10 min at maximum speed in a table-top centrifuge in order to clarify the cell lysate. The supernatant was transferred into the spin column and centrifuged at 14,000g for 1 min. This was followed by a washing step with a wash buffer and elution of the plasmid DNA in a 50µL elution buffer. In order to confirm successful cloning, the KAPA HIFI hotstart ready mix PCR kit was used following the same protocol as described in section 3.5.3.3. However, the primers that were used for cloning confirmation were used, namely the forward primer (5'- ATAGGATCCAGCGCCTTGAC-3') and the reverse primer (5'-GTATTTGGCAAGGGTGTGCC-3').

3.6.2.5 Creating the Adenoviral expression clone/recombinant Adenovirus

To create an expression clone, i.e., the Adenovirus vector expressing the gene of interest, the primary requirement was to perform an LR recombination reaction using the attL-containing entry clone (pENTR™/D-TOPO) expressing the gene of interest and the attR-containing the destination vector (pAd/CMV/V5-DEST™). This mechanism is shown in Figure 3.9. In this process, the gene of interest cloned into the entry clone (pENTR™/D-TOPO) was transferred into the expression clone (pAd/CMV/V5-DEST™) via LR recombination. The product was what is usually used as a vaccine vector.

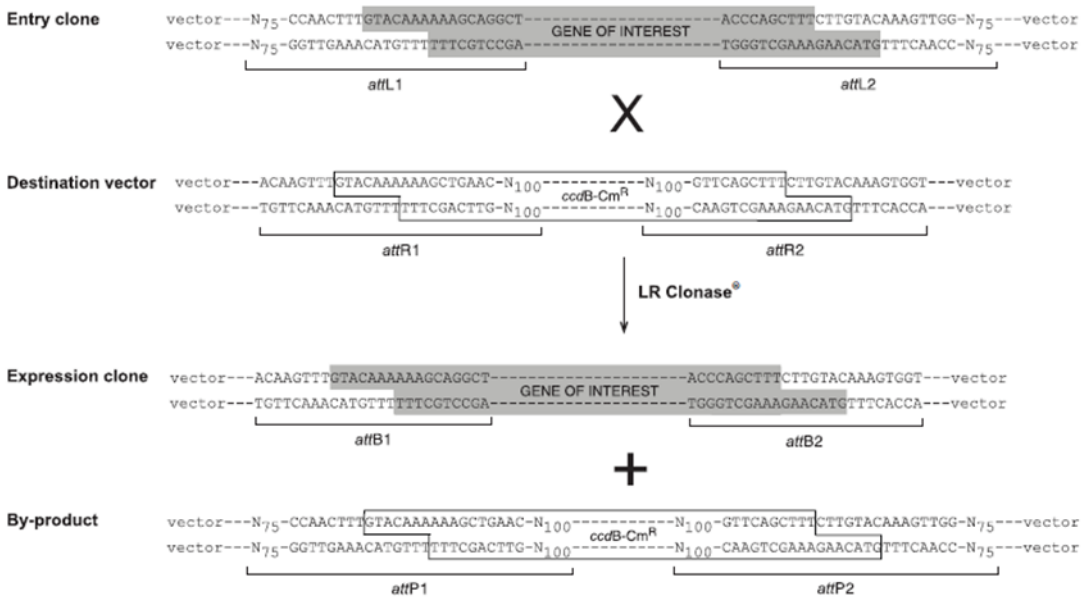

Figure 3.9: An LR recombination reaction between a pENTR™/D-TOPO entry clone and the pAd/CMV/V5-DEST™ destination vector to create an expression clone and a by-product

To perform the LR recombination reaction, the LR clonase® II enzyme mix (Life Technologies, 11791-020) was used according to the manufacturer's instructions. Six (6) µL of the plasmid DNA vector expressing the Matrix gene purified in section 3.6.2.4 and 2µL of the destination vector (pAd/CMV/V5-DEST™) was added in a 0.5mL microcentrifuge tube at room temperature. Then 2µL of the LR clonase® II enzyme mix was also added and mixed well by pipetting up and down. This reaction was incubated at 25ºC for 18 hours in order to increase the level of recombination. This was followed by the addition of 1µL of the proteinase K solution to the reaction and incubation for 10 min at 37ºC. Two (2) µL of the LR recombination reaction was transferred into the TOP10 chemically competent *E.coli* using a similar method as described in section 3.6.2.4. Then 200µL of the transformation mixture was spread on pre-warmed LB plates consisting of 1L distilled water, 32g of LB agar, and 100µg/mL Ampicillin. The plates were incubated overnight at 37ºC. Five (5) to 10 colonies were selected and cultured overnight in LB medium containing10g of tryptone, 10g sodium chloride, and 5g yeast extract in 1L distilled water at pH 7, supplemented with 100µg/mL Ampicillin. The plasmid DNA was extracted using the PureLink™ HQ mini plasmid purification and by following the same protocol as described in section 3.5.3.2.

To confirm that the Matrix gene was successfully cloned in the pAd/CMV/V5-DEST™ and also in the correct frame, PCR was conducted using the KAPA HIFI hotstart ready mix PCR kit and the primers T7 promoter forward primer (5'-TAATACGACTCACTATAGGG-3') and Matrix reverse primer (5'- GTATTTGGCAAGGGTGTGCC-3'). The PCR mixture was prepared in the manner described in section 3.5.3.3. The thermocycling program that was followed is shown in Table 3.7.

The PCR products were resolved on a 1% agarose gel electrophoresis for amplification confirmation.

Table 3.7: PCR thermocycling steps for the confirmation of the recombinant Adenovirus

Steps	Temperature and time	Cycles
Preincubation	at 95ºC for 180 s	1
Initiation	at 98ºC for 20 s	25
Annealing	at 47ºC for 15 s	
Extension	at 72ºC for 15 s	
Final extension	at 72ºc for 60 s	1

3.6.3 293T cell transfection with the recombinant Adenovirus

The purified plasmid (recombinant Adenovirus) was first digested using the PacI enzyme before transfecting it into 293T cells to allow the left and right viral ITRs to be exposed and also for the bacterial sequences (pUC origin and Ampicillin resistant gene) to be removed. To achieve this, a Pac I enzyme (Thermo Scientific, #ER2201) was used according to the manufacturer's instructions. Briefly, 17µL of the 5.9 x 10^4 ng/mL purified DNA plasmid of the pAd/CMV/V5-DEST™ expression construct, 2µL of the 10 x PacI buffer, and 2µL of the PacI enzyme were gently mixed together. The reaction was incubated at 37ºC for 16 hours for the plasmid to be completely digested. This was followed by incubation at 65ºC for 20 min to inactivate the PacI enzyme. To prepare the cells for transfections, 5 x 10^5 293T cells were seeded in one well in a 6-well plate using 2mL DMEM supplemented with 10% FBS and 0.05mg Gentamicin. After 24 hours of incubation, the spent culture medium was removed from the 293T cells and replaced with 1.5mL of DMEM containing 10% FBS. To perform a transfection reaction, the DNA-Lipofectamine® 2000 (Life Technologies, 11668-019) complex was prepared in the following manner: Exactly 20µL of PacI digested pAd/CMV/V5-DEST™ expression plasmid was diluted in 250µL Opti-MEM® I reduced serum medium (Life Technologies, 31985-062) in a microcentrifuge tube and mixed gently. In a different microcentrifuge tube, 3µL of the Lipofectamine® 2000 was diluted in 250µL Opti-MEM® I reduced serum medium, mixed gently, and incubated at room temperature for 5 min. The diluted DNA was then combined with the diluted Lipofectamine® 2000 and mixed gently. This mixture was incubated for 20 min at room temperature, allowing the formation of the DNA-Lipofectamine® 2000 complexes. These complexes were added dropwise to one well of a 6-well plate containing 293T cells and 1.5mL DMEM containing 10% FBS. The plate was rocked back and forth to gently mix the medium in the well and the added DNA-Lipofectamine® 2000 complexes. The cells were incubated overnight in a CO_2 incubator at 37ºC.

After incubation for 24 hours, the medium containing the DNA-Lipofectamine® 2000 complexes was removed and replaced with 2mL DMEM supplemented with 10% FBS and 0.05mg Gentamicin. After 48 hours, the cells were trypsinised, added to DMEM containing 10% FBS, and transferred into a sterile 10c.m tissue culture plate. The spent culture medium was replaced with fresh DMEM containing 10% FBS every 2-3 days until regions of CPE were visible.

Once 80% of CPE was observed, the Adenovirus containing cells were harvested by squirting cells off the plate with a 10mL tissue culture pipette. The cells and medium were then transferred to a sterile 15mL tightly closed centrifuge tube. To lyse the cells, the tube was stored at -80ºC for 30 min, followed by thawing it in a 37ºC water bath for 15 min. The freezing and thawing steps were repeated twice. The cell lysate was centrifuged in a table-top centrifuge at 1106xg at room temperature for 15 min to pellet the cell debris. The supernatant containing viral particles were transferred in aliquots to 2mL Eppendorf tubes. Some of the viral stocks were stored at -80ºC for future use while others were used for PCR to confirm that the crude virus contained the NCDV Matrix gene. To confirm the presence of the NCDV Matrix gene, the same PCR protocol as described in section 3.5.3.3 was followed. The following minor modifications were made: The forward (5'- ATAGGATCCAGCGCCTTGAC-3') and reverse (5'-GTATTTGGCAAGGGTGTGCC-3') primers were used instead at an annealing temperature of 57ºC. The PCR products were run on a 1% agarose gel electrophoresis to confirm amplification.

To infect target cells *in vitro*, the Adenovirus crude viruses usually have to first be amplified twice or thrice to obtain 100% transfection efficiency, depending on the cell type being studied. To amplify the crude virus prepared above, 3 x 10^6 293T cells with 10mL DMEM supplemented with 10% FBS were plated on a 10c.m tissue culture plate and incubated in a CO_2 incubator at 37ºC. Once the cells were 80% confluent, 400µL of the stored crude Adenovirus stock was thawed and added to the cells, followed by the swirling of the plate gently to mix. The cells were incubated at 37ºC in a CO_2 incubator until 80% CPE was reached. The Adenovirus containing cells were harvested by squirting cells off the plate with a 10mL tissue culture pipette and transferring both the cells and medium to a 15mL sterile tube and then tightly closing it. The amplified viruses were collected using the same freeze and thaw method as described in the paragraph above. The supernatant containing the viral particles was transferred to cryovials in 1mL aliquots and stored at -80ºC. The virus amplification was repeated three times.

3.6.4 Next generation sequencing (NGS) for the recombinant Adenovirus vector to confirm the Matrix inserted in the vector

The Ion Torrent PGM system (Thermo Fisher Scientific, 4462921, USA) was used for the targeted next-generation sequencing of the recombinant Adenovirus vector. Adenovirus plasmid DNA

(200ng) was digested into uniform fragments of approximately 200bp using the AB Library Builder™ system (Thermo Fisher Scientific, USA). This was done in duplicate.

To differentiate between the duplicate sample libraries, barcoded adapters (Ion Express™ Barcode Adapters kit) (Life Technologies, USA) were used. To ensure that sufficient library fragments were generated for the downstream experiment, a Qubit dsDNA HS Assay kit (Thermo Fisher Scientific, USA) was used for quantification of the library samples. The libraries were pooled together in equimolar amounts of 200pM to ensure equal representation of each barcoded library in the sequencing run. This was followed by clonal amplification using the Ion OneTouch™ 2 system (Thermo Fisher Scientific, USA). In this reaction the barcoded libraries attached to the ion sphere particles (ISPs), thus forming template-positive ISPs. The template-positive ISPs were then enriched for using the Ion OneTouch™ ES system. To determine the ratio of the template-positive ISPs to all ISPs present in the mixture, the Ion Sphere Quality Control assay kit was used together with the Qubit 2.0 fluorometer (Life Technologies, USA). This provided the percentage templated ISPs. It is noteworthy that it is an important quality control measure prior to commencing sequencing. The pooled samples (templated ISPs) were loaded onto a 314™ chip v2 for sequencing using the Ion Torrent PGM system. For the analysis of the sequencing data (FASTQ format), the CLC Genomics Workbench software (CLC BIO, Denmark) was used. The known sequence of the Adenovirus control vector (pAd/CMV/V5-GW/lacZ) was aligned with the current sequence that was obtained while sequencing the recombinant Adenovirus.

3.6.5 Assessing the RNA expression of the designed recombinant Adenovirus in 293T cells

About 5 x 10^5 293T cells were seeded per well in a 6-well plate using 2mL DMEM supplemented with 10% FBS and 0.05mg Gentamicin. The cells were incubated at 37ºC in a CO_2 incubator. At 24 hours after incubation, the spent culture medium was removed from the cells and replaced with 2mL DMEM containing 10% FBS. Then 200µL of the amplified crude recombinant Adenovirus was added to each of the four wells and mixed gently. No virus was added to the other two wells. Two (2) hours later, cells from one well infected with the crude recombinant Adenovirus and cells from the two wells not infected with the virus were harvested by squirting the cells off the wells using a 5mL tissue culture pipette. Both the cells and medium were transferred into a 15mL sterile tube and tightly closed. The tubes were centrifuged at 1106xg for 5 min at room temperature. The supernatant was discarded, and the cells were stored at -80ºC. The infected cells in the three remaining wells were harvested in a similar manner after 6, 12, and 24 hours respectively and stored at -80°C.

Once ready for RNA extraction, the cells were thawed, and RNA extraction was performed using the RNeasy® mini kit (QIAGEN®) according to the manufacturer's instructions. Exactly 350µL of the RLT lysis buffer containing β-mercaptoethanol (β-ME) was added to each of the harvested cell pellets and mixed by vortexing. The lysate was centrifuged for 3 min at maximum speed. The supernatant was removed by pipetting it into a new sterile tube. Then 1 volume of 70% ethanol was added to the lysate and mixed well by pipetting. The sample was transferred to a RNeasy mini spin column placed in a 2mL collection tube and centrifuged at ≥8000xg for 15s. The flow-through was discarded. The spin column was washed and centrifuged for 15 s at ≥8000xg first with 700µL RW1 buffer, then 500µL buffer RPE, and lastly with 500µL RPE buffer for 2 min. The RNA was eluted in 30µL of RNase-free water. DNase digestion in the extracted RNA samples was performed using the TURBO DNA-free™ kit (Life Technologies, AM1907) according to the manufacturer's instructions. For each sample, 0.1 volume of the 10 x TURBO DNase buffer and 3µL of the TURBO DNase were added to the RNA and mixed gently. This reaction was incubated at 37ºC for 30 min. After the incubation, 0.2 volume of the resuspended DNase inactivation reagent was added and mixed well. This was followed by incubation at room temperature for 5 min and mixing occasionally. Finally, the reaction was centrifuged at 10 000xg for 1.5 min and the RNA was transferred to a fresh sterile tube. For each RNA sample, cDNA was synthesised using the Transcriptor first strand cDNA synthesis kit and following the method as described in section 3.3.2.

To confirm the expression of the recombinant Adenovirus in the synthesised cDNA, PCR was performed using Ssofast™ EvaGreen® Supermix (BIO-RAD, #172-5202) and by following the manufacturer's instructions. To set up a 20µL PCR, the following were mixed together: 10µL of 2 x SsoFast EvaGreen supermix (BIO-RAD, #172-5202), 0.8µM of each of the T7 promoter forward (5'-TAATACGACTCACTATAGGG-3') and Matrix reverse (5'-GTATTTGGCAAGGGTGTGCC-3') primers, 6.4µL of nuclease free water, and 2µL cDNA. Using the ROCHE lightCycler®, thermocycling was conducted using the following steps: Preincubation at 95ºC for 30 s, 45 cycles at 95ºC denaturation for 10 s, 47ºC annealing for 10 s, and 60ºC extension for 40 s. The melting cycle was done at 95ºC for 10 s, 60ºC for 60 s, and 97ºC for 1 s. The PCR product was resolved on a 1% agarose gel to confirm amplification.

3.6.6 Assessing the DNA expression of the recombinant Adenovirus in chicken embryo fibroblasts (CEFs)

This part of the methodology is illustrated in section b.3.2 of the protocol workflow (Figure 3.1). Approximately 3 x 10^6 of CEFs cells and 10mL DMEM supplemented with 10% FBS were cultured per plate in two 10c.m tissue culture plates and incubated in a CO_2 incubator at 37ºC. Once the

cells had reached 70% confluency, the spent medium was removed and replaced in one plate with 10mL DMEM containing 10% FBS and 2mL of the amplified crude recombinant Adenovirus. The contents of the other plate was replaced with10mL DMEM containing 10% FBS only. The cells were incubated for 4 days at 37ºC in a CO_2 incubator. Four (4) days after infection, the spent medium was removed from each culture plate and the cells were harvested by trypsinization. The trypsin was inactivated by the addition of DMEM with 10% FBS to the cells. The cells, together with the inactivated trypsin, were centrifuged at 1106xg for 5 min and removed the supernatant. The cells were resuspended in 200µL PBS. To extract genomic DNA from the cells, the PureLink® genomic DNA kit (Life Technologies, K1820-01) was used according to the manufacturer's instructions. Twenty (20) µL of the proteinase K was added to each of the samples, followed by the addition of 20µL RNase A to each of the samples. The samples were mixed well by brief vortexing and incubated at room temperature for 2 min. After the incubation, 200µL PureLink® genomic lysis/binding buffer was added to each sample and mixed well by vortexing. The samples were incubated at 55ºC for 10 min for protein digestion. The 200µL of 96-100% ethanol was added to the lysate, which was mixed well by vortexing for 5 s. The lysates were each added to the PureLink® spin column. This was centrifuged at 10 000xg for 1 min at room temperature. The columns were washed with 500µL wash buffer and centrifuged at room temperature at 10 000xg for 1 min. The column was washed for the second time with 500µL wash buffer 2 and centrifuged at maximum speed for 3 min at room temperature. The genomic DNA was eluted with 25µL PureLink® genomic elution buffer. To assess the expression of the recombinant Adenovirus in the chicken embryo fibroblasts genomic DNA, PCR was used following the method as described in section 3.5.3.3. The following minor modifications were made: The forward (5'-ATAGGATCCAGCGCCTTGAC-3') and reverse (5'-GTATTTGGCAAGGGTGTGCC-3') primers were used instead at an annealing temperature of 57ºC. The PCR products were then run on a 1% agarose gel electrophoresis to confirm amplification.

3.6.7 Mass spectrometry (MS) protein expression analysis

3.6.7.1 Protein extraction from the recombinant Adenovirus crude lysate

The crude recombinant Adenovirus was purified using the ViraBind™ Adenovirus purification kit (Cell Biolabs, Inc., VPK-100) according to the manufacturer's instructions. Prior to virus purification, the virus supernatant was clarified by passing it through a 0.45µm sterile filter. The clarified viral supernatant was then passed through the purification filters (each pre-rinsed with 5mL of 1 x wash buffer) by gravity flow. This was followed by two washes with 10mL of a wash buffer using gravity flow. The virus sample was eluted in 3mL of an elution buffer using gravity flow.

The purified Adenovirus sample was diluted 5-fold in lysis buffer (4% SDS, 50mM Tris-HCL pH 8.0) and heated at 90ºC for 5 min. The lysate was pulse sonicated on ice for 90 s (10 s per pulse and 10 s intermission between pulses) and incubated with 25 units of benzonase (Merck) at 37ºC for 30 min. This was followed by centrifugation at 15 000xg for 10 min. The supernatant was collected, and the protein concentration was determined using the Qubit® 2.0 Fluorometer and Qubit™ protein assay kit. A final concentration of 10mM Dithiothreitol (DTT) (Amresco) was used to reduce the protein at 37ºC for 45 min. The protein was then alkylated using a final concentration of 25mM Iodoacetamide (IAA) (Sigma) for 30 min in the dark. The IAA (Sigma) was quenched with a final concentration of 10mM DTT (Amresco).

3.6.7.2 Protein extraction from CEFs

Approximately 3 x 10^6 of CEFs cells with 10mL DMEM supplemented with 10% FBS were cultured per plate in two 10c.m tissue culture plates and incubated in a CO_2 incubator at 37ºC. Once the cells reached 70% confluency, the spent medium was removed and replaced into one plate with 10mL DMEM containing 10% FBS and 2mL of the amplified crude recombinant Adenovirus. The other plate was replaced with10mL DMEM containing 10% FBS only. The cells were incubated for 4 days at 37ºC in a CO_2 incubator. Four days after infection, the spent medium was removed from each culture plate and the cells were scraped off the wells in a final volume of 1mL PBS and transferred into a sterile Eppendorf tube. The cells were centrifuged at 1145xg for 2 min using the bench top mini centrifuge to pellet the cells. The supernatant was discarded and whole protein was extracted from the cell pellet using the same method as described in section 3.5.4. Protein concentration was determined using the Qubit® 2.0 Fluorometer and Qubit™ protein assay kit (Life Technologies, USA).

3.6.7.3 Mass spectrometry (MS) protein expression analysis of the recombinant Adenovirus in CEFs

Twenty (20) µg of each protein sample (crude recombinant Adenovirus, CEFs infected with the recombinant Adenovirus, and non-infected CEFs) was purified of salts and detergents in an automated manner using MagReSyn® HILIC particles (ReSyn Biosciences) with on-particle protein digestion using sequencing-grade trypsin (Promega). The resultant peptides were analysed using a Dionex Ultimate 3000 RSLC system coupled to an AB Sciex 6600 TripleTOF mass spectrometer. Injected peptides were inline de-salted using an Acclaim PepMap C18 trap column (100 µm x 2 cm: 2 min at 15 µl.min 1 using 2% ACN/0.2% FA). Trapped peptides were gradient eluted and separated on an Acclaim PepMap C18 RSLC column (300 µm x 15 cm, 3 µm particle size) using a flowrate of 8µl.min 1 with a gradient of 4-30% B over 60 min (A: 0.1% FA;

B: 80% ACN/0.1% FA). The 6600 TripleTOF mass spectrometer was operated in positive ion mode. Precursor (MS) scans were acquired from m/z 360-1500 (2+-5+ charge states) using an accumulation time of 500ms followed by 50 fragment ion (MS/MS) scans, acquired from m/z 100-1800 with 50ms accumulation time each.

Spectral data from MS analysis was searched in Search GUI (Compomics) using the X!Tandem, MS-GF+ and Comet search engines. The sequences of the NDV Matrix protein and common contaminants were added to the whole proteome of dsDNA viruses (with no RNA stage) database found in Swiss-Prot. Decoy sequences were created by reversing the sequences in the target database in Search GUI. A 1% false discovery rate cut-off was applied at the PSM (peptide-spectrum match) and protein level.

CHAPTER 4

POINT-OF-CARE (POC) DIAGNOSIS FOR AI USING LAMP: RESULTS AND DISCUSSIONS

4.1 Sequence Alignment of AI Viruses

In an attempt to develop a POC LAMP for the detection of all AI viruses by targeting the Matrix gene and also for the detection of HPAI (H5 and H7), sequences of the South African origin of these viruses were retrieved from the influenza research database (http:www.fludb.org/). Twenty-seven (27) Matrix genes originating from various South African AI viruses were aligned (Figure 4.1). This was followed by an alignment of 12 hemagglutinin genes of the H5 subtypes from various avian species (Figure 4.2). Finally, the alignment of 5 hemagglutinin genes of the H7 subtypes isolated from various avian species was also performed (Figure 4.3). The alignment for all these genes was done using the MUSCLE multiple sequence alignment tool which is described in the influenza research database. These alignments were performed in order to identify conserved regions for each gene alignment. The specific names of the virus sequences that were aligned are indicated on the left panel of the alignments performed for each gene. This is shown in Figure 4.1, Figure 4.2, and Figure 4.3. The nomenclature is such that a unique number is given to each outbreak, the type of influenza it is, the animal in which the virus was isolated, and the region where it was isolated. The alignment results revealed high nucleotide sequence variation within the Matrix gene of different avian influenza viruses. These variations make it difficult to design primers that are specific for AI subtypes. For the Matrix gene alignments (Figure 4.1), only 5 AI viruses (accession #: CY014985, JX069084, JX069092, JX069100 and JX069108) had conserved regions in the first 60 bases. Similar levels of variation in the alignment results were obtained in the processing of the H5 and H7 subtypes (Figure 4.2 and Figure 4.3 respectively). Due to the sequence variability of the AIVs, one sequence for each gene which seemed to have more common sequence regions with the other aligned sequences was used for primer design. Variability occurred not only in the first 60 bases, but throughout the entire gene sequence alignments.

Figure 4.1: Sequence alignment of the conserved Matrix gene regions of the South African AI viruses aligned using the MUSCLE multiple sequence alignment (influenza research database). Only the first 60 aligned bases are shown.

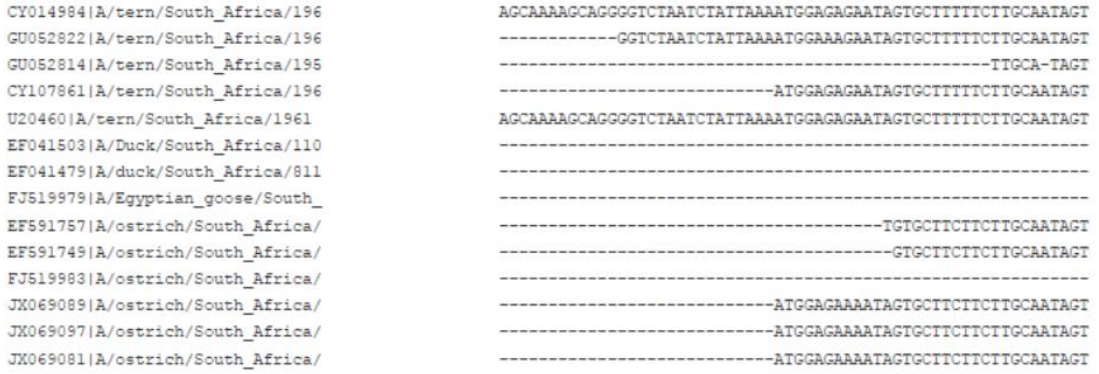

Figure 4.2: Sequence alignment of the conserved hemagglutinin (HA) gene of the H5 subtypes of the South African AI viruses aligned using the MUSCLE multiple sequence alignment (influenza research database). Only the first 60 aligned bases are shown.

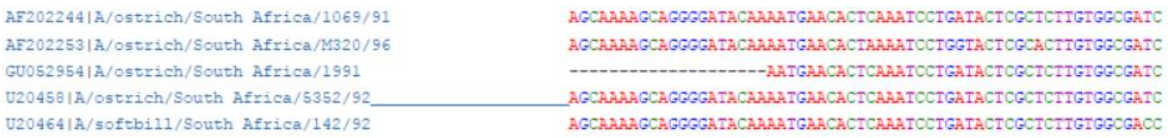

Figure 4.3: Sequence alignment of the conserved hemagglutinin (HA) gene of the H7 subtypes of the South African AI viruses aligned using the MUSCLE multiple sequence alignment (influenza research database). Only the first 60 aligned bases are shown.

4.2 Testing the functionality of the LAMP primers

The selected sequences with the conserved regions for each gene (Matrix, Hemagglutinin H5 and H7 subtypes) were uploaded into the LAMP primer designing software, namely the LAMP primer explorer (http: primerexplorer/jp/e/) using the default settings of the software. More than 10 sets of the LAMP primers for each gene were generated. Each set comprised of the BIP, FIP, B2/B loop, F2/F loop, B3 and F3. The first two best primer sets were chosen.

To determine whether these primers would work for the LAMP assays, the B3/F3 and the B2/F2 for two of the chosen sets of each gene were carried out using conventional PCR. These primers were tested using three AI viruses, namely HP-H5N2 (11060333C), LP-H5N2 (12060229), and LP-H7N1 (12080123A). To confirm that the viruses that were tested with the LAMP primers were AI viruses, the OIE approved AI detection primers were used in conventional PCR.

Figure 4.4 shows the PCR products of the amplified Matrix gene in HP-H5N2 (11060333C), LP-H5N2 (12060229), and LP-H7N1 (12080123A) using the two sets of B3/F3 and B2/F2 and the OIE AI approved detection primers. The OIE detection primers for the AI showed that the three samples were indeed AI as is evident on the middle set of amplifications in Figure 4.4. Set 1A (B2 and F2) as shown on the first set of amplification products in Figure 4.4 was chosen over set 2A (B2 and F2 from segment 7), which is shown on the second set of amplifications in Figure 4.4, due to the fact that set 1A primers showed more specificity than those of Set 2A, which only amplified sample LP-H5N2 (12060229). Similarly, set 1B (B3 and F3), as shown on the second last set of amplification products in Figure 4.4, was chosen over set 2B (B3 and F3), which is shown on the last set of amplifications in Figure 4.4, due to the specificity of set 1B over set 2B. Although the first PCR using set 1B primers and the LP-H7N1 (12080123A) sample amplified a wrong product size of ~500bp of the Matrix gene, it was concluded that it might have been due to contamination as the second PCR (a duplicate reaction) gave rise to the correct product size of

249bp, which is similar in size to the products of the other samples amplified using the set 1B PCR primers.

To choose primers for use in the H5 and H7 subtype specific LAMP assays, the same technique that had been used in choosing primers for the Matrix gene LAMP assay was followed.

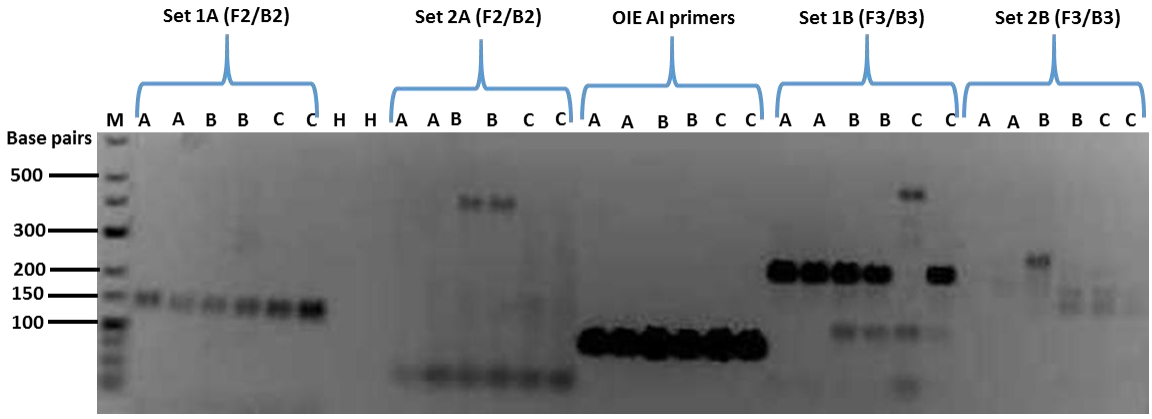

Figure 4.4: Image of 1% Agarose gel electrophoresis showing PCR products of the tested LAMP primers. M: Low range DNA ladder (Thermo Scientific, # sm1193), Lanes 2-7: PCR products using Set 1A(F2/B2), Lanes 8-9: Negative control (H_2O), Lanes 10-15: PCR products using Set 2A(F2/B2), Lanes 16-21: PCR products using OIE AI primers, Lanes 22-27: PCR products using Set 1B(F3/B3), Lanes 28-33: PCR products using Set 2B(F3/B3), A: HP-H5N2 (11060333C), B: LP-H5N2 (12060229), C: LP-H7N1 (12080123A), H: Negative control (H_2O).

4.2.1 Development and optimisation of the LAMP method

4.2.1.1 Samples used for LAMP optimisation

Primers were designed specifically for the detection of South African strains. It would have been preferable to include South African outbreak strains, but the laboratory could not access such samples. Colleagues abroad who had such strains were unable to make them available owing to legal implications or regulatory frameworks that govern the distribution of such samples for research work in South Africa. Similarly placed strains were obtained from Italy and the specific genes targeted variability, as would have been the case had South African strains been used.

4.2.1.2 Viral RNA concentrations

The samples extracted using the QIAamp® viral RNA mini kit were in the range of 1.24 x 10^3 – 9.96 x 10^3ng/L (Table 4.1). The extraction concentrations for each viral sample were from single extractions. These concentrations were high enough for LAMP detection. In previous studies LAMP was used to detect animal pathogens at concentrations which were much lower than the ones obtained in this study (Pham *et al.*, 2005; Peng *et al.*, 2011; Farooq *et al.*, 2015).

Table 4.1: RNA concentrations quantified using the Qubit® 2.0 Fluorometer (Life Technologies, Singapore) and Qubit® RNA high sensitivity kit (Life Technologies, USA)

Sample	Numbering	RNA Concentration (ng/mL)
H5N1 inactivated antigen: ANHUI/1/2005 (H5N1) IBCDC - RG-6 07/290	1	6.64 x 10^3
H5N1 inactivated antigen: A/Cambodia/R040505/2007 (H5N1) NIBRG-88	2	5.12 x 10^3
H5N1 A/mallard/Italy/3401/05	3	1.24 x 10^3
H5N1 A/turkey/Turkey/1/05	4	2.03 x 10^3
H5N2 A/turkey/Italy/80	5	2.98 x 10^3
H5N2 A/turkey/Italy/1258/V05	6	2.4 x 10^3
H5N3 A/duck/Italy/775/04	7	4.44 x 10^3
H5N9 A/chicken/Italy/22A/98	9	2.92 x 10^3
H6N8 A/turkey/Italy/4776-52/2015	10	7.88 x 10^3
H7N1 inactivated antigen: AV98/00 984v00/OST/ITALY P2	11	3.28 x 10^3
H7N9 inactivated antigen: A/Anhui/1/2013 (H7N9) (NIBRG-268)	12	1.80 x 10^3
H7N1 A/turkey/Italy/1067/99	13	5.08 x 10^3
H7N1 A/starling/Africa/983/79	14	2.21 x 10^3
H7N3 A/turkey/Italy/9289/02	15	2.03 x 10^3
H7N4 A/mallard/Italy/4810-79/04	16	2.42 x 10^3
H7N7 A/macaw/England/626/80	17	3.0 x 10^3
H8N4 A/turkey/Ontario/6118/68	18	7.16 x 10^3
H9N2 A/mallard/Italy73817-34/05	19	9.96 x 10^3
A/Turkey/Canada H6N8 NOV84	20	1.82 x 10^3
A/Chick/Scotland/59 H5N1 A/S 7/89	21	2.5 x 10^3
NCDV	22	2.08 x 10^3

4.2.2 Detected viral RNA from samples (Table 4.1) using the Matrix specific LAMP detection assay

The LAMP reaction was carried out in 25µL at 65ºC for 30 min on the Roche light cycler using viral RNA (Table 4.1) as templates. This translates to a minimum concentration of 0.3 to 2ng/µL per sample. These concentrations were above the minimum LAMP starting concentrations for RNA, which is usually 0.8µg/µL or less (Pham *et al.*, 2005; Peng *et al.,* 2011; Farooq *et al.*, 2015). Positive LAMP results were visualised as characteristic ladders on agarose gel. This is shown in Figure 4.5 on the left side of the panel as the first three wells representing Samples 1, 2 and 4. This result indicated successful amplification using the LAMP designed primers assay targeting the Matrix gene when the template used was RNA.

The ladder-like patterns indicate that stem-loop DNAs with inverted repeats of the gene of interest were produced (Notomi *et al.*, 2000). To improve the virus amplification for this assay, the use of cDNA as a template was tested.

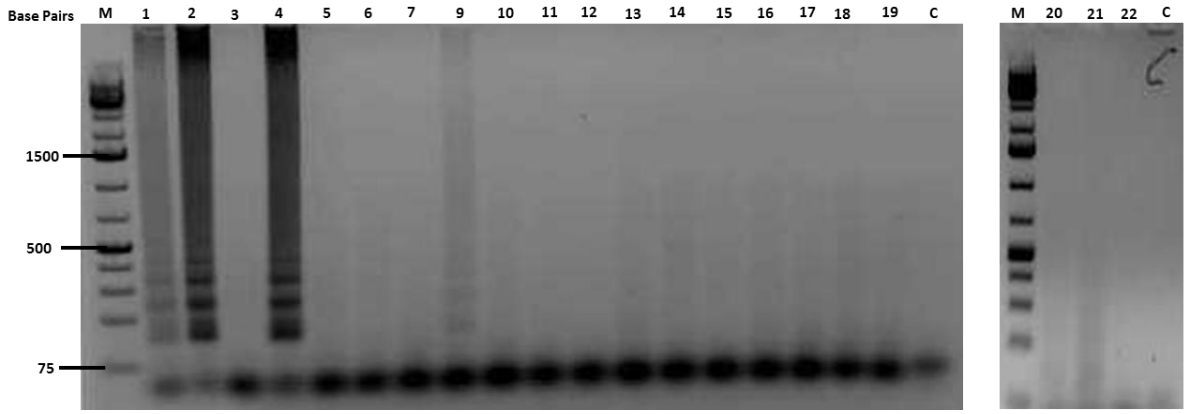

Figure 4.5: LAMP screening of AI using RNA as a template. Lane M: 1Kb DNA molecular ladder, Lanes 1-22: Samples shown in Table 4.1, C: Negative control.

Because only three samples were detected with the LAMP assay specific for the Matrix gene, a few optimisation steps had to be followed. RNA was used as a template in the first instance and, as RNA is known to degrade easily, the first step to optimise was to test whether using RNA as a template could be the problem. The aim was to determine the best LAMP template amongst RNA, random hexamer cDNA, and specific B3/F3 cDNA. This time, the LAMP master mix included SYBR® green (Invitrogen, USA). The three different templates were synthesised from samples 1, 2 and 3 that had been selected randomly to avoid sample bias. Using the three different templates from the three different samples, the results showed that the best template to use to obtain optimum LAMP results was cDNA that was synthesised using F3 and B3 LAMP specific

primers. These results are presented in Figure 4.6, Figure 4.7, and Figure 4.8. These figures also show that the cDNA that was synthesised using B3 and F3 LAMP specific primers was always detected earlier than the other templates. This was consistent with theoretical expectations, given that the cDNA synthesis in the case of F3/B3 primers had already been selected for the desired template rather than random production of complementary RNA. Furthermore, cDNA would be considerably more stable than RNA as a template.

4.2.3 cDNA synthesised with Matrix specific primers is the best template for obtaining optimum LAMP results

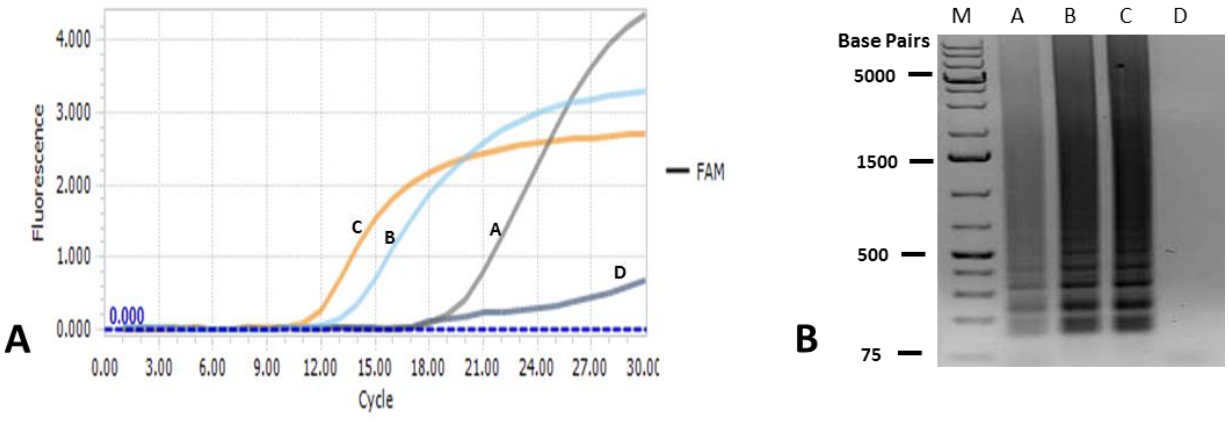

C

Sample Name	Cq/Ct	Call
A: RNA	17.67	Positive
B: Random primer Cdna	12.06	Positive
C: F3B3 LAMP primer cDNA	10.51	Positive
D: Negative control	-	Negative

Figure 4.6: H5N1 inactivated antigen: ANHUI/1/2005 (H5N1) IBCDC - RG-6 07/290 (sample 1) processed in different ways to improve the sensitivity of LAMP. 4.6(A): Real-time LAMP results of samples A, B, C, and D, 4.6(B): LAMP results of samples A, B, C, and D resolved on 1% agarose gel, 4.6(C): Table showing the times (Cq/Ct) at which the samples were detected

A

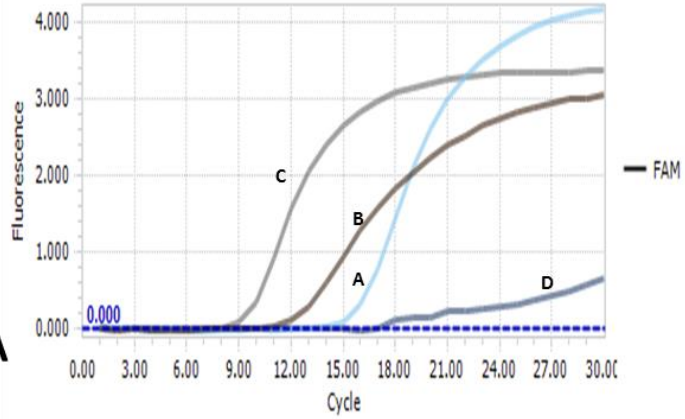

B

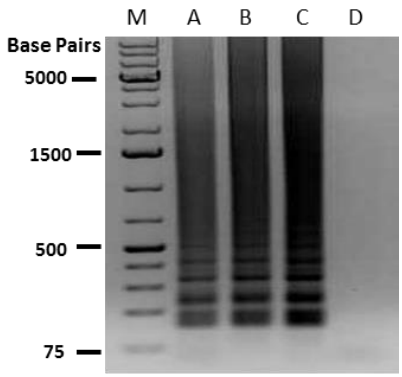

C

Sample Name	Cq/Ct	Call
A: RNA	14.27	Positive
B: Random primer cDNA	11.16	Positive
C: F3B3 LAMP primer cDNA	8.5	Positive
D: Negative control	-	Negative

Figure 4.7: H5N1 inactivated antigen: A/Cambodia/R040505/2007 (H5N1) NIBRG-88 (Sample 2) processed in different ways to improve the sensitivity of LAMP. 4.7(A): Real-time LAMP results of samples A, B, C, and D, 4.7(B): LAMP results of samples A, B, C, and D resolved on 1% agarose gel, 4.7(C): Table showing the times (Cq/Ct) at which the samples were detected

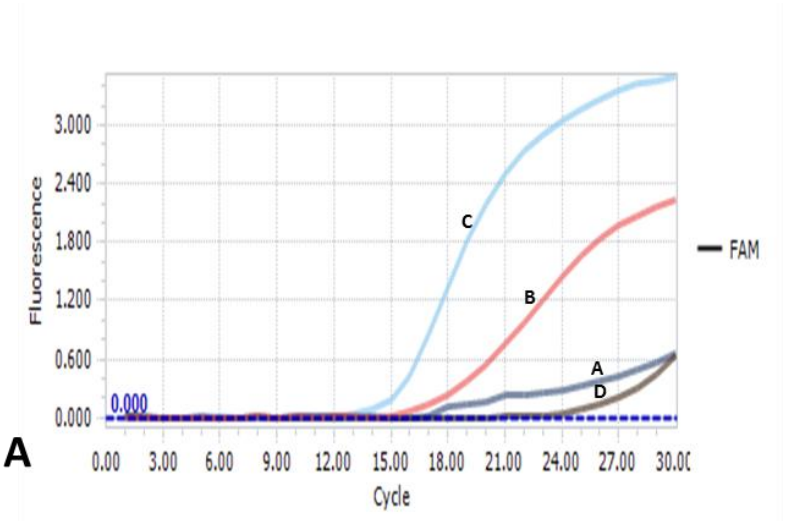

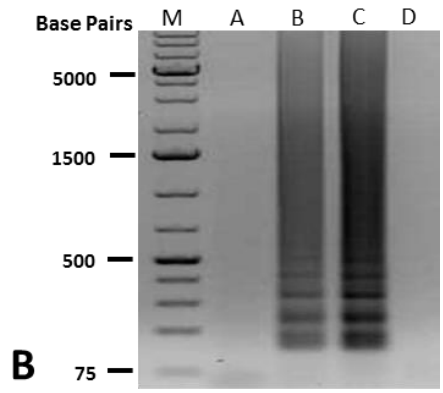

C

Sample Name	Cq/Ct	Call
A: RNA	17.75	Positive
B: Random primer cDNA	15.48	Positive
C: F3B3 cDNA	13.53	Positive
D: Negative control	-	Negative

Figure 4.8: H5N1 A/mallard/Italy/3401/05 (sample 3) processed in different ways to improve the sensitivity of LAMP. 4.8(A): Real-time LAMP results of samples A, B, C, and D. 4.8(B): LAMP results of samples A, B, C, and D resolved on 1% agarose gel, 4.8(C): Table showing the times (Cq/Ct) at which the samples were detected

4.2.4 Concentrations of the cDNA synthesised for all samples using the Matrix specific primers

The synthesised cDNA concentrations were in the range 1.61 x 10^4 to 2.22 x 10^4 ng/mL. These concentrations were above the conventional LAMP starting concentration for DNA which is usually at less than 100fg/µL (Pham *et al.*, 2005; Peng *et al.*, 2011; Xie *et al.*, 2013; Abbasi *et al.*, 2016). This meant that the template preparation method would yield acceptable concentrations for the LAMP method.

Table 4.2: cDNA concentrations quantified using the Qubit® 2.0 Fluorometer (Life Technologies, Singapore) and Qubit® double stranded DNA (dsDNA) high sensitivity kit (Life Technologies, USA)

Sample	Numbering	cDNA concentration (ng/mL)
H5N1 inactivated antigen: ANHUI/1/2005 (H5N1) IBCDC - RG-6 07/290	1	2.19×10^4
H5N1 inactivated antigen: A/Cambodia/R040505/2007 (H5N1) NIBRG-88	2	2.22×10^4
H5N1 A/mallard/Italy/3401/05	3	2.01×10^4
H5N1 A/turkey/Turkey/1/05	4	1.96×10^4
H5N2 A/turkey/Italy/80	5	1.86×10^4
H5N2 A/turkey/Italy/1258/V05	6	1.81×10^4
H5N3 A/duck/Italy/775/04	7	1.93×10^4
H5N9 A/chicken/Italy/22A/98	9	1.99×10^4
H6N8 A/turkey/Italy/4776-52/2015	10	1.94×10^4
H7N1 inactivated antigen: AV98/00 984v00/OST/ITALY P2	11	1.93×10^4
H7N9 inactivated antigen: A/Anhui/1/2013 (H7N9) (NIBRG-268)	12	1.81×10^4
H7N1 A/turkey/Italy/1067/99	13	2.05×10^4
H7N1 A/starling/Africa/983/79	14	1.78×10^4
H7N3 A/turkey/Italy/9289/02	15	1.61×10^4
H7N4 A/mallard/Italy/4810-79/04	16	1.76×10^4
H7N7 A/macaw/England/626/80	17	1.78×10^4
H8N4 A/turkey/Ontario/6118/68	18	1.76×10^4
H9N2 A/mallard/Italy73817-34/05	19	1.93×10^4
A/Turkey/Canada H6N8 NOV84	20	1.93×10^4
A/Chick/Scotland/59 H5N1 A/S 7/89	21	1.94×10^4
NCDV	22	1.89×10^4

4.2.5 AI detection by targeting the Matrix gene

The real-time LAMP assay was performed in a final volume of 25µL (equivalent to 3ng/µL – 4ng/µL final template concentration per reaction) at 65ºC for 30 min on the Roche light cycler. Specific B3/F3-derived cDNAs synthesised as described in section 4.2.4 (Table 4.2) were used as templates for each reaction. Figure 4.9A shows real-time detection of 20 AI samples and two negative controls (NCDV and water) using the LAMP method on the Roche thermo cycler with SYBR® green as a detection dye. The real-time LAMP results showed that all the samples were amplified while the negative controls remained negative, as was expected. The detected samples did, however, show a variety of patterns. Other samples were detected much earlier in less than 18 min, and these are shown in Figure 4.9A panel 1. This was indicative of higher concentrations

of starting template and/or better complementarity with the primers used. Others were detected later, after 21 min. These are also shown in Figure 4.9A panel 2. The amplified products were resolved on a 1% agarose gel stained with ethidium bromide to confirm the real-time LAMP results. The stained agarose gel results (Figure 4.9B) also showed that all the tested samples, except samples 12 (H7N9), 2 (H6N8), 21 (H5N1), and the negative controls (22: NCDV and water) were true positives. The false positive samples, 12 (H7N9), 2 (H6N8), 21 (H5N1), and the negative controls (22: NCDV and water) appeared as though they were amplified on the real-time amplification graphs due to non-specific amplification which is usually detected on a real-time instrument when a non-specific dye such as SYBR green is used in an amplification reaction.

The threshold (Cq/Ct) values in Figure 4.9C show how quickly the samples were amplified in terms of assay time. All the true positives were detected in less than 16 min. This then relates to the suitability of the designed primers and related oligonucleotides against the available samples. This result illustrates that the primers, with their degenerate nucleotide substitutions to compensate for minor variations among various AI subtypes, did work. The prominent laddering pattern on the agarose gel that is visible in Figure 4.9B and the threshold levels shown in Figure 4.9A account for this success. It can therefore be concluded that the design of the relevant primers and probes, as well as the optimum template processing described earlier, was efficacious.

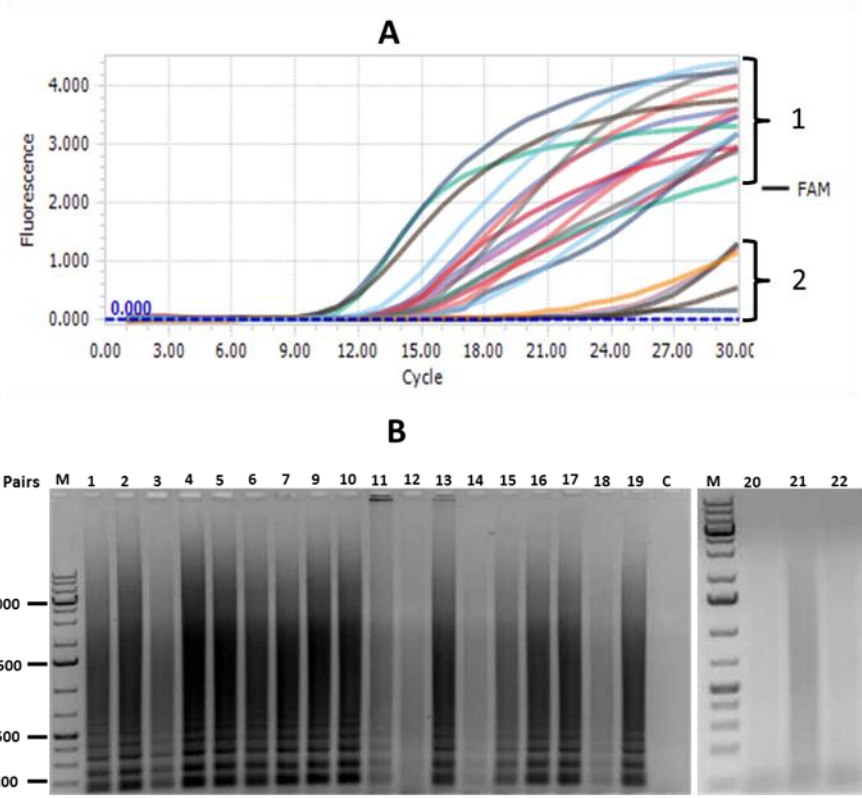

C

Sample Name	Cq	Call
1	11.53	Positive
2	9.31	Positive
3	14.48	Positive
4	9.51	Positive
5	10.16	Positive
6	12.86	Positive
7	11.93	Positive
9	12.7	Positive
10	12.84	Positive
11	14.66	Positive
12	22.84	Positive
13	12.38	Positive
14	14.22	Positive
15	12.91	Positive
16	13.65	Positive
17	12.3	Positive
18	18.33	Positive
19	13.46	Positive
20	21.78	Positive
21	23.65	Positive
22	21.23	Positive
Negative control	-	Negative

Figure 4.9: Screening of AI viruses using LAMP. Figure 4.9A shows the real-time sigmoidal graphs of the LAMP products. Figure 4.9B shows the LAMP products that ran on a 1% agarose gel. M: 1Kb DNA molecular marker. 1-22: Samples listed in Table 4.2 and C: Negative control. Figure 4.9C shows the times at which the samples were detected.

4.2.6 The H5 subtype specific detection

Once an area has been defined as AI positive, it is always important to determine whether the AI viruses circulating in that area are highly pathogenic or not. This is an important consideration that the authorities tasked with reporting and notifying the OIE have to be sure of. It is therefore critical to have an assay that will indicate the pathogenicity of the strain based on hemagglutinin known gene classification. To this end, primers targeting the hemagglutinin gene specific for H5 subtypes were designed and tested. To determine whether the designed H5 LAMP primer set was specific for H5 influenza virus amplification, the primers were tested on 20 AI viruses of different subtypes as shown in Table 4.2. Two negative controls (NCDV and water) were also included. The LAMP reactions were examined by real-time fluorescence detection and by agarose gel stained with ethidium bromide. The H5 specific primer set used for the RT-LAMP amplified only the H5 influenza virus subtypes (Figure 4.10A and Figure 4.10C). None of the non-specific amplification products were observed, as shown in Figure 4.10A and Figure 4.10C. To confirm the amplified LAMP products' specificities, ethidium bromide stained 1% agarose gel was used. Figure 4.10B shows visibly distinct ladder-like patterns for the amplified H5 influenza virus subtypes. Similar to the real-time sigmoidal graph, non-specific amplification products were not observed. Figure 4.10C shows just how quickly the H5 samples were detected. The specific H5 samples were all detected as positive in less than 21 min, while the samples that were not H5 serotypes showed as negative, as did the negative controls as (Figure 4.10).

This result has two important implications. First, it is important to note that not only avian AI can test positive for the Matrix gene, but that most influenza A viruses will. However, to have a positive H5 profile and be accepted as AI H5 subtype, both the Matrix gene-based LAMP assay and the H5 assay should be positive. This then gives the assurance that one will not end up with false negatives or false positives. Although the complementarity of the H5 primers for the LAMP assay seemed to be less effective compared to the Matrix gene-based assay (16 min vs 21 min), this will still be good enough in an outbreak situation because H5 assay will be the secondary test after Matrix gene assay. It can therefore be concluded that the design for H5 specific degenerate primers and probes is sufficiently applicable for use in samples such as the ones used in the study.

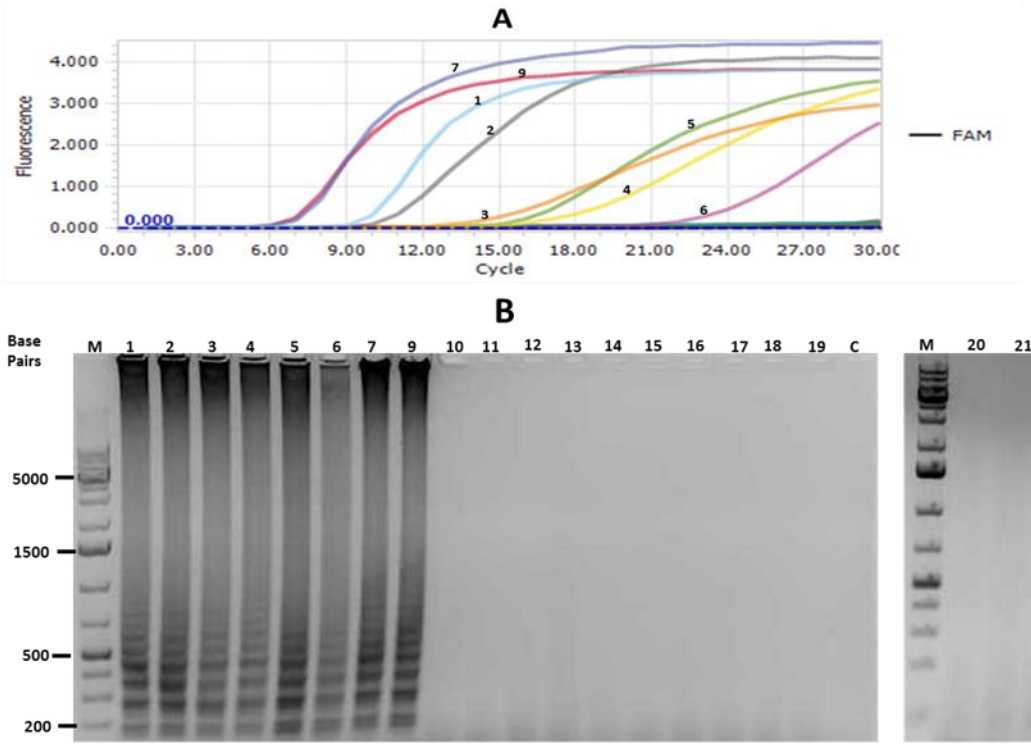

C

Sample Name	Cq	Call
1	8.62	Positive
2	9.5	Positive
3	12.57	Positive
4	14.63	Positive
5	14.2	Positive
6	20.21	Positive
7	5.99	Positive
9	5.75	Positive
10	-	Negative
11	-	Negative
12	-	Negative
13	-	Negative
14	-	Negative
15	-	Negative
16	-	Negative
17	-	Negative
18	-	Negative
19	-	Negative
20	-	Negative
21	-	Negative
22	-	Negative
Negatice control	-	Negative

Figure 4.10: Testing the specificity of the H5 detection assay. Figure 4.10A shows a real-time LAMP graph of samples amplified and labelled with specific numbers for identification. Figure 4.10B indicates the 1% agarose gel products with corresponding lanes indicating the sample number. Lane M: 1Kb DNA molecular marker, 1-22: Samples listed in Table 4.2, and C: Negative control. Figure 4.10C: Table showing the threshold values and result type with numbering corresponding to panel A and B.

4.2.7 The H7 subtype specific detection

Similar to the H5 AI viruses described in the previous section, the H7 AI viruses are also known for their high pathogenicity in poultry. Therefore, to determine whether an area is free from H7 AI subtypes, an H7 specific assay was designed. The cross reactivity of the H7 subtyping primer sets was assessed on the available 20 AI viruses of different subtypes listed and negative controls (NCDV and water) (Table 4.2). The H7 specific primer sets amplified all the H7 influenza viruses but did not amplify any other subtype (Figure 4.11A and Figure 4.11C). The H7 primer set did weakly amplify samples 4 (H5N1), 18 (H8N4), and 19 (H9N2), as shown in Figure 4.11B. This should not happen if the primers are properly designed to fit only H7 amplification. However, the non-specific or cross-reactive amplified products were clearly distinguishable from the H7 amplified products by agarose-gel electrophoresis and by the Cq values in Figure 4.11C. This is important considering that the agarose gel pattern of the false positives can be distinguished as smears rather than a laddering pattern consistent with LAMP amplification. One can easily distinguish the false positives from the true positives by looking at the gel fragment patterns in Figure 4.11 panel B. Furthermore, these false positives tended to amplify only after 25 min of the 30-min test run. It is therefore possible to eliminate them by running only a 25-min cycle or by rerunning the samples that indicate a positive outcome after 25 min of the test run. Alternatively, the samples that are positive after 25 min may be run on a 1% agarose gel to determine the laddering pattern. Depending on the instrument used to run the assay, a follow-up melting curve could be run to determine the nature of the positive run. If a different pattern to the validated one is produced, the sample can safely be reallocated as negative. The NCDV sample, together with the negative water control, was not amplified by the H7 specific primer set. One can therefore conclude that the primers were specific for H7 subtypes and the fact that the cycles were positive in as early as 4 min indicates that this is an overly suitably sensitive test for H7 detection.

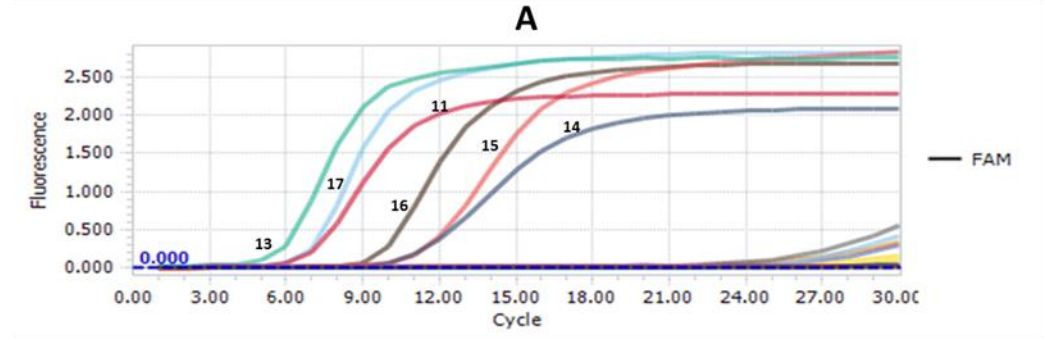

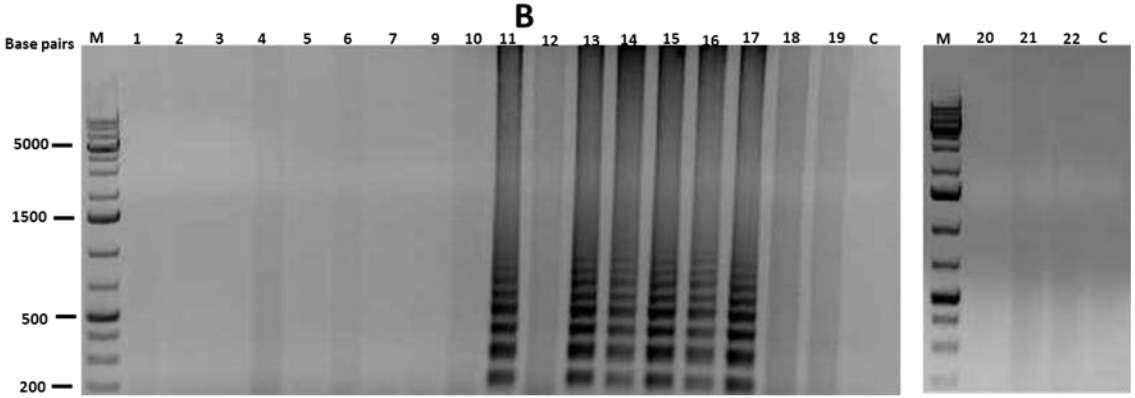

C

Sample Name	Cq	Call
1	-	Negative
2	-	Negative
3	-	Negative
4	25.06	Positive
5	-	Negative
6	-	Negative
7	-	Negative
9	-	Negative
10	-	Negative
11	5.9	Positive
12	-	Negative
13	4.27	Positive
14	9.63	Positive
15	9.58	Positive
16	8.62	Positive
17	5.7	Positive
18	23.13	Positive
19	-	Negative
20	-	Negative
21	-	Negative
22	-	Negative
Negative control	-	Negative

Figure 4.11: Testing the specificity of the H7 detection assay. Figure 4.11A shows a real-time LAMP graph of samples amplified and labelled with specific numbers for identification. Figure 4.11B indicates the 1% agarose gel products with corresponding lanes indicating the sample number. Lane M: 1Kb DNA molecular marker, 1-22: Samples listed in Table 4.2, and C: Negative control. Figure 4.11C: Table showing the threshold values and result type with numbering corresponding to panel A and B.

4.2.8 Summary of the RT-LAMP results

In summary, the RT-LAMP for the Matrix gene amplification in all the AI samples was able to detect most of the AI samples tested, except for samples 12 (H7N9), 20 (H6N8), and 21 (H5N1) that are highlighted in red in Table 4.3. The reason for the non-detection of these samples could be attributed to the fact that the sequences of these samples varied significantly with the samples that were detected, which of course would explain why the Matrix primers were not able to amplify these samples in the LAMP assay. Another reason could simply be that these three samples were not avian at all. Non-avian influenza samples, NCDV and negative control samples tested negative with the RT-LAMP for the Matrix gene amplification.

The H5 RT-LAMP assay detected all the H5 subtypes, except for sample 21 (highlighted in red in Table 4.3). This assay did not amplify the other subtypes, including the negative controls (NCDV and water). The H7-specific LAMP assay detected all H7 subtypes, except for sample 12 (H7N9) which is highlighted in red in Table 4.3. There seemed to be some non-specific amplification in the H7 assay on other subtypes which was only detected late according to the Cq values and also as viewed on the agarose gel (highlighted in grey in Table 4.3).

Table 4.3: Summary of the RT-LAMP assays for the detection of avian influenza viruses (Matrix gene, H5 and H7 detection). (+): shows that the sample is positive for either the H5 or H7 subtype, (-): shows that the sample is negative for either the AI (Matrix gene), H5 or H7. Not applicable (N/A) means that the sample was not tested using that particular method.

		Real time graphs			Agarose gels		
SAMPLE	**Labelling**	H5	H7	Matrix	H5	H7	Matrix
H5N1 inactivated antigen: ANHUI/1/2005 (H5N1) IBCDC - RG-6 07/290	1	+	-	+	+	-	+
H5N1 inactivated antigen: A/Cambodia/R040505/2007 (H5N1) NIBRG-88	2	+	-	+	+	-	+
H5N1 A/mallard/Italy/3401/05	3	+	+	+	+	+	+
H5N1 A/turkey/Turkey/1/05	4	+	-	+	+	-	+
H5N2 A/turkey/Italy/80	5	+	-	+	+	+	+
H5N2 A/turkey/Italy/1258/V05	6	+	-	+	+	-	+
H5N3 A/duck/Italy/775/04	7	+	-	+	+	-	+
H5N9 A/chicken/Italy/22A/98	9	-	-	+	+	+	+
H6N8 A/turkey/Italy/4776-52/2015	10	-	-	+	-	+	+
H7N1 inactivated antigen: AV98/00 984v00/OST/ITALY P2	11	-	+	+	-	+	+
H7N9 inactivated antigen: A/Anhui/1/2013 (H7N9) (NIBRG-268)	12	-	-	-	-	-	-
H7N1 A/turkey/Italy/1067/99	13	-	+	+	-	+	+
H7N1 A/starling/Africa/983/79	14	-	+	+	-	+	+
H7N3 A/turkey/Italy/9289/02	15	-	+	+	-	+	+
H7N4 A/mallard/Italy/4810-79/04	16	-	+	+	-	+	+
H7N7 A/macaw/England/626/80	17	-	+	+	-	+	+
H8N4 A/turkey/Ontario/6118/68	18	-	-	+	-	+	+
H9N2 A/mallard/Italy73817-34/05	19	-	-	+	-	-	+
A/Turkey/Canada H6N8 NOV84	20	-	-	-	-	-	-
A/Chick/Scotland/59 H5N1 A/S 7/89	21	-	-	-	-	-	-
New castle disease virus	22	-	-	+	-	-	+
HP-H5N2 (11060333C)	A	N/A	N/A	+	N/A	N/A	+
LP-H5N2 (12060229)	B	N/A	N/A	+	N/A	N/A	+
LP-H7N1 (12080123A)	C	N/A	N/A	+	N/A	N/A	+

Some of the samples were not detected by all the designed RT-LAMP assays as is evident in Table 4.3. These samples were 12 (H7N9), 20 (H6N8), and 21 (H5N1), which could not be detected by the Matrix specific RT-LAMP and the H5 or H7 specific RT-LAMP assays. In this particular investigation, these samples were tested using the OIE approved RT-PCR for AI detection. This assay uses a probe that always shows a true positive on the real-time graphs. Sample 1 (H5N1), which was detected in both the Matrix-specific RT-LAMP and the H5 specific RT-LAMP, was used as a positive control in the RT-PCR confirmation test. Sample 1 (H5N1) was successfully amplified by the OIE approved RT-PCR assay, while the other three samples tested (sample 12, 20 and 21) were not successfully amplified, as shown in Figure 4.12. These results correlated with all the RT-LAMP assay results. This means that the LAMP assay is comparable with the OIE recommended RT-PCR assay in terms of the specificity of sample detection. All the samples detected on the OIE primer panel were also detectable on the LAMP assay.

A

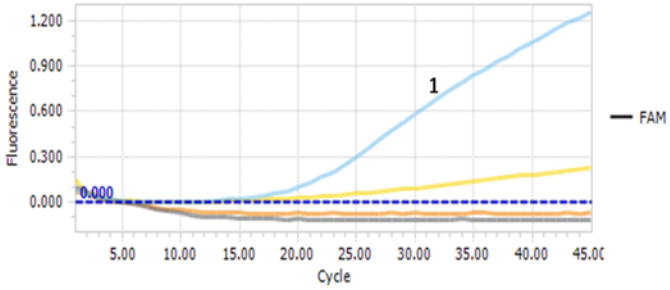

B

Sample Name	Cq	Call
1	17.94	Positive
12	-	Negative
20	-	Negative
21	-	Negative
H20	-	Negative

Figure 4.12: Verification of the RT-LAMP non-detected samples (12-H7N9, 20-H6N8 and 21-H5N1) as avian influenza or not, using the OIE approved RT-PCR detection method for avian influenza. Figure 4.12A shows a real-time PCR graph of samples tested. 4.12B: Table shows the Cq values and explanations of results indicated in Figure 4.12A.

4.2.9 LAMP vs PCR sensitivity

If one has to use a POC assay, it does have to be sensitive enough so that the advent of false negatives is reduced. It is always important when performing an assay to know what the virus detection limits of that assay are. In that way, it is possible to determine what levels of virus shedding from the host are required before the assay is able to detect the virus. To determine this aspect, a series of sample 4 (H5N1) cDNA 10-fold dilutions ranging from 10^{-1} to 10^{-9} was used to analyse the sensitivity of the RT-LAMP and the conventional real-time PCR (using F3 and B3 primers). Although the F3/B3 primers are not designed for PCR, it was important to use the same primers so that a better sensitivity comparison could be conducted. This means that the same gene, the same region, and the same size fragment amplification from both instruments and methods could be compared. The Matrix-specific RT-LAMP was used as it would cover most samples and therefore reduce bias. The detection limit for the RT-LAMP was 10^{-4} dilution factor (Figure 4.13A and Figure 4.13B), while for the RT-PCR it was 10^{-7}, as shown in Figure 4.13C and Figure 4.13D. These results show that the conventional RT-PCR is at least 1 000 times more sensitive than the RT-LAMP. The RT-PCR, however, also showed some non-specific amplification of the 10^{-8} to 10^{-9} dilutions as well as of the negative water control (Figure 4.13C). Again, this was attributed to the fact that SYBR green, which is a non-specific detection dye, was used in this experiment. This was fortunately controlled by the agarose gel results that showed the correct amplified products (Figure 4.13D). These results tend to favour the usage of PCR real-time protocols for AI detection using the Matrix gene. In other words, one would get better sensitivity when using PCR than when using LAMP assay. However, at the point-of-care, PCR protocols are not applicable for use. Even though the LAMP assay is less sensitive than the PCR

assay in the field, it is still significantly high enough to detect AI positive samples given the amount of shedding known to be in the collected samples from an active field outbreak. The samples labelled A, B and C in Table 4.3 are representative field samples that were kindly donated for this study by the Elsenburg veterinary laboratory in Stellenbosch owned by Ms Pieterse. To control for instrument variations, the Roche thermocycler was used for both tests even though it is not the instrument of choice for POC field detection.

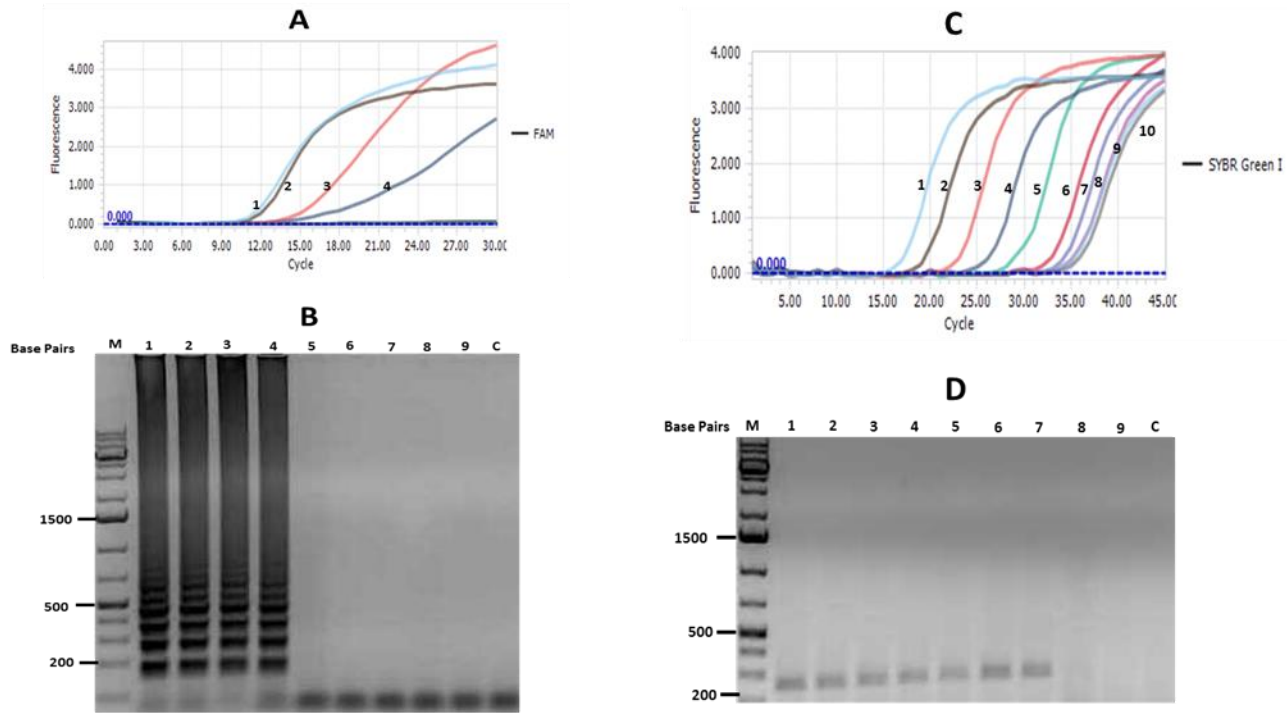

Figure 4.13: The sensitivity of LAMP in comparison to real-time PCR. Ten-fold serial dilutions of H5N1 A/turkey/Turkey/1/05 (concentration: 1.96 x 10^4 ng/mL) from 10^{-1} to 10^{-9} were prepared and tested using both these methods. Figure 4.13A shows a graph for real-time LAMP assay. The products were run on a 1% agarose gel electrophoresis (Figure 4.13B). Figure 4.13A: 1-9 shows amplification products for dilutions 10^{-1} to 10^{-9} and negative control. Figure 4.13B: M: 1Kb DNA molecular marker, 1-9: 10^{-1} to 10^{-9} H5N1 A/turkey/Turkey/1/05 dilutions, C: Negative control. Figure 4.13C shows a graph for real-time PCR assay. The products were run on a 1% agarose gel electrophoresis as shown in Figure 4.13D. Figure 4.13D: amplification products for dilutions 10^{-1} to 10^{-9} and a negative control. Figure 4.13D: M: 1Kb DNA molecular marker, 1-9: 10^{-1} to 10^{-9} H5N1 A/turkey/Turkey/1/05 dilutions, C: Negative control.

4.3 POC RT-LAMP for AI detection using the Axxin T16 isothermal instrument

As the main purpose for the design of the RT-LAMP assay was testing it for use at the point-of-care, the Axxin T16 isothermal instrument, which was designed for use at the point-of-care, was used to test some of the samples that were tested in a laboratory using the Roche thermo cycler. The Matrix-specific LAMP assay was again used to represent the H5 and H7 specific RT-LAMP assays. The Matrix-specific LAMP assay protocol was followed as before. The samples that were tested were samples 1 (H5N1), 2 (H5N1), 4 (H5N1) and 5 (H5N2), which were randomly chosen.

The Axxin T16 isothermal instrument displayed amplification signals in real time. All the samples tested positive, as shown in Figure 4.14. The detection of all these samples occurred in less than 15 min (Figure 4.14A and Figure 4.14B). The positive RT-LAMP products still showed a ladder-like pattern similar to the initial results when the Roche thermo cycler (Figure 4.14C) was used. The negative water control did not amplify, as was expected. The results are shown in Figure 4.14.

The advantage of the T16 Axxin LAMP instrument is that it can plot the graphs as fluorescence versus time, which allows one to see the real-time amplification (Figure 4.14 A). It can also plot the data as a second derivative versus time (Figure 4.14B). This second feature allows one to determine the unambiguous, exact point of amplification without necessarily having to contend with possible high background fluorescence values that may be introduced by pipetting variations. Furthermore, the instrument is light weight and can be battery operated, which makes it ideal for field usage. The adaptation of the assay to the Axxin T16 instrument makes the possibility of point-of-care detection for AI outbreaks highly feasible.

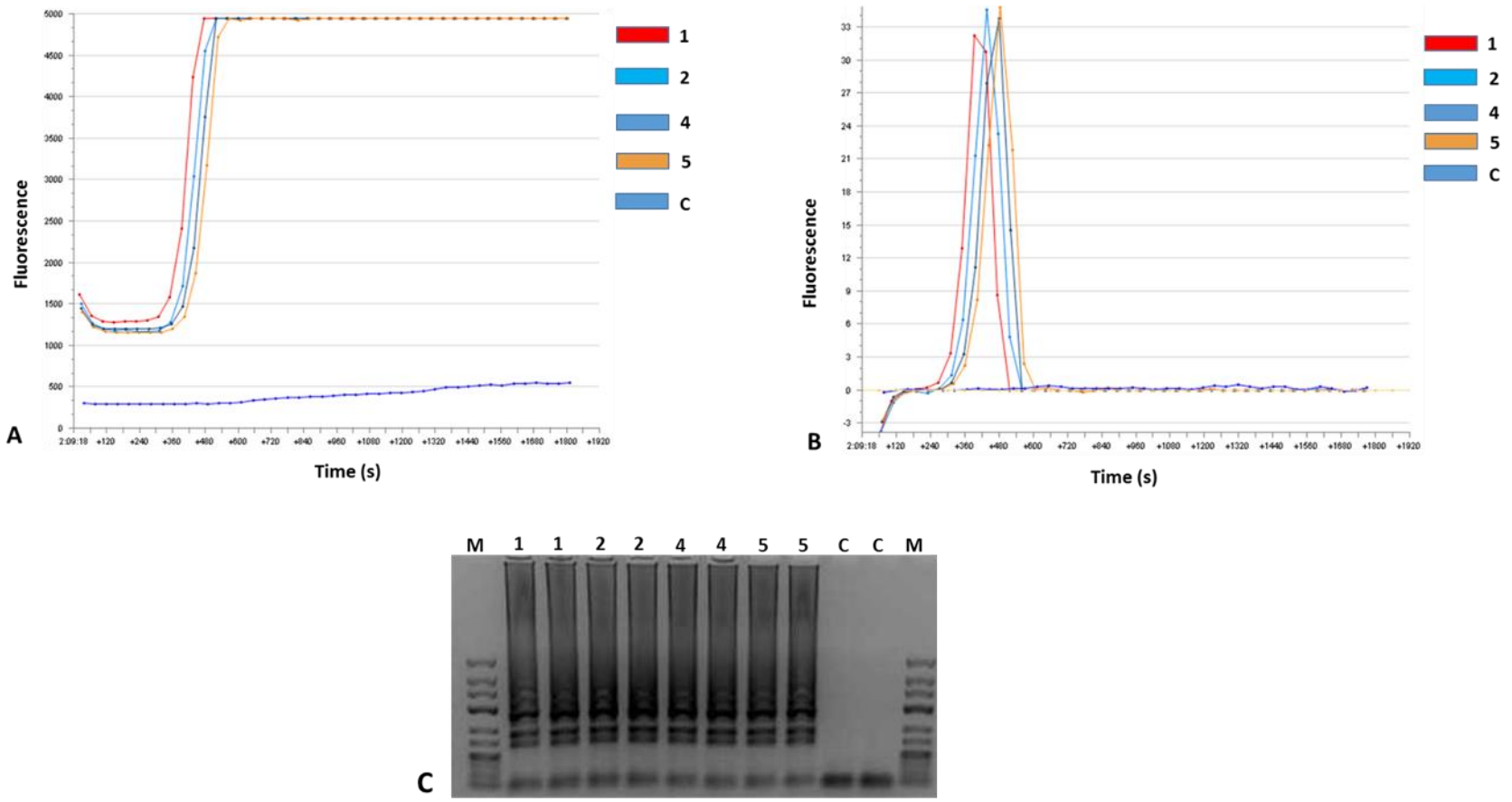

Figure 4.14: POC validation of the Axxin T16 isothermal instrument. Figure 4.14A shows the results of some of the samples (samples 1 (H5N1), 2 (H5N1), 4 (H5N1), and 5 (H5N2) from Table 4.2 which were tested in the field. Figure 4.14B shows the second derivatives of the sigmoidal graphs obtained in Figure 4.14A. Figure 4.14C shows the LAMP products that ran on a 1% agarose gel electrophoresis.

CHAPTER 5

EXPRESSION OF NON-REPLICABLE ADENOVIRUS VECTORS IN 293T, CHICKEN EMBRYO FIBROBLASTS, AND VERO CELLS: RESULTS AND DISCUSSION

5.1 Introduction

Vaccination still remains the primary and most effective strategy for the prevention and management of AI. Current licensed influenza vaccines are manufactured using embryonated chicken eggs according to a production system that was first used in the 1940s (Partridge and Kieny, 2011; Miliän and Kamen, 2015). This production system is not only labour intensive but also has other major drawbacks. For instance, in a pandemic the egg-based production system might not work due to the unavailability of eggs. Moreover, some virus subtypes, such as the H3N2, grow poorly in embryonated chicken eggs while others, including the HPAI subtype H5N1, have been shown to be lethal to chicken embryos, thus causing a production of low viral titres (Lu *et al.*, 2005; Horimoto *et al.*, 2006; Donis, 2014). Due to an increased demand for vaccines against influenza in birds and poultry, new manufacturing strategies have been introduced. The most highly favoured strategy is the use of cell culture for the production of vaccines. The first reason for this is that cell lines can be stored for future use, unlike egg-based methods that always have to be started from scratch. Secondly, in contrast to the egg-based production method, the cell-based production method can produce higher quantities of vaccines in a shorter space of time (Dormitzer *et al.*, 2012; Wong and Webby, 2013; Hilleringmann *et al.*, 2014; Miliän and Kamen, 2015). Thirdly, viruses produced in cell cultures are quite similar to field strains, unlike viruses produced in eggs that might undergo antigenic changes (Hardy *et al*, 1995; Robertson *et al.*, 1995; Robertson *et al.*, 1987; Donis, 2014). Lastly, cell-based production methods can be used for the preparation of viral seeds, thus avoiding the long process required for the egg-based method (Miliän and Kamen, 2015). Several mammalian cells have been successfully assessed for the production of influenza vaccines, which include monkey kidney cells (Vero) (Kistner *et al.*, 1998; Youil *et al.*, 2004), human embryonic retinal cells (PER.C6) (Pau *et al.*, 2001), Madin Darbi canine kidney cells (MDCK) (Rimmelzwaan *et al.*, 1998; Voeten *et al.*, 1999) and 293T HEK cells (Le Ru *et al.*, 2010; Silva *et al.*, 2016).

The aim of the investigation that is discussed in this chapter was to produce a non-replicative Adenovirus control vector in 293T HEK cells and test the produced virus in CEFs generated in-house. The decision to first test the control vector was to demonstrate whether it could infect and

express in CEFs before designing the actual Adenovirus-based vaccine for AI prevention. This part of the experiment is diagrammatically shown in parts b.1 and b.2 of the protocol workflow in Figure 3.1 (Chapter 3). One of the main aims of the larger study was to design an Adenovirus-based vector vaccine against AI in poultry. Testing the Adenovirus vector in live poultry would have been ideal, but due to ethical requirements and regulations the Adenovirus control vector was tested *in vitro* in chicken embryo fibroblasts instead. CEFs were chosen to represent poultry in this study as chicken eggs are always available in all seasons and as only one fertilized egg would be needed for this experiment. Moreover, chicken embryo development is fast as it takes between 9-11 days for the embryo to reach the desired stage for the production of fibroblasts. In contrast, other poultry embryos, such as ostrich embryos, take ~40 days to reach the required stage for use in the production of fibroblasts. Also, chicken embryo development can easily be monitored as chicken eggshell is thin enough to see through it using the egg candling method, which is a method in which a light is shone through the egg in the dark and one can then easily see how far the embryo has developed.

5.2 Preparation of Chicken Embryo Fibroblasts

5.2.1 Egg development stages

One fertilised egg was sterilised using 70% ethanol and incubated at 37ºC in a humid incubator. Egg candling was done daily. Embryo development using egg candling is usually identified either as visible veins or by the darkening of the inside of the egg. After day 1 of incubation, the embryo appeared without a shadow. It was only after day 3 of incubation that the upper 1/5th of the egg started appearing darker. On day 4 and day 5, the shadow started getting darker. On day 6 and day 8, the upper dark part of the egg extended around the air sac. On day 11, the entire egg, except for the air sac, was darker. These stages are shown in Figure 5.1. It is usually on the 11th day that an embryo is suitable for fibroblast preparation, and this was the case in this study (Figure 5.2).

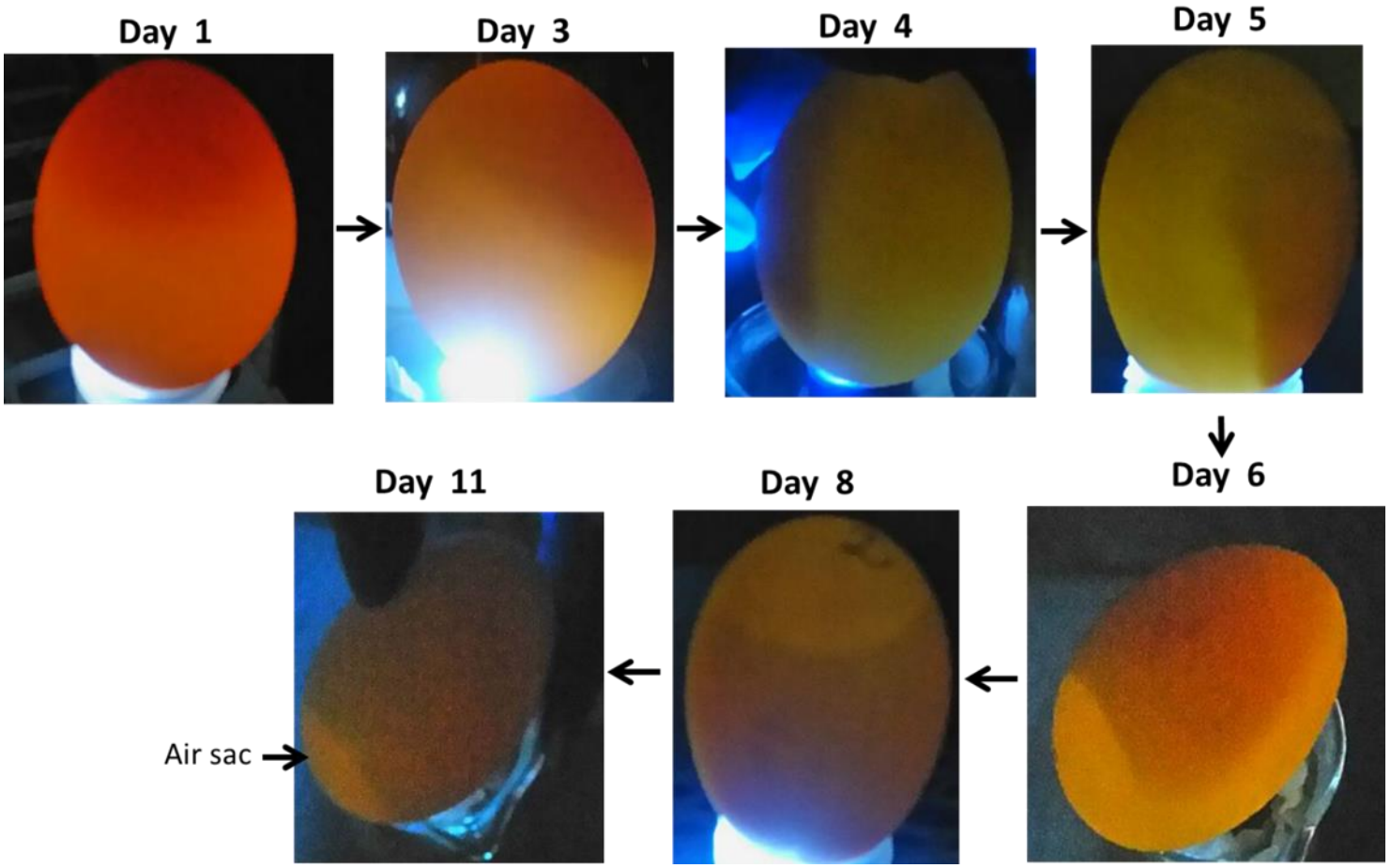

Figure 5.1: Chicken embryo development in a fertilised egg from day 1 to day 11

After 11 days of fertilised egg incubation, the egg was cracked open. The embryo was separated from the rest of the egg contents, rinsed in PBS, and placed in a sterile glass petri-dish in PBS. The chicken embryo was not fully differentiated. Only the eyes, beak and limbs had started to develop (Figure 5.2). No feathers, eyelids, or internal organs had developed yet. This was desirable as fibroblasts are generated from the skin cells only. Should the embryo have passed the stage of development as depicted in Figure 5.2 (i.e., the development of other parts of the body such as feathers), the types of cells produced would have been a mixed culture of fibroblasts, epithelial cells, and other cells. What was needed for reliable results was a pure culture consisting of fibroblasts only. As the desired stage of embryo development had been reached, fibroblasts were therefore successfully generated (Figure 5.3).

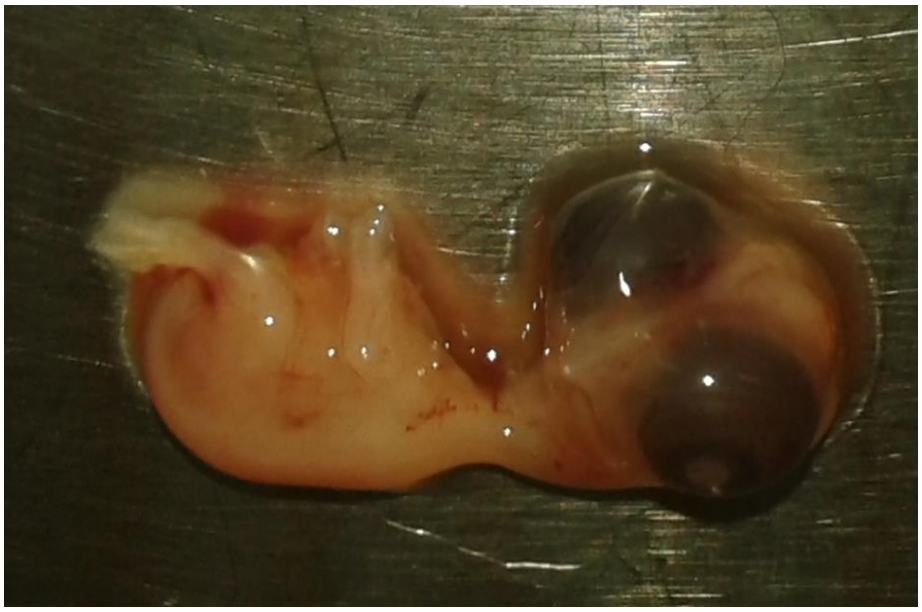

Figure 5.2: An 11-day-old chicken embryo. The embryo was separated from the rest of the egg contents, rinsed in PBS, and placed in a sterile glass petri-dish in PBS.

5.2.2 Chicken embryo fibroblasts viewed under the microscope

The chicken embryo fibroblast cells were routinely cultured at 37ºC in a 5% CO_2 in DMEM supplemented with 10% FBS and 0.05 mg Gentamicin. As the fibroblasts were still at their earliest stage of development, their growth rate was very high in the sense that on every third day they reached approximately 95% confluency. However, as the fibroblast passages went up, the growth rate decreased somewhat. The medium was changed once every three days and replaced with a fresh one. The chicken embryo fibroblasts were sub-cultured once every five days at a confluency of 90%. The fibroblasts appeared to have an elongated and triangular morphology with shiny rings around the cell body. This is shown in Figure 5.3.

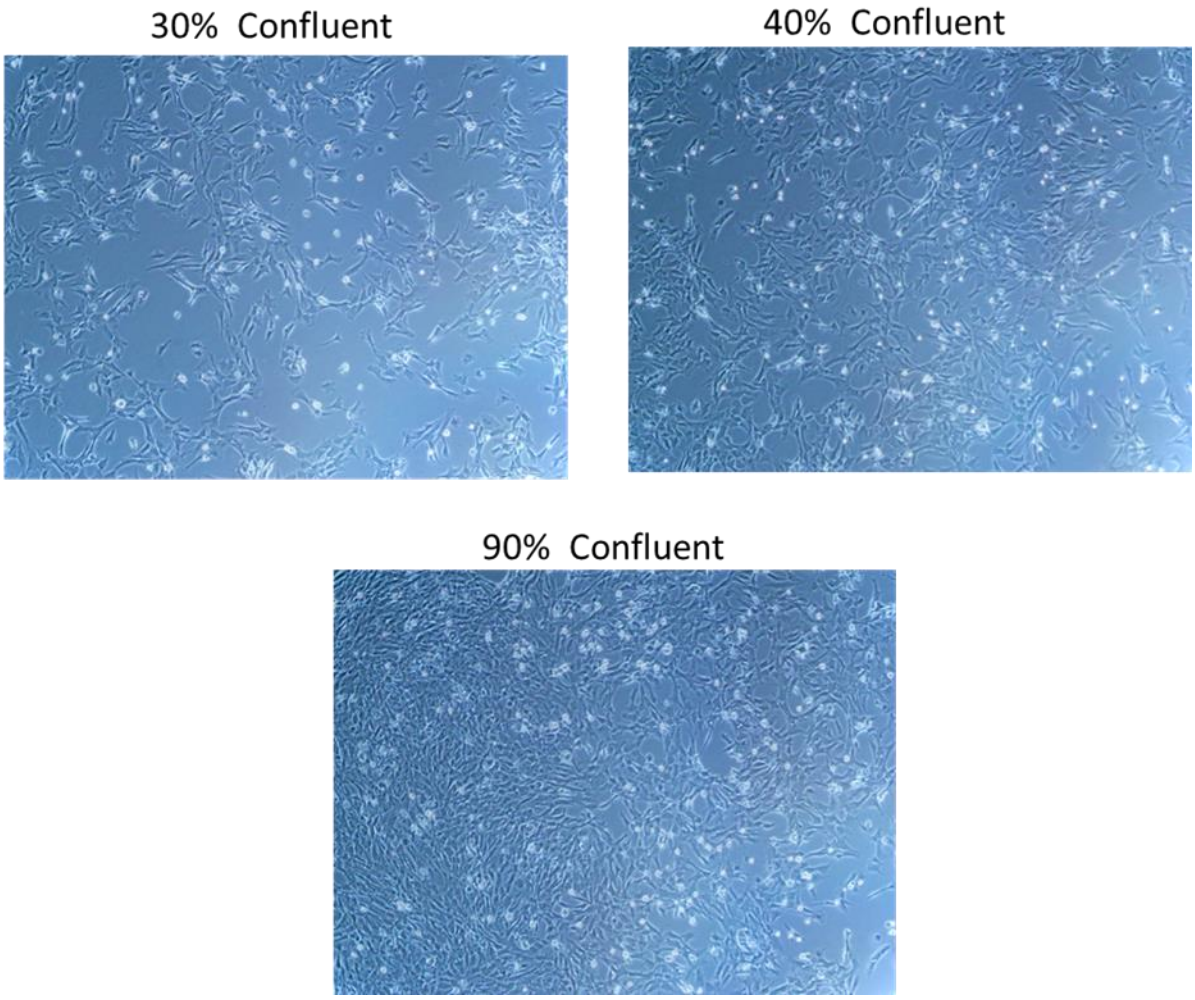

Figure 5.3: Passage three of chicken embryo fibroblasts at different confluence points. Images taken under an OLYMPUS BX53 microscope using phase contrast at 10x magnification.

5.2.3 Amplified Adenovirus: crude virus using PCR

Replication deficient Adenovirus vector (pAd/CMV/V5-GW/lacZ) was infected into 293T HEK cells with 100µL of the stock virus. After a complete CPE had been reached, the culture medium and pellet were collected and separated by centrifugation. Adenovirus DNA was extracted from the supernatant and PCR was performed to detect the presence of the Adenovirus produced in the 293T cells. The expected product size of 1017bp was amplified from the Adenovirus DNA (Figure 5.4). This indicated that the Adenovirus had successfully infected the 293T cells and was also replicated in the cells, thus increasing the Adenovirus titre. A high virus titre is required for infection of target cells in order to achieve a significant transduction efficiency.

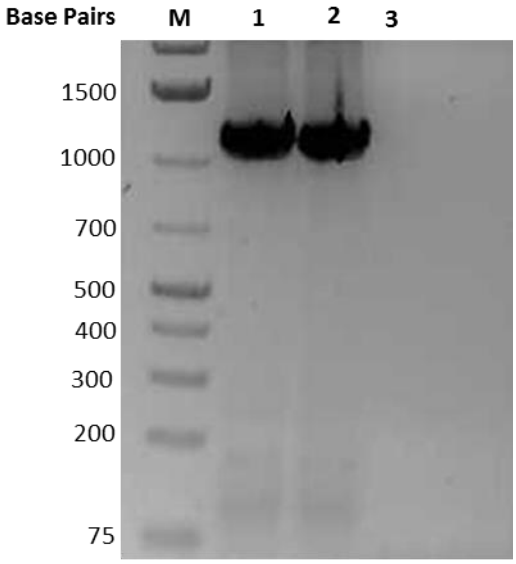

Figure 5.4: Test for the presence of Adenovirus produced in 293T cells. PCR was done using the viral DNA of the Adenovirus produced in 293T cells. The PCR products were run on 1% agarose gel electrophoresis. Lane M: 1Kb plus DNA ladder (#sm1333), Lanes 1 and 2: Crude Adenovirus supernatant PCR product, Lane 3: Negative control

5.3 Expressions of the Adenovirus Protein

5.3.1 Expression of the Adenovirus (pAD /CMV/V5-GW/lacZ control plasmid) protein in 293T cells

It was important to detect whether the desired proteins were translated, as this is the method that shows whether the virus multiplied within the host cell line . This part of the investigation was thus vital as this translation would show that the Adenovirus was able to multiply and that this method could be used for the future production of a desired vaccine for AI in poultry. The Adenovirus (pAD /CMV/V5-GW/lacZ) infected 293T cells were collected after a complete CPE had been formed. The lysates of both the infected and non-infected cells were sampled into SDS-PAGE and transferred into a nitrocellulose membrane. The protein was probed by mouse anti-V5 and the bound antibody was detected by goat anti-mouse IgG-HRP and visualised with the Gel DocTM XR + Documentation system. As depicted in Figure 5.5, four bands with a molecular weight of 120 kDa were detected in the lysates of 293T infected by the Adenovirus (pAD /CMV/V5-GW/lacZ), but not in non-infected cells. This is clearly visible in Figure 5.5B, demonstrating that the V5 protein expressed in pAD/CMV/V5-GW/lacZ was expressed correctly in 293T cells.

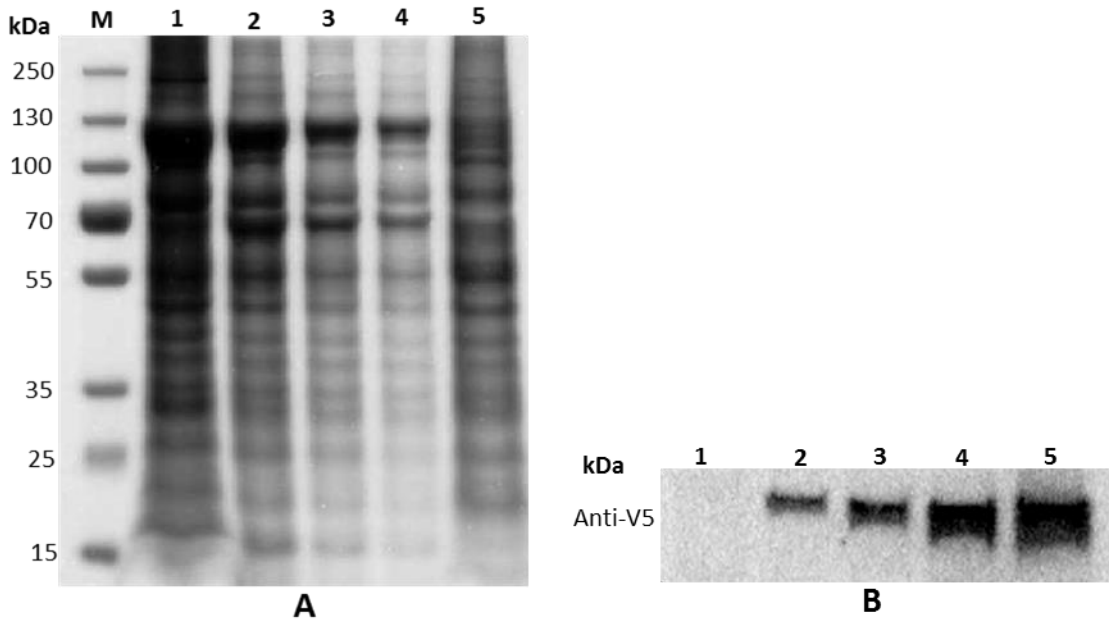

Figure 5.5: A: SDS-PAGE gel of protein extracted from 293T cells infected with Adenovirus vector. Lane 1: 250kDa protein ladder (Thermo Scientific). Lane 2-5: different volumes (10, 5, 2 and 1 µL) of 293T cells' protein infected with Adenovirus vector. Lane 6: uninfected 293T cells' protein. B: western blot analysis of the V5 epitope protein expressed in Adenovirus (pAD /CMV/V5-GW/lacZ) infected 293T cells. Lane 1: uninfected 293T cells. Lane 2-5: 293T cells infected with Adenovirus vector.

5.3.2 Expression of the Adenovirus (pAD /CMV/V5-GW/lacZ control plasmid) protein in 293T, CEFs and Vero cells using western blot analysis

Western blot analysis was conducted in a similar way as described in section 5.3. After three days of incubation, the Adenovirus (pAD /CMV/V5-GW/lacZ) infected 293T cells, Vero cells and CEF cells were collected. The lysates were separated on SDS-PAGE, transferred to nitrocellulose membranes, and incubated with mouse anti-V5 followed by goat anti-mouse IgG-HRP. As is shown in Figure 5.5B, Adenovirus (pAD /CMV/V5-GW/lacZ) infected 293T cells highly expressed the V5 protein compared to the Adenovirus (pAD /CMV/V5-GW/lacZ) infected Vero cells, which showed no expression of the V5 at all (Figure 5.6B). The CEFs, on the other hand, did show an expression of the V5 protein, but it appeared to be weak (Figure 5.6B). These results were expected as there was no sign of CPE in either the Vero cells or the CEFs during the incubation period, thus indicating that there was no virus replication in these cells. The E1 gene of the Adenovirus is responsible for the Adenovirus replication in mammalian cells. However, this gene

was removed from the Adenovirus (pAD/CMV/V5-GW/lacZ) used in this study, thus making it replication deficient (Gao *et al.*, 2006; Jones *et al.*, 2011; Silva *et al.*, 2016). The absence of viral replication was due to the E1 gene which was not expressed in either the Vero cells or the CEFs. In the 293T cells, however, the E1 gene was expressed in the genome, which explained why the CPE occurred 48 hours post infection and became nearly complete after 72 hours. The high expression of the V5 protein in the infected 293T cells also indicated that the E1 gene was expressed in the 293T genome. Even though the V5 expression in CEFs was weak, it still suggests that chicken embryo fibroblasts can be used as Adenovirus cargoes for immunisation purposes. No V5 expression was detected in cells not infected with the Adenovirus (pAD /CMV/V5-GW/lacZ), as is evident in Figure 5.6B.

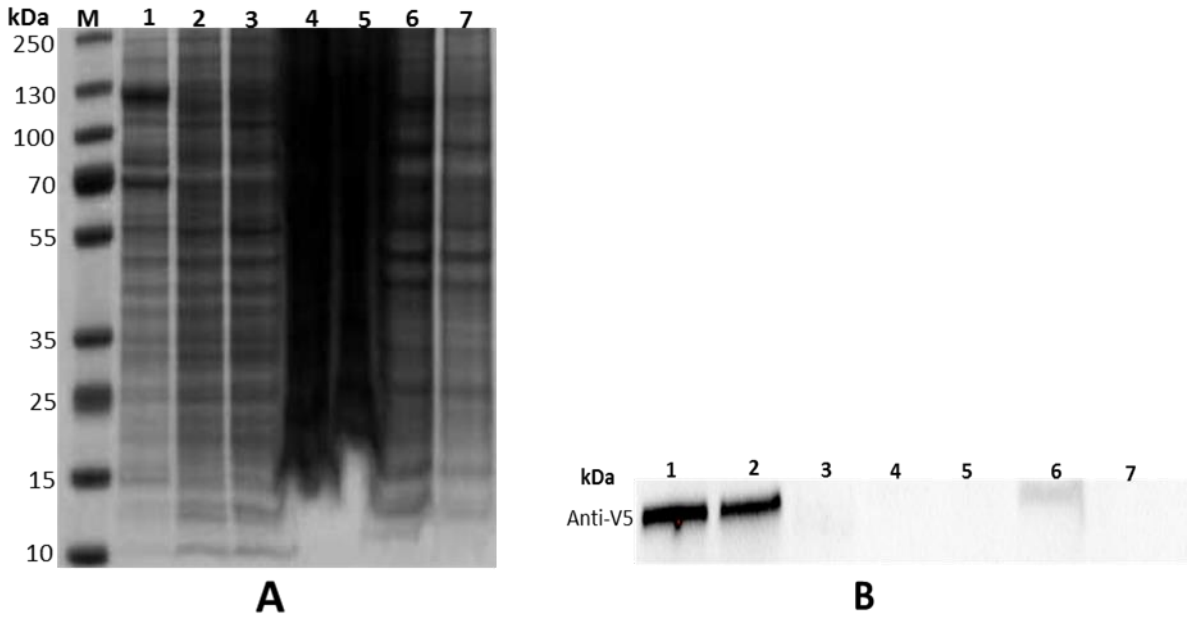

Figure 5.6: A: SDS-PAGE gel of protein extracted from various cell lines and infected and uninfected with Adenovirus vector (pAD /CMV/V5-GW/lacZ). Lane M: 250kDa protein ladder (Thermo Scientific). Lane 1: Adenovirus protein positive control. Lane 2: 293T cells' protein infected with Adenovirus vector. Lane 3: 293T cells' protein uninfected. Lane 4: Vero cells infected with Adenovirus. Lane 5: Vero cells uninfected. Lane 6: CEFs infected with Adenovirus vector. Lane 7: CEFs uninfected. B: western blot analysis of the V5 epitope protein expressed in Adenovirus (pAD /CMV/V5-GW/lacZ) infected 293T cells, Vero cells, and CEFs. Lane 1: Adenovirus protein positive control. Lane 2: 293T cells' protein infected with Adenovirus vector. Lane 3: 293T cells' protein uninfected. Lane 4: Vero cells infected with Adenovirus. Lane 5: Vero cells uninfected. Lane 6: CEF cells infected with Adenovirus vector. Lane 8: CEFs uninfected.

CHAPTER 6

RESULTS AND DISCUSSION: EXPRESSION OF NON-REPLICATIVE, RECOMBINANT ADENOVIRUS VECTOR EXPRESSING THE NCDV MATRIX GENE IN CHICKEN EMBRYO FIBROBLASTS

6.1 Introduction

It was demonstrated in Chapter 5 that the Adenovirus vector undoubtedly infected and expressed in CEFs. This finding positively supports the argument that the vector could be used as a functional delivery system in poultry. Therefore, one could confidently design a vaccine using the same Adenovirus vector as a delivery system in poultry. However, the regulatory framework in South Africa does not allow scientific experimentation using live birds for the purpose of vaccine design to curb and ultimately eradicate avian influenza. To do this work and still fall within the permitted regulations, a virus close to AI had to be identified and targeted. The closest virus for which such work is allowed is NCDV, which was thus targeted in this study.

The broader study attempted to answer two questions:

1. Is it possible to significantly reduce the time period that it takes to detect conclusively that a viral outbreak occurred in livestock, specifically in poultry?

2. How effectively can one design and propagate a vaccine as soon as an outbreak has been detected in a manner that will permit targeting and eradicating a specific viral outbreak in poultry?

The discussion in the section below attempts to answer the second question. In the sections that follow, an attempt is made to show the effectiveness of the proposed protocol for vaccine design to combat AI in poultry (see step b.3 in the workflow diagram, Figure 3.1).

6.2 Authentication of the NCDV Samples for Desired Gene Selection before Cloning

Before one proceeds to insert/clone a gene of interest for vaccine design, one needs to verify the authenticity of the gene function, its nucleotide sequence, and its possible suitability for eliciting the expected immunological response once cloned into the vector of choice. For this reason, RNA was extracted from samples H3090/11 and H3343/11 containing the NCDV from an outbreak at a commercial farming operation.

The inactivated specimens were generously donated for research purposes by the Rainbow farms. Using OIE approved NCDV detection PCR primers, PCR was performed to confirm the identity of the virus. The amplification results are presented in Figure 6.1, and these indicate that approximately 120bp PCR product was successfully amplified. This expected size fragment confirms that the samples actually contained NCDV as reported.

For subsequent experiments, both the H3090/11 and H3343/11 samples were utilised for downstream experiments.

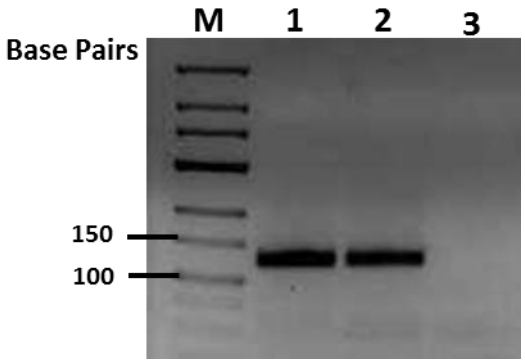

Figure 6.1: PCR products for NCDV samples (H3090/11 and H3343/11). M: low range DNA ladder (Thermo Scientific # SM1193). 1: H3090/11, 2: H3343/11, 3: Negative control

A verification process was followed to confirm that the samples contained NCDV. The gene of interest in this case was the Matrix gene. The reason for the selection of this gene was the Matrix protein product's structural arrangement of the outer shell of the NCDV particle. This arrangement is very similar to that of the AI Matrix gene. Moreover, the protein domains of the two viruses are also largely similar. To verify and compute the nucleotide sequence of the NCDV Matrix gene, total genomic DNA from sample H3090/11 was sequenced in-house using the PGM next generation sequencer procured from Thermo.

To elicit the desired immunological response − or at least to target the desired immunological response − the correct Matrix gene protein product should fold as expected in its native viral state. Furthermore, the sections/motifs that are generally exposed to elicit immunological response should be included in the cloning exercise.

Not knowing the exact sections responsible for this part on the Matrix gene, it was critical that as much as possible of the Matrix gene was incorporated into the cloning vector. In that way the possibility that the cloned gene would not elicit the immunological response, or that it would elicit

a different response, was minimised. However, only when challenge studies have been performed on live animals shall we be certain whether the desired immunological protection is conferred using this approach. This was however not the main thrust of the study and ethical approval for clinical challenge studies was never sought. For this reason, and to remain within all ethical parameters, the Matrix gene was obtained from sequencing the NCDV H3090/11 to design primers specific for this gene. Ten primer sets were generated that were specific to the input template. Of these 10 sets that were generated with different overlapping sizes, 12 primers were grouped together, aiming to put them into sets from which to choose a set that would amplify the largest fragment for later use for cloning into a vaccine vector. In total, 6 sets were grouped together, as was indicated in section 3.6.2.1. These 6 grouped sets were tested in PCR using the cDNAs of the NCDV. The results are shown in Figure 6.2. Of the two samples that were tested (sample A H309011 and B H3343/11), sample A was always detected, and the primer sets always appeared to be specific to this sample. This made sense because the primer design was performed using the sequence of sample A. Set 5 MF8A forward primer (5'-ATAGGATCCAGCGCCTTGAC-3') and MR5 reverse primer (5'-GTATTTGGCAAGGG TGTGCC-3') amplified the largest fragment of 956bp in sample H3090/11, as shown in Figure 6.2. The purified chosen fragment is depicted in Figure 6.3. This set of primers and the amplified fragment were then chosen for use in the cloning experiments to develop a vector vaccine.

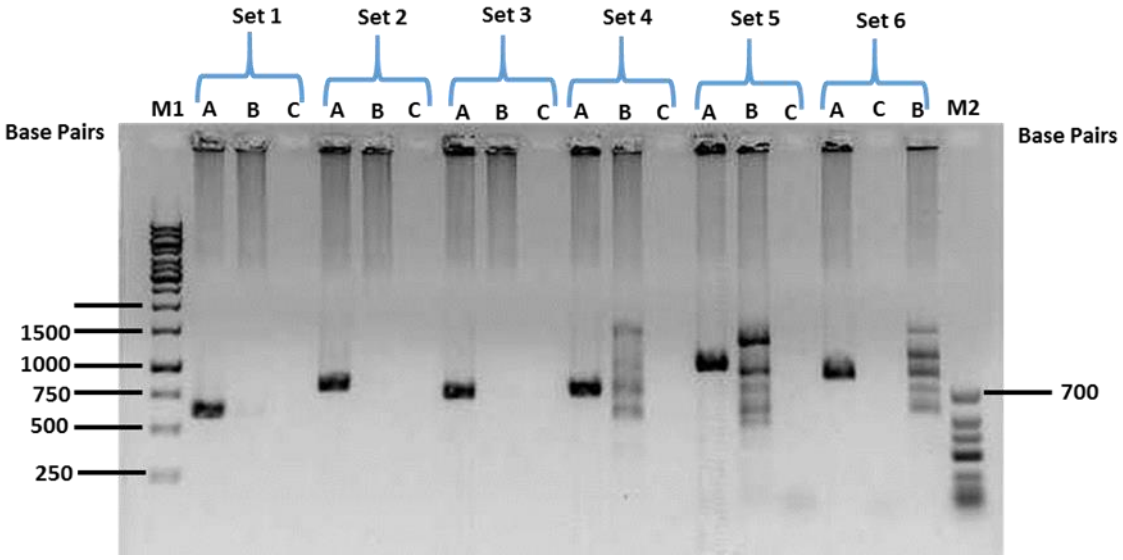

Figure 6.2: PCR products of the NCDV Matrix gene of the H3090/11 and H3343/11 samples using 6 different designed primer sets. M1: 1Kb plus DNA ladder (Fermentas, #sm0311). A: NCDV sample H3090/11, B: NCDV sample H3343/11, C: Negative control, M2: low range DNA ladder (Thermo Scientific, #sm1193). Set 1: MF1A forward primer and MR1A reverse primer, Set 2: MF1A forward primer and MR5 reverse prime, Set 3: MF1A forward primer and MR6 reverse primer, Set 4: MF8A forward primer and MR1A reverse primer, Set 5: MF8A forward primer and MR5 reverse primer, Set 6: MF8A forward primer and MR6 reverse primer. The primer sequences are presented in section 4.5.1 (Table 4.4).

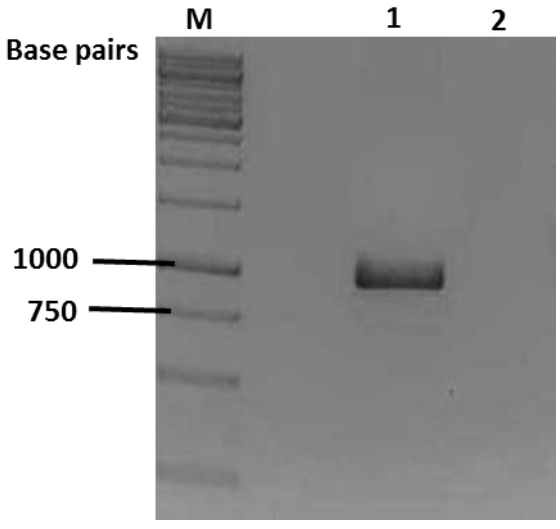

Figure 6.3: Purified PCR product of a NCDV H3090/11 amplified using set 5 of the Matrix specific gene. M: 1Kb plus DNA ladder, 1: gel purified Matrix gene PCR product, 2: Negative control (gel with no PCR product gene purified)

6.3 Primary Cloning of the Gene of Interest as a Step in Devising a Vaccine Model

The purified PCR product (see section 6.2) was amplified using cloning primers to produce a blunt end PCR product. Such primers are designed in a manner that includes digestion enzyme sites so that they are able to facilitate integration of the gene of choice into the donor vector directionally. The amplification was successful, resulting in the expected 956bp PCR product (Figure 6.4). The primers used for this purpose were designed with overhangs on either side of the amplified fragment. The necessary sticky ends were introduced by adding the CACC sequence at the 5' end of the forward primer. The successful amplification (Figure 6.4) therefore confirms that the overhangs were successfully introduced on the Matrix gene PCR product, thus rendering this product ready for cloning into the pENTR™/D-TOPO® vector.

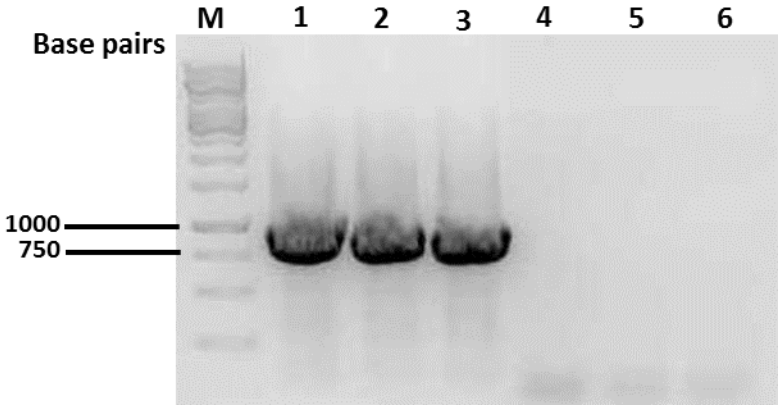

Figure 6.4: PCR products of the Matrix gene with the added overhangs/blunt end PCR products using the designed cloning primers. M: 1Kb plus DNA ladder (Fermentas, #sm0311), 1-3: Blunt end NCDV Matrix gene PCR products, 4-6: Negative control

The blunt end PCR products were purified from the gel and directionally cloned into the pENTR™/D-TOPO® vector, which is a donor/intermediate vector. Purification was necessary to increase the efficiency of cloning. To confirm that the Matrix gene was successfully cloned in the vector, amplification using set 5 (MF8A and MR5) PCR primers was performed using PCR. Once again, the amplification of the NCDV Matrix gene was successful, indicating the presence of the NCDV Matrix gene within the pENTR™/D-TOPO® vector (Figure 6.5).

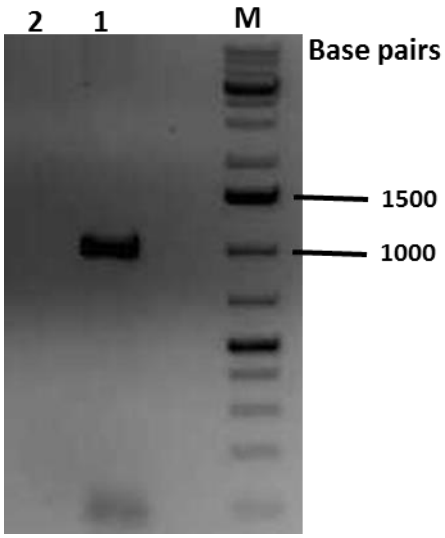

Figure 6.5: PCR products of the NCDV Matrix gene cloned into the pENTR™/D-TOPO® vector. M: 1Kb plus DNA ladder (Thermo scientific, #SM1333), 1: NCDV Matrix gene PCR product, 2: Negative control

6.4 Secondary NCDV Matrix Gene Cloning through Homologous Recombination into pAD/CMV/V5-DEST™

For a vaccine to be effective in combating poultry viral outbreak it needs to be propagated in a vector that is known to be compatible with the species of interest. Therefore, as the Adenoviral vector has been successfully utilised in chickens (Gao *et al.*, 2006; Toro and Tang, 2009; Singh *et al.*, 2010; Baron *et al.*, 2018), it was selected for this study. However, this vector has never been licensed for commercial application and therefore it is mainly used as a research tool. Other vectors will have to be investigated in the same manner if possible, commercialisation is to be pursued.

To create an expression clone (Adenovirus vector expressing the NCDV Matrix gene), an LR recombination reaction using the attL-containing entry clone (pENTR™/D-TOPO®) expressing the NCDV Matrix gene and the attR containing the destination vector (pAD/CMV/V5-DEST™) was performed. Once homologous recombination had been completed, the purified plasmid DNA was tested using PCR to confirm the success or failure of the process. To confirm the presence of the gene of interest in the final vector, one needs to use one primer that is specific for the gene of interest, which was the NCDV Matrix gene in this case. Secondly, a primer specific for the vector should be used as well, as in that way the amplified product will include the actual inserted gene as well as part of the original vector, thus amplification will confirm cloning success as well as the correct directional cloning.

For this reason, the sets of primers selected for this purpose were the Matrix gene reverse primer (MR5) and the Adenovirus forward primer attaching to the T7 promoter of the vector. The compatibility of the melting temperature of the primers was critical to encourage specific fragment amplification. Furthermore, seeing that the expected fragment was over 1Kb in length, the choice of the amplification polymerase enzyme was vital. For this reason, the KAPA hotstart master mix was selected due to its high-fidelity property where long fragments are concerned. The 1149bp PCR product was detected as anticipated (Figure 6.6). This indicates that: (1) the LR recombination was successful; (2) the expression clone was properly constructed; and (3) the NCDV Matrix gene was in the correct orientation as the Matrix gene reverse primer and the forward primer attaching to the T7 promoter of the vector were used.

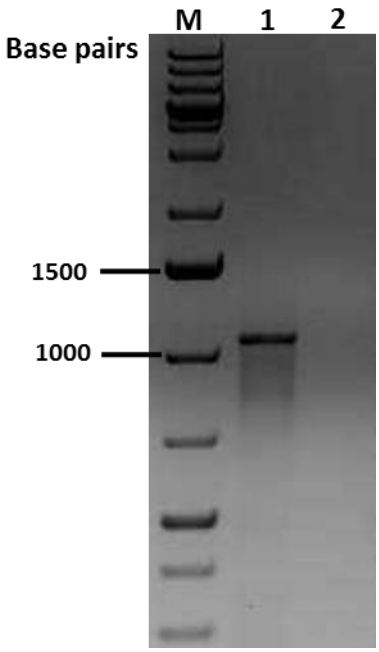

Figure 6.6: Image depicting 1% agarose gel electrophoresis of the PCR products of the NCDV Matrix gene. M: 1Kb plus DNA ladder (Thermo Scientific, # sm1333). 1: PCR product of the NCDV Matrix gene plus part of the T7 promoter of the Adenovirus vector, 2: Negative control

6.5 Recombinant Virus Vaccine Confirmation and Authentication

The choice of Adenovirus, which is replication deficiency, was based on two desired functions. First, it can be used as is without necessitating attenuation because it is unlikely to replicate without the necessary E1 gene factor required for its replication within the host cells. Therefore, vaccine design using this vector is efficient as one can control the virus concentration by

effectively determining the required dose during manufacture. Manufacturing literally involves propagating the virus in 293T cells that contain the replication factor E1 gene, which is absent in poultry (Bett *et al.*, 1994; Tatsis and Ertl, 2004; Kovesdi and Hedley, 2010; Ura *et al.*, 2014; Silva *et al.*, 2016; Ma and Guan, 2018). Secondly, the vector is compatible with other formulation regimes that are known to further elicit and enhance immune response to the vaccine.

6.5.1 Propagation of the Adenovirus vector pAD/CMV/V5-DEST™ expressing the NCDV Matrix gene

The 293T cells were transfected with PacI digested pAD/CMV/V5-DEST™ expressing the NCDV Matrix gene. This was done to expose the left and right viral ITRs and to remove the bacterial sequences for proper packaging of the viral proteins. To show that the 80% CPE observed in the cells was due to the multiplication of the virus, the cells and the medium, were collected and lysed using the freezing/thaw method, thus leaving the viruses floating in the medium. At this point, if a functional virus was formed, it would indicate that the Adenovirus propagated well, hence the cloning of the gene of interest had not affected the function of the genes involved in the replication mechanism of the virus. It would therefore be necessary to verify whether the Adenovirus propagated included the cloned gene of interest. If it did, this would indicate successful cloning of the gene of interest while retaining original and full virus functionality. The viral DNA was subsequently extracted from the medium. PCR amplification was then performed to test whether the viral DNA that was extracted contained the NCDV Matrix gene using the MF8A and MR5 Matrix specific primers. As expected, the 956bp Matrix gene was successfully amplified as shown in Figure 6.7A. It therefore seemed to indicate that the transfection of the secondary vector into 293T cells and subsequent free infection of the 293T cells by packaged viruses had been effectively accomplished and that the viruses had successfully multiplied in the 293T cells. This confirmed the possibility of propagating the virus as an effective vaccine for Newcastle disease should the vaccine prove to be effective clinically.

In a typical virus production facility, seed virus stocks are usually kept and used for batch propagation of the viral vaccine. The results stock that resulted as described above could thus have been used as seed stock if locked in such a bank for speedy propagation of virus vaccine formulation in future production cycles.

For actual batch production to be formulated and packaged accordingly, it was necessary to use virus seed stock to infect appropriate host cell lines, in this case the 293T cells. To mimic this process, two samples were used for comparison, namely the pure Adenovirus control with no inserted gene and the vector with the Matrix gene. Two petri-dishes of 293T cells were prepared. At 80% confluency, one dish of cells was infected with 200µL of the Adenovirus control while the

other dish with cells was infected with the Adenovirus with the Matrix gene. Three days later, 100% CPE was reached in both dishes. The media were collected from both the experiment and control vector dishes. Adenovirus DNA was then extracted from the crude (non-purified) viruses. PCR was performed using the extracted viral DNA to check whether batch production had been successful. The Matrix gene reverse primer was used together with the T7 promoter forward primer. It was evident that the 1149bp Matrix gene, plus part of the T7 promoter of the Adenovirus, had been successfully amplified (Figure 6.7B).

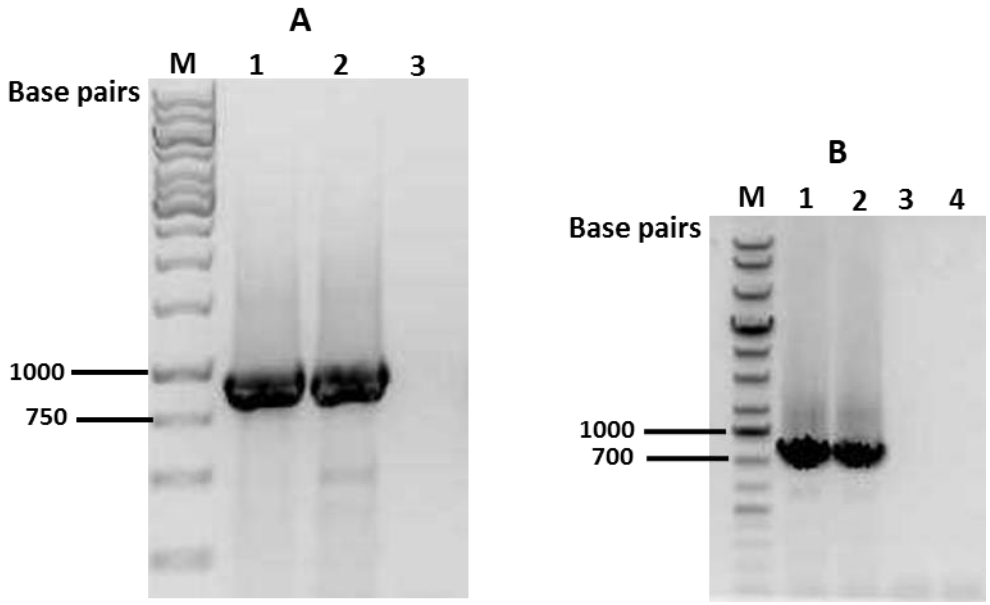

Figure 6.7: Images of 1% agarose gel electrophoresis. Image A: M: 1Kb plus DNA ladder (Fermentas, #sm0311), 1-2: NCDV Matrix gene PCR product. 3: Negative control. B: M: 1Kb plus DNA ladder (Thermo Scientific, # sm1333), 1-2: PCR products of the Matrix gene plus a part of the T7 promoter of the Adenovirus vector, 3: Negative control

The propagation of the virus and the subsequent amplification of the desired fragment confirmed two facts. First, that the virus structure was compatible with virus propagation as had been expected of Adenovirus within an appropriate host cell line. It further affirmed that the replicated Adenovirus contained the gene of interest, in this case the NCDV Matrix gene. However, whether the gene of interest was in effect being expressed in this process was not necessarily clear at this stage. It was thus argued that a protein product of the gene of interest was required to elicit immunological response within the target animal for which the vaccine was intended.

6.5.2 Next generation sequencing (NGS) for the Adenovirus vector pAD/CMV/V5-DEST™ expressing the NCDV Matrix gene

To further verify that the Adenovirus propagated included the cloned gene of interest, NGS was performed on the viral DNA. The sequencing results that are presented in Figure 6.8 show that the pAD/CMV/V5-DEST™ vector on its own was 36686bp in size. During the process of recombination, part of the sequence from the pENTR™/D-TOPO®, including the Matrix gene, replaced the region between bases 1414 and 3657, thus reducing the new designed vector to a smaller size of 35465bp. Figure 6.8 shows only part of the vector from 25021bp to 26220, with the Matrix gene inserted from 25142bp to 26048bp. This is highlighted in yellow in Figure 6.8.The pink highlights the DNA sequence that was transferred from the pENTR™/D-TOPO® into the pAD/CMV/V5-DEST™ following LR recombination. Both the inserted Matrix gene and the sequence recombined in the pAD/CMV/V5-DEST™ show that the cloning process was not only successful, but that the Matrix gene was inserted in the correct orientation.

The sequencing results also revealed that the V5 epitope was present in the pAD/CMV/V5-DEST™ virus from 26,165-26,202bp (highlighted in green in Figure 6.8), while in the pAd/CMV/V5-GW/lacZ control vector the epitope was located from 4578-4619bp (highlighted in green in Figure 6.9). In both these vectors, the V5 epitope was in the correct codon frame.

Figure 6.8: Part of a sequence of the pAD/CMV/V5-DEST™ vector expressing the NCDV Matrix gene. The part of the sequence highlighted in yellow shows the Matrix gene inserted from 25142bp to 26048bp. The pink highlights the DNA sequence that was transferred from the pENTR™/D-TOPO® into the pAD/CMV/V5-DEST™ following LR recombination

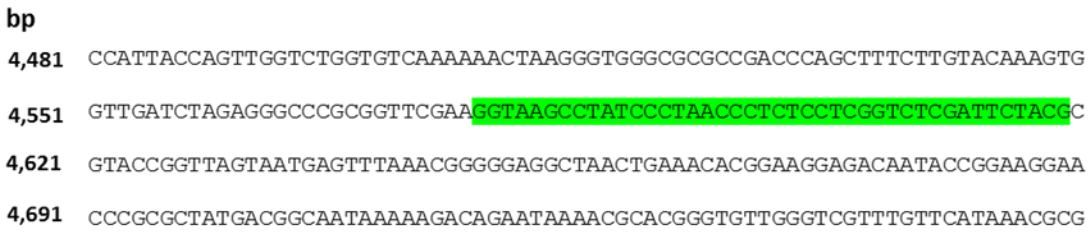

Figure 6.9: Part of a sequence of the pAd/CMV/V5-GW/lacZ control vector showing the position of the V5 epitope highlighted in green

6.5.3 Assessing the RNA expression of the recombinant Adenovirus in 293T cells

The 293T infected with the Adenovirus construct expressed the NCDV Matrix gene for 2, 6, 12, and 24 hours in separate wells. Non-infected control cells were also included in the experiments and RNA extraction was performed on both the infected and non-infected cells. cDNA was synthesised from the extracted RNA and real-time PCR (RT-PCR) was performed to test the Adenovirus construct expressing the NCDV in the 293T cells. The results showed successful amplification of the NCDV Matrix gene plus a part of the T7 promoter of the Adenovirus vector (Figure 6.10). All the infected experimental cell sets that contained the viruses showed a high expression of the NCDV Matrix gene with an anticipated PCR product size of 1149bp. This result is presented in Figure 6.10 panel 4. However, the expression of the recombinant Adenovirus after a 2-hour infection time in 293T cells was lower than after 6 to 24 hours' infection time. This is attributed to the fact that most of the cells might not yet have been infected by the virus after a 2-hour incubation period, thus rendering the RNA expression in these cells lower in comparison to the other infected cells.

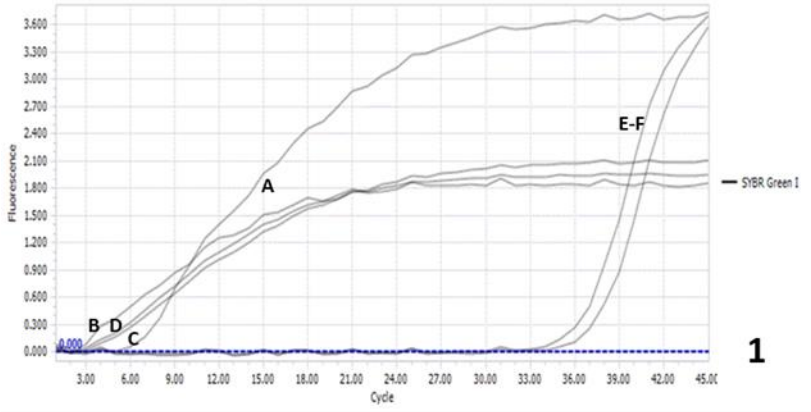

1

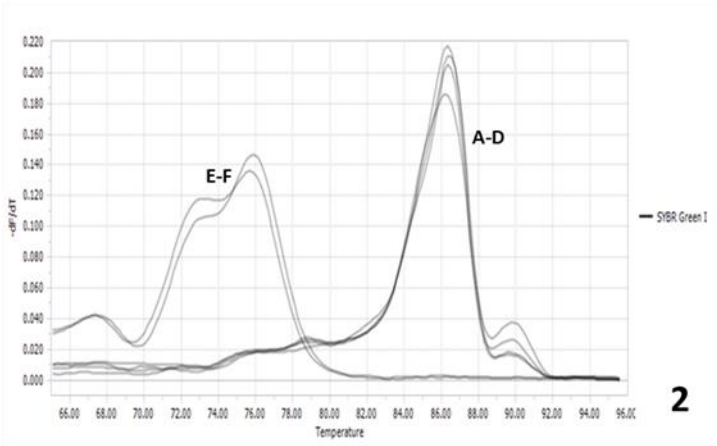

2

Position	Sample name	Cq
A	2h virus incubation	7.2
B	6h virus incubation	3.71
C	12h virus incubation	5.42
D	24h virus incubation	4.92
E	Negative control	36.69
F	Negative control	35.56

3

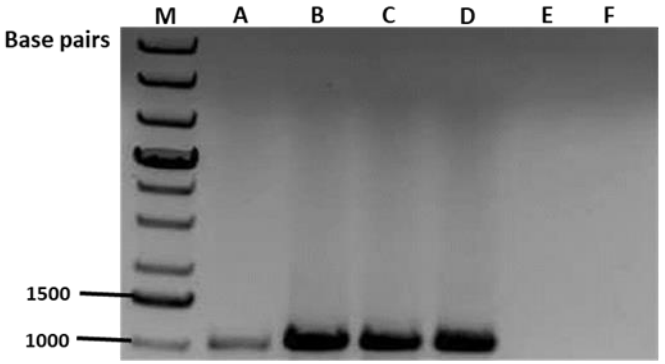

4

Figure 6.10: Amplification curves (Figure 6.10.1), Melting curves (Figure 6.10.2), Cq table (Figure 6.10.3), and 1% agarose gel electrophoresis (Figure 6.10.4) showing RT-PCR products of the recombinant Adenovirus containing the NCDV Matrix gene expressed in 293T cells. M: 1Kb plus DNA ladder (Thermo Scientific, # sm 1333), A: 2h virus infected 293T cells, B: 6h virus infected 293T cells, C: 12h virus infected 293T cells, D: 24h virus infected 293T cells, E-F: non infected 293T cells

6.6 Assessing the Functionality of the Recombinant Adenovirus Expressing the NCDV Matrix in CEFs

6.6.1 RNA analysis of the recombinant Adenovirus vector by PCR

The 293T host cell line has been used for years to propagate different types of Adenoviruses (Graham and Prevec, 1992; Choi and Chang, 2013; Silva *et al*, 2010; Silva *et al*, 2016). In the current study, a Life Technologies Adenovirus vector (pAD/CMV/V5-DEST^{TM}) was manipulated by inserting a NCDV Matrix gene to test it as a potential vaccine for NCDV and possibly other chicken/poultry diseases. As a first step, the recombinant Adenovirus was propagated in 293T cells to increase the titre of the viruses for downstream analysis. This was followed by assessing the RNA expression following infection with the vaccine model Adenovirus. The results that were discussed in the previous section showed that the recombinant Adenovirus that had been designed was expressed at an RNA level using RT-PCR. These results also showed that the vaccine vector had been designed appropriately and was ready to be tested *in vitro* in CEFs.

To assess the RNA expression level in CEFs, the cells were seeded on two 10cm sterile culture plates. Twenty-four (24) hours later, which is the maximum time that mammalian cells in general take to divide, one plate was infected with the recombinant Adenovirus. It was then incubated for four days to ensure maximum viral infection in the cells.

Genomic DNA extraction of both the infected and non-infected cells was subsequently conducted. PCR was performed to test the expression of the recombinant Adenovirus in the infected CEFs. CEFs were used because they are the closest to a live chicken. Using a live chicken would have given us a true reflection, but animal trials can only be done when vaccine tests were done *in vitro* first. The reason that the expression of the Adenovirus was assessed at DNA level in CEFs is that the Adenovirus can only replicate in cells such as 293T cells expressing the E1 gene, which suggests that the expression of Adenovirus late genes is dependent upon the E1 gene. Once the Adenovirus is in the nucleus of the 293T cells, transcription and translation of the E1 proteins may be initiated, followed by the expression of the adenoviral late genes and viral replication (Graham and Prevec, 1992; Choi and Chang, 2013; Silva *et al*, 2010; Silva *et al*, 2016). In chicken embryo fibroblasts, however, the E1 gene is absent, meaning that the Adenovirus will be replication deficient in these cells (Graham *et al*, 1977; Kamen and Henry, 2004; Silva *et al*, 2010; Silva *et al*, 2016). Once the Adenovirus is transduced into the chicken embryo fibroblasts and is transported to the nucleus, it does not integrate into the genome of the fibroblasts, therefore the expression of the Adenovirus can only be detected by assessing the DNA expression rather than

the mRNA or protein expression. The Adenovirus DNA was successfully detected in the CEFs using PCR, and an expected band size of 1149bp was obtained (Figure 6.11).

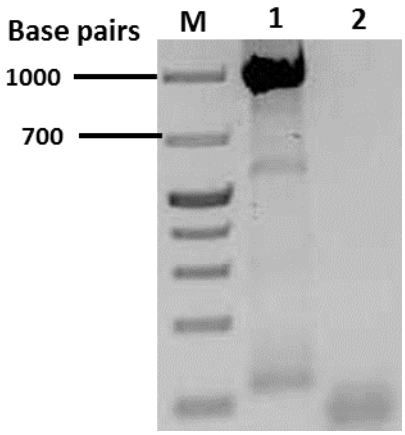

Figure 6.11: Image of 1% Agarose gel electrophoresis showing the expression of the Adenovirus with an inserted NCDV Matrix gene in CEFs. M: 1Kb plus DNA ladder (Thermo Scientific, #sm 1333), 1: PCR product of the amplified Matrix gene containing a few bases of the T7 promoter of the Adenovirus vector expressed in chicken embryo fibroblasts, 2: PCR product of non-infected chicken embryo fibroblasts (negative control)

6.6.2 Protein analysis of the recombinant Adenovirus vector by mass spectrometry (MS)

To aid the universal application of the designed vaccine strategy, mass spectrometry was used instead of western blotting to confirm the expression of the target antigen (Matrix) by the recombinant Adenovirus, because mass spectrometry is not dependent on the availability of commercial antibodies related to the antigen of interest. While mass spectrometry may not necessarily be cheap or readily available, such analyses can be performed by designated laboratories at relatively reasonable costs. The combination of accuracy and fast turnaround times of mass spectrometry dictates the preferential use of this strategy. Mass spectrometry confirmed that the CPE formed in the 293T cells was due to Adenovirus infection (see Figure 6.12, Figure 6.13, Figure 6.14, and Table 6.1). This method also confirmed that the PCR and sequencing results were correct given the presence of the Matrix gene protein on the virus coat.

The recombinant Adenovirus contained all five the peptides that were identified in the Matrix protein with a 19% protein coverage (Table 6.1). However, the protein of the CEFs infected with the recombinant Adenovirus contained only four of the peptides identified in the Matrix protein with a 16% protein coverage. These percentage coverages were significant enough to consider

the Matrix protein to be expressed in the Adenovirus vector and the CEFs. As anticipated, the control non-infected CEFs contained none of the peptides identified in the Matrix protein.

YRIQRLDLWTDSKEDSVFITTYGFIFQVGNEEATVGIIDDKPKRELLSAAMLCLGSVPNT

GDLIELARACLTMMVTCKKSATNTERMVFSVVQAPQVLQSCRVVANKYSSVNAVKHVKAP

EKIPGSGTLEYKVNFVSLTVVPKKDVYKIPAAVLKISGSSLYNLALNVTINVEVDPRSPL

VKSLSKSDSGYYANLFLHIGLMTTVDRKGKKVTFDKLEKKIRSLDLSVGLSDVLGPSVLV

KARGARTKLLAPFFSSSGTACYPIANASPQVAKILWSQTACLRSVKIIIQAGTQRAVAVT

ADHEVTSTKLEKGHTLAKY

Figure 6.12: The NCDV Matrix protein sequence which was cloned in the Adenovirus vector (pAD/CMV/V5-DEST™). This sequence shows where the protein was cleaved during the on-particle protein using trypsin. The highlighted regions show the peptides that were formed when the recombinant Adenovirus was digested.

The relevant protein fragments that were parts of the Matrix gene are shown in Figure 6.12. The position and size of each fragment are visible. The coverage and the uninterrupted amino acid sequences of the fragments were significant and unique enough to confirm the presence of the cloned in Matrix gene product from the actual Adenovirus coat. Figure 6.13 reveals the mass over charge size of each of the fragments, hence the unique profile of the full protein sequence was confirmed. The specific fragments that are labelled in red corresponded to the oligopeptides (see Figure 6.12) that ranged in mass from 500mz upwards. This was expected for such large fragments. A similar profile was observed (see Figure 6.14), which was produced from the CEF proteins infected with the recombinant Adenovirus. Apart from the unique extra fragment size of about 300mz, the rest of the fragments were identical, and the same fragments were identified in both designs. One can therefore conclude that:

1. The recombinant Adenovirus expresses the gene of interest, namely the Matrix gene, from the NCDV.

2. The expression and abundance of the resultant Matrix coat protein is high enough to be detected in the Adenovirus coat by means of the mass spectrometry method.

A summary of the results is presented in Table 6.1. This table indicates the number of peptides identified and their uniqueness as a measure of the fidelity of the identification method. A single unique peptide is usually enough to identify a specific protein presence. In this case, no fewer

than four fragments were identified from both the recombinant Adenovirus and the CEFs infected with the recombinant Adenovirus that were uniquely those of the Matrix gene protein product. It is therefore concluded that the vector design may function as a vaccine production system and that 293T cells can be used as a host cell line for virus propagation for seed stock.

Overall, these findings suggest that the vaccine design strategy used in this study may be a promising approach for developing protective vaccines that may be effective against poultry viral diseases. However, more *in vivo* studies/clinical trials will have to be performed as such tests in live chickens will give a true reflection of whether these Adenovirus-based vaccines can provide immunity by inducing the production of antibodies in chickens against the disease for which they are vaccinated, in this case the NCDV. Many researchers have successfully expressed target genes *in vivo* in a multitude of tissues such as the lung, heart, and brain using adenoviral-based vectors (Wivel, 1999; Russell, 2000; Wang and Huang, 2000; Baron *et al.*, 2018).

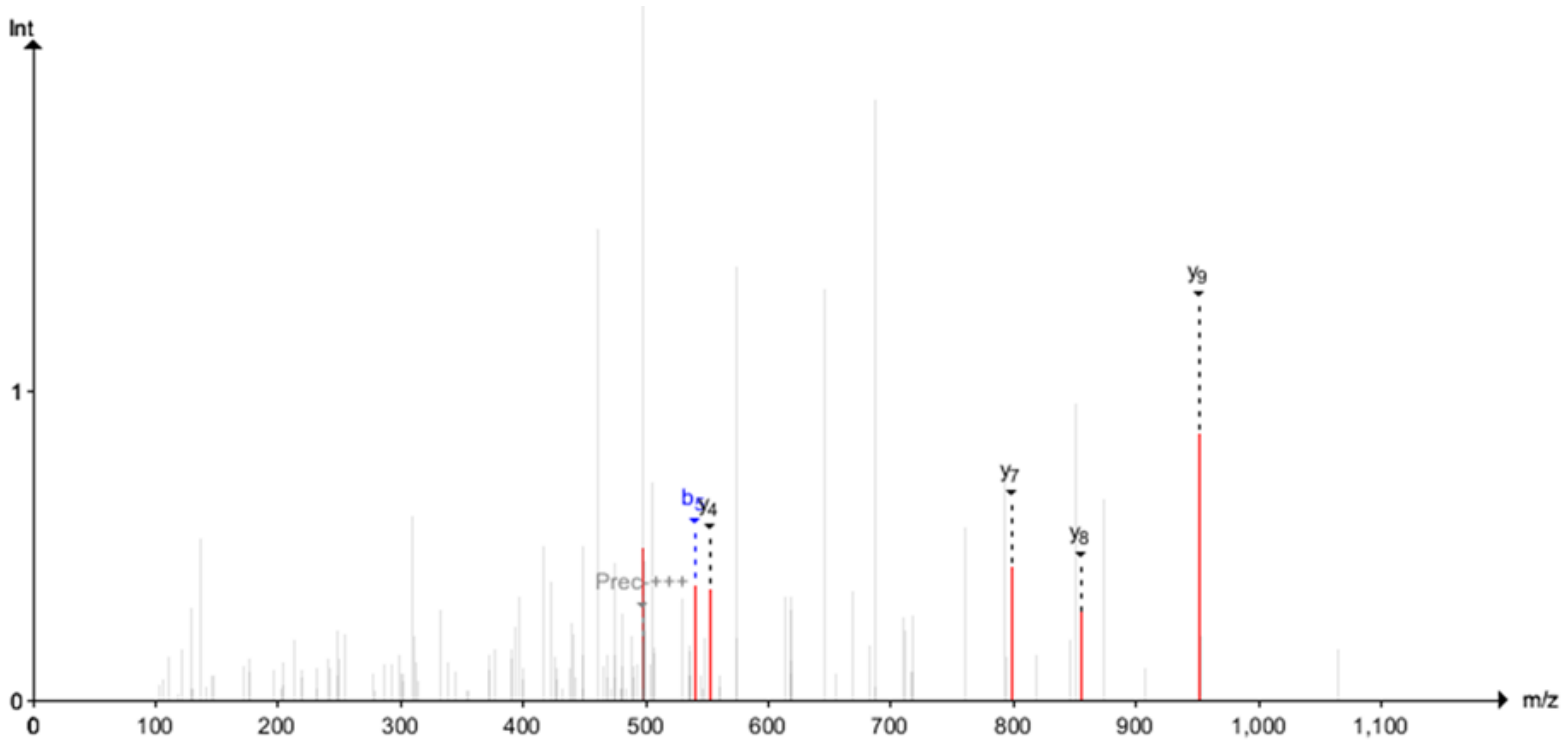

Figure 6.13: Mass spectrometry-based detection of the Matrix gene in recombinant Adenovirus purified stock. This figure shows the fragmentation spectra of N-APEKIPGSGTLEYK-C and highlighted dominant fragment ions.

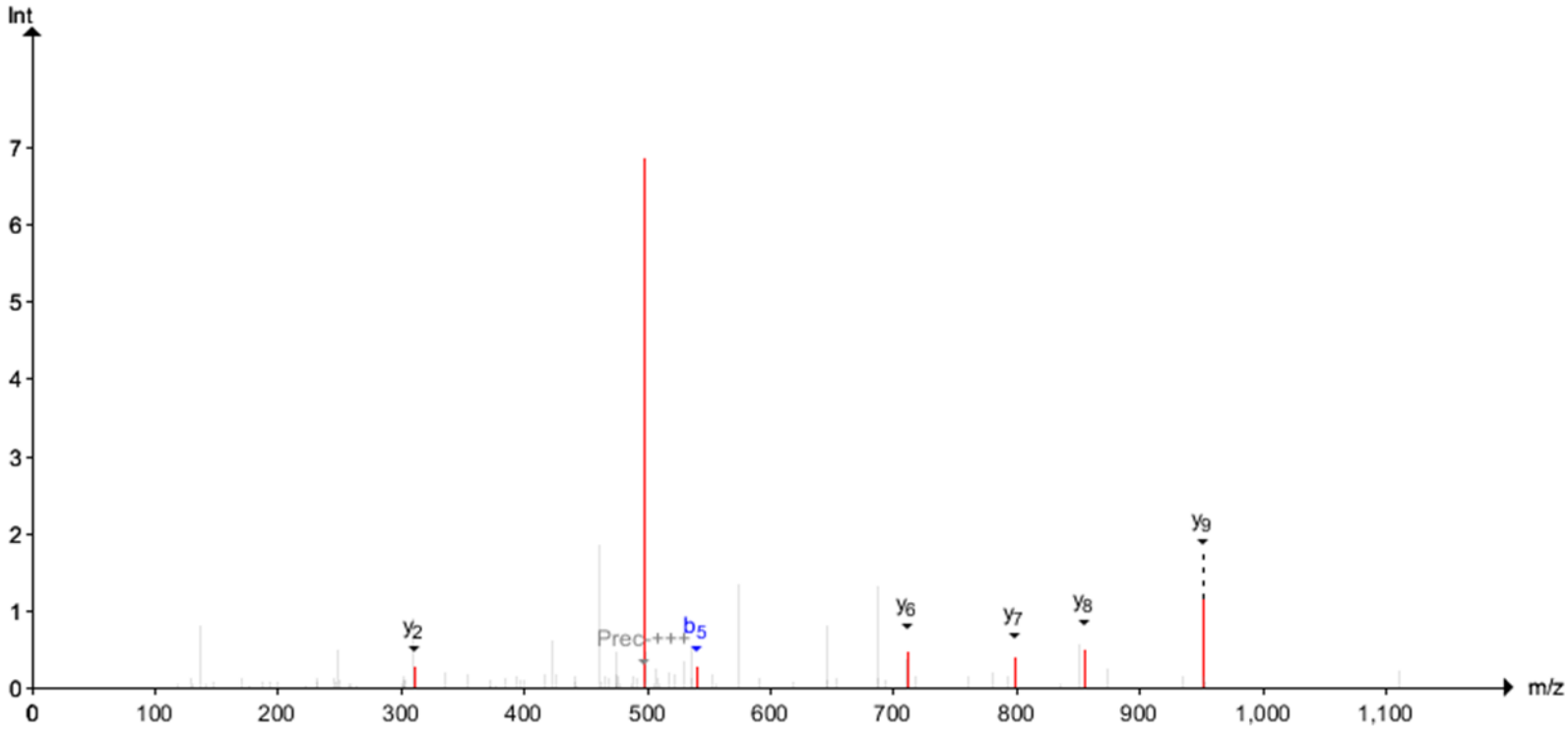

Figure 6.14: Mass spectrometry-based detection of the Matrix gene in the CEFs infected with the recombinant Adenovirus. This figure shows the fragmentation spectra of N-APEKIPGSGTLEYK-C and highlighted dominant fragment ions.

Table 6.1: NCDV Matrix protein identification in the recombinant Adenovirus and the CEFs infected with the recombinant Adenovirus. The numbers of different peptides that were identified in the samples are indicated. These unique peptides were identified using the fragmentation spectra in Figure 6.13 and Figure 6.14.

Sample	Recombinant Adenovirus	Infected CEFs	Non-infected CEFs (control)
Matrix protein coverage (%)	19	16	-
No. of unique peptides	5	4	-
Peptides identified (+)			
N-APEKIPGSGTLEYK-C	+	+	-
N-VNFVSLTVVPK-C	+	+	-
N-ILWSQTACLR-C	+	-	-
N-IIIQAGTQR-C	+	+	-
N-AVAVTADHEVTSTKLEK-C	+	+	-

CHAPTER 7

GENERAL DISCUSSION, CONCLUSION, AND RECOMMENDATIONS FOR FUTURE STUDIES

7.1 Introduction

AI is an infectious disease that targets many species of birds and affects their respiratory, digestive, and nervous systems (Peiris *et al.*, 2007; The Poultry Site, 2017; Shi *et al.*, 2019; Scott *et al.*, 2020). Outbreaks caused by avian influenza viruses often lead to significant economic losses in the poultry industry worldwide (Alexander *et al.*, 2006; FAO, 2011; Baron *et al.*, 2018; Chatziprodromidou *et al.*, 2018; Kim *et al.*, 2019; Scott *et al.*, 2020; Song *et al.*, 2020; Almayahi *et al.*, 2020). The methods that are currently used for the detection and control of these viruses are too laborious for real-time efficacy and are also time consuming (GAO, 2000; Lee and Suarez, 2004; Ng *et al.*, 2005, Payungporn *et al.*, 2006; Partridge and Kien, 2011, Shi *et al.*, 2019). An early detection and more effective control strategy for these viruses is thus urgently needed if the disruption to animal health following AI outbreaks and the concomitant commercial losses that follow are to be curbed. The current work focused on developing point-of-care detection assays for AI viruses and a protective vaccine that will not only be effective against AI pandemic strains, but that may also be produced quickly enough to prevent AI shedding and spreading.

7.2 LAMP

LAMP is a nucleic acid amplification technique that operates at isothermal temperatures of between 60-65ºC. What makes this technique so fascinating is its simplicity, specificity, and rapidity (Notomi *et al.*, 2000; Tomlinson *et al.*, 2010; Bhat *et al.*, 2013; Camp and Nowotny, 2016; Maan *et al.*, 2016; Kim *et al.*, 2018; Zeng *et al.,* 2018; Pumford *et al.*, 2020). Three LAMP assays were developed in this study. The first was to detect all AI strains by targeting the Matrix gene, while the last two were applied for the specific detection of the H5 and H7 AI subtypes that have often been identified as highly pathogenic. These assays were first optimised on a real-time PCR machine but were later tested on the Axxin T16 isothermal instrument (Axxin (Pty) Ltd), which produced the same results as the PCR machine. The best features of the Axxin T16 are that it is portable, produces results real-time, and most importantly is an instrument that operates on rechargeable batteries, which makes it ideal for usage in field operations. The three assays were tested on 20 Italian sourced avian influenza subtypes. Two negative controls, the NCDV and nuclease free water, were also included in the assays in order to compare the AI samples to non-AI samples.

All the AI samples were detected by means of these assays, except for three samples that were later shown not to be AI positive by testing them with the OIE approved PCR detection assay for all AI strains. However, the sensitivity of the LAMP assay method was found to be at least three logs less than that of the PCR method. Fortunately, this was not a major drawback as the samples that were used to validate the LAMP assays were field samples and the AI samples were all detected without any difficulty.

7.3 Developing a Vaccine against NCDV

According to the DALRRD vaccination against AI is prohibited in South Africa (DAFF, 2017). This is because poultry vaccinated for protection against AI using standard vaccines have always been found to test seropositive for AI, and this makes it impossible to differentiate between vaccinated and infected poultry. Moreover, when this occurs it interferes with surveillance programmes as well as export testing protocols for poultry. It was for these reasons that no vaccine against AI could be designed and/or developed in the current study as not only the study but also the resultant vaccine would not be approved by the National Ministry of Agriculture. As an alternative, and also as proof of concept that an effective vaccine against AI can be developed that can differentiate between a true and false AI infection, a vaccine against NCDV was designed and developed. NCDV was appropriate for this purpose because it is closely related to the AI virus in terms of the animals it infects, its genetics, and the symptoms it causes (Miller and Torchetti, 2014; Shekaili *et al.*, 2015; Bertran *et al.*, 2017). The vaccine was thus developed using human Adenovirus vectors because they have been shown to be suitable recombinant vaccine vectors due to their ability to infect a wide variety of cell types and grow to high titres *in vitro*, while they also have high levels of transgene expression and they do not integrate with the host genome (Robert-Guroff, 2007).

The Matrix gene of the NCDV was inserted in the Adenovirus expression vector using the Gateway cloning technology (Life Technologies Ltd, California). It would have been most informative if the final Adenovirus vector-based vaccine that was validated in 293T HEK cells could have been tested in live chickens, but ethically one is only allowed to test a first-time designed vaccine *in vivo* as an initial step. Due to this limitation, CEFs were prepared from a 9-day old chicken embryo. Ethical approval for this part of the study was obtained from the Research Ethics Committee of the Council for Scientific and Industrial Research (CSIR) (Approval no. 73/2013).

The expression of the recombinant Adenovirus DNA was then tested in the CEFs, and the recombinant Adenovirus was found to successfully express in these fibroblasts. The results were highly promising and suggest that this design strategy has the potential for use in vaccine

development against NCDV in live chickens. It is even more exciting that the possibility exists that the same strategy can be used to design and develop a vaccine against AI viruses, the reason being that this type of vaccine will not interfere with epidemiological survey strategies of natural AI infections because only one gene of the AI virus will be present in the vaccine. In light of the current COVID-19 pandemic, the Ad5-nCoV Adenovirus-based vaccine against the COVID-19 disease is already undergoing clinical trials (Al-Rohaimi and Al-Otaibi, 2020).

In combination, the LAMP-POC assays and the vaccine developed seem a promising approach for controlling poultry viral diseases in general. The strategy that was designed in the current study to improve the turnaround time for the detection and control of poultry viral diseases is summarised schematically in Figure 7.1. In this strategy, samples are collected from an area where poultry viral infection occurred or is suspected of having occurred. The samples are tested immediately at the POC using the developed LAMP assays. This process takes a maximum of a day as shown in Figure 7.1. Once the samples have been tested and the type of virus circulating in that particular area has been identified, the sample/s are taken to the laboratory for sequencing. This usually takes 3-5 days using NGS (Thermo Fisher Scientific, 4462921, USA). As soon as the sequence of the virus is known, the Adenovirus vector-based vaccine for the circulating viral strain/s will therefore be designed. This procedure takes 7 days to be completed. The designed recombinant Adenovirus is then propagated in the pre-cultured 293T cells until 100% CPE is reached. This usually takes a maximum of 14 days, depending on the concentration of the virus that was initially used to infect the cells. The viral medium is then separated from the cells by centrifugation, followed by viral DNA purification from the medium. This can then be formulated into a vaccine. This entire process takes a maximum of 5 weeks, which is a massive improvement considering that the conventional strategy for detecting viral diseases and producing a suitable vaccine for AI in poultry usually take 6 to 8 months (GAO, 2000).

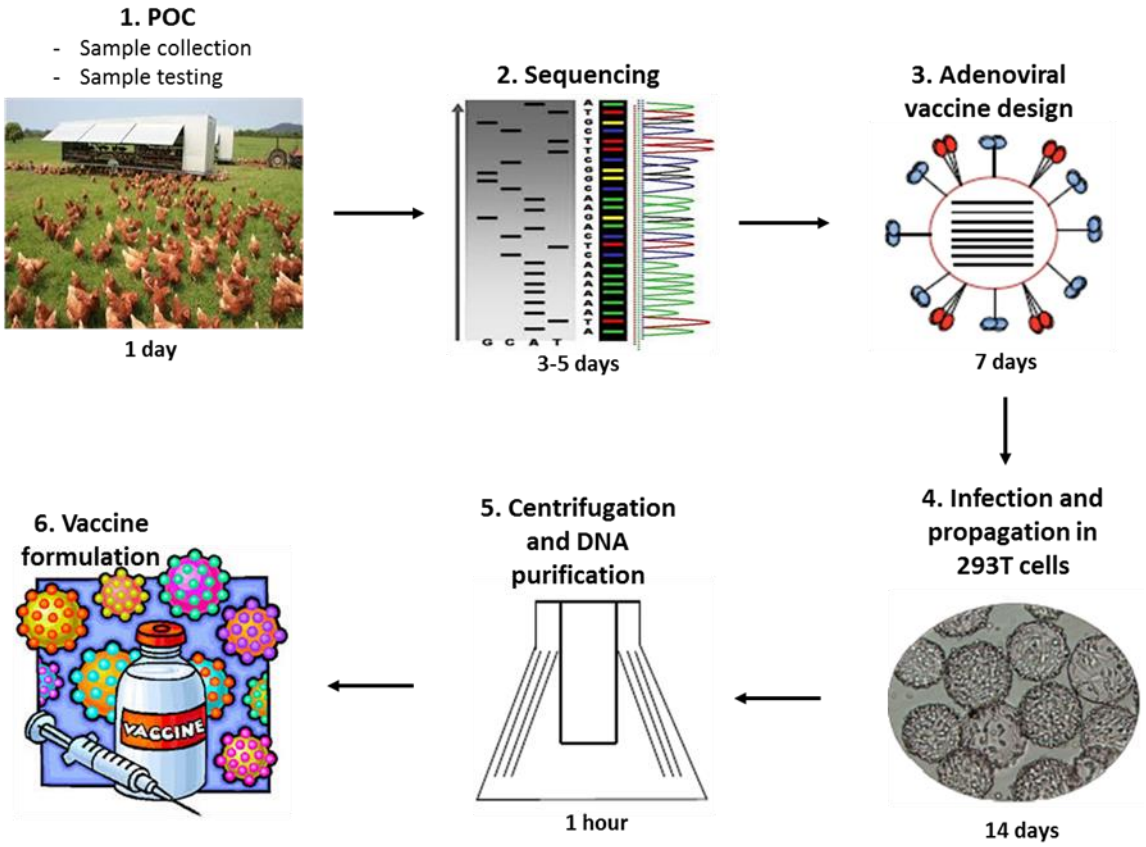

Figure 7.1: Timeline for avian influenza detection and vaccine production as developed in the current study

7.4 Recommendations for Future Studies

Although the results achieved by this study are very promising, there is still a lot of room for improvement. For example, with regards to the design of the POC detection assays, only 20 AI samples were used to validate these assays, therefore future research should involve a large sample size of at least 1000 samples. Such studies should also include proficiency testing in various laboratories where the same samples that were tested in the current laboratory should be tested using the same assays to compare the results.

Another interesting type of assay to include in future research is the multiplexing LAMP assay. In this testing process, the results obtained for one assay can show more than one outcome. For example, the following information can be obtained from only one assay: the type of virus found, the virus subtype, and also whether the virus is highly pathogenic or low pathogenic. In the current study the focus was on avian influenza viruses, whereas other investigations that are in the pipeline will include designing POC assays for the detection of other poultry diseases as well.

7.5 Conclusion

The recombinant Adenovirus vaccine strategy that was designed looks promising for controlling chicken viral diseases as the Adenovirus expressing the NCDV Matrix gene was shown to express in chicken embryo fibroblasts. However, *in vivo* studies/clinical trials of this recombinant Adenovirus vaccine will still have to be performed in live chickens. The reasoning behind this suggestion relates to the dose determination, adverse effects analysis, and general clinical prognosis of vaccinated animals compared to a control cohort. For a study of this nature, ethical approval will of course have to be granted first. It may also be valuable to design an Adenovirus vaccine expressing multiple genes for immunity against various viral diseases that are problematic in the poultry industry. There is also a need for the mass production of such vaccines should they be as successful as this researcher envisions them to be. This challenge can be addressed by culturing the virus propagation cells in large-scale bioreactor systems. Previously, Adenovirus vectors were successfully produced in large-scale bioreactor systems using 293T HEK cells (Stöhr, 2013) or PER.C6 and 293(F) cells (Vemula and Mittal, 2010). If the same results are obtained using the vaccine design strategy implemented in this study, the crisis caused by various viral disease outbreaks among poultry flocks will be eradicated and such outbreaks will become a thing of the past.

REFERENCES

Abbasi, I., Kirsten, O.D., Hailu, A. and Warburg, A. 2016. Optimization of loop-mediated isothermal amplification (LAMP) assay for the detection of Leishmania DNA in human blood samples. *Acta Tropica,* 162:20-26.

Afzal, A. (2020). Molecular diagnostic technologies for COVID-19: limitations and challenges. *Journal of Advanced Research*, 26:149-159.

Ahi, Y.S. and Mittal, S.K. 2016. Components of Adenovirus genome packaging. *Frontiers in Microbiology*, 7:1503.

Akarsu, H., Burmeister, W.P., Petosa, C., Petit, I., Muller, C.W., Ruigrok, R.W. and Baudin, F. 2003. Crystal structure of the M1 protein-binding domain of the influenza A virus nuclear export protein (NEP/NS2). *EMBO Journal,* 22(18):4646-55.

Akey, B.L. 2003. Low-pathogenicityH7N2 avian influenza outbreak in Virginia during 2002. *Avian Disease* 47:1099-1103.

Alders, R.G. and Bagnol, B. 2007. Effective communication: the key to efficient HPAI prevention and control. *World's Poultry Science Journal,* 63:139-147.

Alexander, D.J. 1997. Highly pathogenic avian influenza (fowl plague). In: *Manual of standards for diagnostic tests and vaccines: list A and B diseases of mammals, birds, and bees*. 3rd Edition: 155-160. Paris: Office International des Epizooties (OIE).

Alexander, D.J. 2000. A review of avian influenza in different bird species. *Veterinary Microbiology,* 74(1-2):3-13.

Alexander, D.J. 2006. An overview of the epidemiology of avian influenza. *Vaccine*, 25:5637-5644.

Almayahi, Z.K., Kindi, H.A., Davies, C.T., Al-Rawahi, B., Al-Jardani, A., Al-Yaqoubi, F. and Al-Abri, S. 2020. First report of human infection with avian influenza A (H9N2) virus in Oman: the need for a one health approach. *International Journal of Infectious Diseases,* 91:169-173.

Al-Rohaimi, A.H. and Al-Otaibi, F. (2020). Novel SARS-CoV-2 outbreak and COVID19 disease: a systemic review on the global pandemic. *Genes and Diseases,* 7(4):491-501.

Alsahami, A., Ideris, A., Omar, A., Ramanoon, S.Z. and Sadiq, M.B. 2018. Seroprevalence of Newcastle disease virus in backyard chickens and herd-level risk factors of Newcastle disease in poultry farms in Oman. *International journal of veterinary science and medicine*, 6(2):186-191.

Amanollahi, R., Keramat, A. and Bahman, A. 2020. Effect of Newcastle disease and infectious bronchitis live vaccines on the immune system and production parameters of experimentally infected broiler chickens with H9N2 avian influenza. *Comparative immunology, microbiology, and infectious diseases,*71:101492.

Atila Biosystems: iAMP COVID-19 detection kit. Atila Biosyst Inc.2020. https://atilabiosystems.com/our-products/covid-19/ Accessed 31 October 2020.

Bankowski, R.A. 1985. Report of the committee on transmissible disease of poultry and other avian species. Proceedings of the 88th annual meeting of the U.S. Animal Health Association: 474-483.

Baron, M.D., Iqbal, M. and Nair, V. 2018. Recent advances in viral vectors in veterinary vaccinology. *Current opinion in virology*, 29:1-7.

Belgrad, J.P., Rahman, M.A., Abdullah, M.S., Rashid, M.H., Sayeed, M.A., Anwer, M.S. and Hoque, M.A. 2018. Newcastle disease sero and viro-prevalence in rural poultry in Chittagong, Bangladesh. *Preventive veterinary medicine*, 160:18-25.

Bello, M.B., Yusoff, K.M., Ideris, A., Hair-Bejo, M., Peeters, B.P.H., Jibril A.H. and Omar, A.R. 2018. Genotype diversity of Newcastle disease virus in Nigeria: Disease control challenges and future outlook. *Advances in virology*, Article ID D6097291.

Berk, A.J. 2007. Adenoviridae: The viruses and their replication. In: D.M. Knipe and P.M. Howley (Eds.), *Fields virology*. Wolters Kluwer Health/Lippincott Williams & Wilkins, Philadelphia, pp. 2355-2394.

Bertran, K., Susta, L. and Miller P.J. 2017. Chapter 51-Avian influenza virus and Newcastle disease virus. *Egg innovations and strategies for improvements*. pp. 547-559.

Bett, A.J., Haddara, W., Prevec, L. and Graham, F.L. 1994. An efficient and flexible system for construction of Adenovirus vectors with insertions or deletions in early regions 1 and 3. *Proceedings of the national academy of sciences U.S.A*, 91:8802-8806.

Bhat, A.I., Siljo, A. and Reshma, K.P. 2013. Rapid detection of Piper yellow mottle virua and Cucumber mosaic virus infecting black pepper (Piper nigrum) by loop-mediated isothermal amplification (LAMP). *Journal of virological methods*, 193:190-196.

Bomfanti, L., Monne, I., Tamba, M., Santucci, U., Massi, P., Patregnani, T. and Marangon, S. 2014. Highly pathogenic H7N7 avian influenza in Italy. *Veterinary record*, 174:382.

Boulo, S., Akarsu, H., Ruigrok, R.W. and Baudin, F. 2007. Nuclear traffic of influenza virus proteins and ribonucleoprotein complexes. *Virus Research*, 124(1-2):12-21.

Bourret, V. 2018. Avian influenza viruses in pigs: An overview. *The veterinary journal*, 239: 7-14

Bouvier, N.M. and Palese, P. 2008. The biology of influenza viruses. Vaccine 4: D49-53.

Branton, P.E. 1999. Early gene expression. In Adenoviruses: Basic biology to gene therapy (P.Seth,Ed.), pp 39-55. Landes Bioscience, Georgetown, TX.

Bublot, M., Pritchard, N., Swayne, D.E., Selleck, P., Karaka, K., Suarez, D.L. and Mickle T.R. 2006. Development and use of fowl pox vectored vaccines for avian influenza. *Annals of the New York academy of sciences*, 1081:193-201.

Bublot, M., Richard-Mazet, A., Chanavat-Bizzit, S., Le Gross, F.X., Duboeuf, M., Stoll, A. and Dren, NC. 2010. Immunogenicity of poxvirus vector avian influenza vaccines in Muscovy and Pekin ducks. *Avian diseases*, 54:232-238 .

Business Day live.2012. New bird flu case dashes ostrich export plans. http://www.bdlive.co.za/articles/2012/03/02/new-bird-flu-case-dashes-ostrich-export-plans;jsessionid=51784A2B3C47204CBAF926EBAAA3F3B6.present1.bdfm. Accessed 28 February 2013.

Camp, J.V. and Nowotny, N. 2016. Rapid detection of European orthobunyaviruses by reverse transcription loop-mediated isothermal amplification assays. *Journal of virological methods*, 236:252-257.

Campbell, A.M. 1962. Episomes. *Advanced genetics*, 11:101-145.

Capua, I. and Alexander, D.J. 2001. Avian influenza and Newcastle disease. A field and laboratory manual: *Ecology and epidemiology of Newcastle disease*, 39-46.

Capua, I., Terregino, C., Cattoli, G., Mutinelli, F. and Rodriguez. J.F. 2003. Development of a DIVA (differentiating infected from vaccinated animals) strategy using a vaccine containing a heterologous neuraminidase for the control of avian influenza. *Avian pathology*, 32:47-55.

Capua, I. and Marangon, S. 2003. The use of vaccination as an option for the control of avian influenza. *Avian pathology*, 32(4):335-343.

Capua, I. and Alexander, D.J. 2004. Avian influenza: recent developments. *Avian Pathology*, 33:393-404.

Capua, I., Cattoli, G. and Marangon, S. 2004. DIVA- a vaccination strategy enabling the detection of field exposure to avian influenza. *Developments in biologicals (Basel)*, 119:229-233.

Capua, I., Terregino, C., Cattoli, G. and Toffan, A. 2004. Increased resistance of vaccinated turkeys to experimental infection with an H7N3 low-pathogenicity avian influenza virus. *Avian pathology*, 133:47-55.

Capua, I. and Marangon, S. 2006. Control of avian influenza in poultry*. Emerging infectious diseases*, 12(19):1319-1324.

CDC (Centres for disease control and prevention).2017. Avian influenza in birds. https://www.cdc.gov/flu/avianflu/avian-in-birds.htm. Accessed 13 December 2018.

Charlton, H. (2018). Warning that SA is still at risk for bird flu in 2018. *News24*, 28 Jan https://www.fin24.com/Companies/Agribusiness/warning-that-sa-is-still-at-risk-for-bird-flu-in-2018-20180128-2. Accessed 12th of December 2018.

Chatziprodromidou, I.P., Arvanitidou, M., Guitian, J., Apostolou, T., Vantarakis, G. and Vantakis, A. 2018. Global avian influenza outbreaks 2010-2016: a systematic review of their distribution, avian species and virus subtype. *Systematic reviews*, 7(1):17.

Chen, H. 2009. Avian influenza vaccination: The experience in China. *Revue scientifique et technique (Office International des Épizooties)*, 28:267-274.

Chen, E., Chen, Y., Fu, L., Chen, Z., Gong, Z., Mao, H. and Yu, H. 2013. Human infection with avian influenza A (H7N9) virus re-emerges in China in winter 2013. *Euro surveilance*, 18(pii):20616.

Chen, N., Zhou, M., Dong, X., Qu, J., Gong, F., Han, Y. and Zhang, L. 2020. Epidemiological and clinical characteristics of 99 cases of 2019 novel Coronavirus pneumonia in Wuhan, China: a descriptive study. *Lancet London England*, 395:507-513.

Choi, Y.K., Goyal, S.M., Kang, S.W., Farnham, M.W. and Joo, H.S. 2002. Detection and subtyping of swine influenza H1N1, H1N2 and H3N2 viruses in clinical samples using two multiplex RT-PCR assays. *Journal of virological methods*, 102:53-59.

Choi, Y. and Chang, J. 2013. Viral vectors for vaccine applications. *Clinical and experimental vaccine research*, 2:97-105.

Chua, T.H., Ellis, T.M., Wong, C.W., Guan, Y., Ge, S.X., Peng, G. and Parkinson, J. 2007. Performance evaluation of five detection tests for avian influenza antigen with various avian samples. *Avian diseases*, 51(1):96-105.

Collins, R.A., Ko, L.S., Fung, K.Y., Chan, K.Y., Xing, J., Lau, L.T. and Yu, A.C. 2003. Rapid and sensitive detection of avian influenza virus subtype H7 using NASBA. *Biochemical and biophysical research communications*, 300:507-515.

Corman, V.M., Landt, O., Kaiser, M., Molenkamp, R., Meijer, A., Chu, D.K. and Drosten, C. 2020. Detection of 2019 novel coronavirus (2019-nCov) by real-time RT-PCR. *Euro surveillance*, 25:2000045.

Couceiro, J.N., Paulson, J.C. and Baum, L.G. 1993. Influenza virus strains selectively recognize sialyloligosaccharides on human respiratory epithelium, the role of the host cell in selection of hemagglutinin receptor specificity. *Virus research*, 29(2):155-165.

Cox, N.J. and Subbarao, K. 2000. Global epidemiology of influenza: Past and present. *Annual review of medicine*, 51(1):407- 421.

Cros, J.F. and Palese, P. 2003. Trafficking of viral genomic RNA into and out of the nucleus: influenza, Thogoto and Borna disease viruses. *Virus research*, 95:3-12.

CSB (Computational Systems Biology). 2011. Influenza virus structure and function. https: //www.csblab.kr/1160. Accessed: 12 October 2017.

DAFF (Department of Agriculture, Forestry and Fisheries. 2017. Media statement: Avian influenza confirmed in Mpumalanga. [Online]. Available: http://www.nda.agric.za/docs/media/AVIAN%20INFLUENZA%20CONFIRMED%20IN%20MPUMALANGA.pdf. Accessed 18 October 2017.

Darre, M.J. 2015. Signs and symptoms of avian influenza in poultry. https://www.aphis.usda.gov/publications/animal_health/2015/fs_hpai_biosecurity.pdf. Accessed: 16 December 2017.

Das, K., Aramini, J.M., Ma, L-C. and Krug, R. M. 2010. Structures of influenza A proteins and insights into antiviral drug targets. *Nature structural & molecular biology*, 17:530-538.

de Villiers, J. 2017. Over 2 million birds now dead in Western Cape's worst bird flu outbreak. *News24*, 02 Oct. https://www.fin24.com/Economy/over-2-million-birds-now-dead-in-western-capes-worst-bird-flu-outbreak-20171002. Accessed 12 December 2018.

Dei, H.K., Alidu, I., Otchere, E.O., Donkoh, A., Boa-Amponsem, K. and Adam, I. (2009). Improving the brooding management of local guinea fowl (*Numida meleagris*). *Family poultry*, 18(1&2):3-8.

Ding, X.X., Hu, D.M., Chen, Y., Di, B.A., Jin, J., Pan, Y.X. and Che, X.Y. 2011. Full serotype and group specific NS1 capture enzyme-linked immunosorbent assay for rapid differential diagnosis of dengue virus infection. *Clinical and vaccine immunology*, 18:430-434.

Donis, R.O. 2014. The influenza cell culture working group. Performance characteristics of qualified cell lines for isolation and propagation of influenza viruses for vaccine manufacturing. *Vaccine*, 32:6583-6590.

Dormitzer, P.R., Tsai, T.F. and Del Giudice, G. 2012. New technologies for influenza vaccines. *Human vaccines and immunotherapeutics*, 8(1):45-58.

Doyle, T.M. 1935. Newcastle disease of fowls. *The journal of comparative pathology and therapeutics*, 48:1-20.

Drake, J.W. 1993. Rates of spontaneous mutation among RNA viruses. *Proceedings of the national academy of sciences U.S.A*, 90(9):4171-4175.

Durães-Carvalho, R. and Salemi, M. 2018. In-depth phylodynamics, evolutionary analysis and in silico predictions of universal epitopes of influenza A subtypes and influenza B viruses. *Molecular phylogenetics and evolution*, 121: 174-182.

Ellis, J. S. and Zambon, M. C. 2002. Molecular diagnosis of influenza. *Reviews in medical virology*, 12: 375–389.

Esser, M.T., Marchese, R.D., Kierstead. L.S., Tussey, L.G., Wang, F., Chirmule, N. and Washabaugh, M.W. 2003. Memory T cells and vaccines. *Vaccine*, 21: 419-430.

Fallaux, F.J., Bout, A., Van der Velde, I., Van den Wollenberg, D.J., Hehir, K.M., Keegan, J. and Hoeben, R.C.1998. New helper cells and matched early region 1-deleted Adenovirus vectors prevent generation of replication-competent Adenoviruses. *Human gene therapy*, 9:1909-1917.

FAO (Food and Agricultural Organization of the United Nations). 2007. Communication about highly pathogenic avian influenza with special emphasis on village poultry farmers by B.Bagnol. Consultancy report, January 2007. Emergency centre for Transboundary Animal Diseases (ECTAD). Bankok, FAO Regional office for Asia and the Pacific.

FAO (Food and Agricultural Organization of the United Nations). 2011. http://empres-i.fao.org. Accessed 14 March 2013.

Farooq, U., Latif, A., Irshad, H., Ullah, A., Zahur, A.B., Naeem, K. and Smoliga, G. 2015. Loop-mediated isothermal amplification (RT-LAMP): a new approach for the detection of Foot-and-mouth disease virus and its sero-types in Parkistan. *Iranian Journal of veterinary research*, 16(4):331-334.

Fasina, F.O., Wai, M.D., Mohammed, S.N. and Onyekonwu, O.N. 2007. Contribution of poultry production to household income: a case of Jos South local government in Nigeria. *Family poultry*, 17(1&2):30-34.

Ferhadian, D., Contrant, M., Printz-Schweigert, A., Smyth, R.P., Paillart, J. and Marquet, R. 2018. Structural and functional motifs in influenza virus RNAs. *Frontiers in microbiology*, 9(559):1-11.

Flory, G.A. and Peer, R.W. 2010. Verification of Poultry carcass composting research through application during actual avian influenza outbreaks. *ILAR journal*, 51(2):149-157.

Fogg, P.C.M., Colloms, S., Rosser, S., Stark, M. and Smith M.C.M. 2014. Review: New applications for phage integrases. *Journal of molecular biology*, 426:2703-2716.

Fouchier, R.A., Schneeberger, P.M., Rozendaal, F.W., Broekman, J.M., Kemink, S.A., Munster, V. and Osterhaus, A.D. 2004. Avian influenza A virus (H7N7) associated with human conjunctivitis and a fatal case of acute respiratory distress syndrome. *Proceedings of the national academy of sciences of the USA*, 101:1356-1361.

Gabitzsch, E.S., Xu, Y., Balcaitis, S., Balint, J.P. and Jones, F.J. 2011. An Ad5 [E1-, E2b-]-HER2/neu vector induces immune responses and inhibits HER2/neu expressing tumor progression in Ad5 immune mice. *Cancer gene therapy*, 18(5):326-335.

GAO (General Accounting Office) (2000). Influenza pandemic: Plan needed for federal and state response. http://www.gao.gov/new.items/d014.pdf . Accessed 20 December 2004

Gao, G., Soloff, A.C., Lu, X., Montecalvo, A., Nguyen, D.C., Matsuoka, Y. and Gambotto, A. 2006. Protection of mice and poultry from lethal H5N1 avian influenza virus through Adenovirus-based immunization. *Journal of virology*, 80:1959-1964.

Gao, P., Haoyun, D., Lei, F., Libin, C., Ming, L., Chenggang, X. and Tao, R. 2018. Human infection with an avian-origin influenza A (H7N4) virus in Jiangsu: A potential threat to China. *Journal of infection*, 77(3):249-257.

Gawande, S.S., Kalita, N., Barua, N. and Sahara, K.K. 2007. Indigenous chicken farming in rural conditions of Assam. *India family poultry*, 17(1&2):15-29.

Glass, K., Barnes, B., Scott, A., Toribio, J.A., Moloney, B., Singh, M. and Hernandez-Jover, M. 2019. Modelling the impact of biosecurity practices on the risk of high pathogenic avian influenza outbreaks in Australian commercial chicken farms. *Preventive veterinary medicine*, 165:8-14.

Gonzales, J.L., Koch, G., Elbers, A.R.W. and van der Goot, J.A. 2017. Similar transmissibility of the Italian H7N1 highly pathogenic avian influenza virus and its low pathogenic avian influenza virus predecessor. *The veterinary journal*, 232:20-22.

Graham, F.L., Smiley, J., Russel, W.C. and Nairn, R. 1977. Characteristics of a human cell line transformed by DNA from human Adenovirus type 5. *Journal of General virology*, 36: 59-72.

Graham, F.L. and Prevec, L. 1992. Adenovirus-based expression vectors and recombinant vaccines. *Biotechnology*, 20:363-390.

Grillo, V., Arzey, K., Hansbro, P., Hurt, A., Warner, S., Bergfeld, J. and Postp, L. 2015. Avian influenza in Australia: a summary of 5 years of wild bird surveillance. *Australian veterinary journal*, 93: 387-393.

Guo, Y., Li. J. and Cheng, X. 1999. Discovery of men infected by avian influenza A (H9N2) virus. *Chinese journal of experimental and clinical virology*, 13:105-108.

Guo, Y., Dong, J., Wang, M., Zhang, Y., Guo, J. and Wu, K. (2001). Characterization of hemagglutinin gene of influenza A virus subtype H9N2. *Chinese medical journal (English Edition)*, 114: 76-79.

Hale, B.G., Randall, R.E., Ortin, J. and Jackson, D. 2008. The multifunctional NS1 protein of influenza A viruses. *Journal of general virology*, 89: 2359-2376.

Halvorson, D.A. 2002. Twenty-five years of avian influenza in Minnesota. In: Proceedings of the 53rd North central avian disease conference, Minneapolis, 65-69.

Hambly, E. and Suttle, C.A. 2005. The viriosphere, diversity, and genetic exchange within phage communities. *Current opinion in microbiology*, 8:444-450.

Hamilton, S., East, I., Toribio, J.-A. and Garner, M. 2009. Are the Australian poultry industries vulnerable to large outbreaks of highly pathogenic avian influenza? *Australian veterinary journal*, 87(5):165-174.

Hardy, C.T., Young, S.A., Webster, R.G., Naeve, C.W. and Owens, R.J. 1995. Egg fluids and cells of the chorioallantoic membrane of embryonated chicken eggs can select different variants of influenza A (H3N2) viruses. *Virology*, 211 (1):302-306.

Hartley, J.L., Temple, G.F. and Brasch, M.A. 2000. DNA cloning using in vitro site-specific recombination. *Genome research*, 10:1788-1795.

Hay, A.J., Skehel, J.J. and McCauley J. 1982. Characterization of influenza virus RNA complete transcripts. *Virology*, 116(2):517-522.

Hilleringmann, M., Jobst, B. and Baudner, B.C. (2014). Influenza cell-culture vaccine production, in molecular vaccines, M.Giese, Ed., pp.823-837, Springer international publishing, Cham, Switzerland.

Hillgenberg, M., Tönnies, H. and Strauss, M. 2001. Chromosomal integration pattern of a helper-dependent minimal Adenovirus vector with a selectable marker inserted into a 27.4-kilobase genomic stuffer. *Journal of virology*, 75:9896-9908.

Hirst, M., Astell, C.R., Griffith, M., Coughling, S.M., Moksa, M., Zeng, T., Smailus, D.E. and Paetzel, M. 2004. Novel avian influenza H7N3 strain outbreak, British Columbia. *Emerging infectious diseases*, 10:2192-2195.

Hoelscher, M.A., Jayashankar, L., Garg, S., Veguillla, V., Lu, X., Singh, N. and Sambhara, S. 2007. New pre-pandemic influenza vaccines: an egg- and adjuvant-independent human adenoviral vector strategy induces long-lasting protective immune responses in mice. *Clinical Pharmacology and Therapeutics*, 82(6):665-671.

Horimoto, T. and Kawaoka, Y. 2001. Pandemic threat post posed by avian influenza A viruses. *Clinical microbiology reviews*, 14(1): 129-149.

Horimoto, T., Takada, A., Fujii, K., Goto, H., Hatta, M., Watanabe, S. and Kawaoka, Y. 2006. The development and characterization of H5 influenza virus vaccines derived from a 2003 human isolate. *Vaccine*, 24:3669-3676.

Hu, D., Lou, X., Xu, Z., Meng, N., Xie, Q., Zhang, M. and Wang, F. 2020. More effective strategies are required to strengthen public awareness of COVID-19: Evidence from Google Trends. *Journal of global health*, 10(1):011003.

Huang, C., Wang, Y., Li, X., Ren, L., Zhao, J., Hu, Y. and Jin, Q. 2020. Clinical features of patients infected with 2019 novel Coronavirus in Wuhan, China. *Lancet*, 395:497-506.

Imai, M., Ninomiya, A., Minekawa, H., Notomi, T., Ishizaki, T., Tashiro, M. and Odagiri, T. 2006. Development of H5-RT-LAMP (loop-mediated isothermal amplification) system for rapid diagnosis of H5 avian influenza virus infection. *Vaccine*, 24:6679–6682.

Imai, M., Ninomiya, A., Minekawa, H., Notomi, T., Ishizaki, T., Tu, PV. and Odagiri, T. 2007 Rapid diagnosis of H5N1 avian influenza virus infection by newly developed influenza H5 hemagglutinin gene-specific loop-mediated isothermal amplification method. *Journal of virological methods*, 141:173–180.

Ismail, A.M., Lee, J.S., Lee, J.Y., Singh, G., Dyer, D.W., Seto, D. and Rajaiya, J. 2018. Adenovirimics: mining the human Adenovirus species D genome. *Frontiers in microbiology*, 9:2178.

Ito, T., Goto, H., Yamamoto, E., Tanaka, H., Takeuchi, M., Kuwayama, M. and Otsuki, K. 2001. Generation of a highly pathogenic avian influenza A virus from an avirulent field isolate by passing in chickens. *Journal of virology*, 75(9):4439-4443.

Ito, M., Watanabe, M., Nakagawa, N. and Okuno, Y. 2006. Rapid detection and typing of influenza A and B by loop-mediated isothermal amplification: comparison with immunochromatography and virus isolation. *Journal of virological methods*, 135:272–275.

Jones, F.K., Gabitzsch, E.S., Xu, Y., Balint, J.P., Borisevich, V., Smith, J. and Paessler, S. 2011. Prevention of influenza virus shedding and protection from lethal H1N1 challenge using a consensus 2009 H1N1 HA and NA Adenovirus vector vaccine. *Vaccine*, 29:7020-7026.

Kamen, A. and Henry, O. 2004. Development and optimization of an Adenovirus production process. *Journal of general medicine*, 6(1):S184-S192.

Kapczynski, D.R., Esaki, M., Dorsey, K.M., Jiang, H., Jackwood, M., Moraes, M. and Gardin, Y. 2015. Vaccine protection of chickens against antigenically diverse H5 highly pathogenic avian influenza isolates with a live HVT vector vaccine expressing the influenza hemagglutinin gene derived from a clade 2.2 avian influenza virus. *Vaccine*, 33:1197-1205.

Ke, C., Mok, C.K.P., Zhu, W., Zhou, H., He, J., Guan, W. and Liu, J. 2017. Human infection with highly pathogenic avian influenza A (H7N9) virus, China. *Emerging infectious disease journal*, 23: 1332-1340.

Kilic, T., Weissleder, R. and Lee, H. 2020. Molecular and immunological diagnostic tests of COVID-19: Current status and challenges. *iScience*, 23: 101406.

Kim, J-G., Baek, S.H., Kim, S., Kim, H.I., Lee, S.W., Phan, L.M.T. and Park, T.J. 2018. Rapid discriminative detection of dengue viruses via loop-mediated isothermal amplification. *Talanta*, 190:391-396.

Kim, G-S., Kim, T-S., Son, J-S., Lai, V.D., Park, J-E., Wang, S-J., Jheong, W-H. and Mo, I-P. 2019. The difference of detection rate of avian influenza virus in the wild bird surveillance using various methods. *Journal of veterinary science*, 20(50):e56.

Kistner, O., Barrett, P.N., Mundt, W., Reiter, M., Schober-Bendixen, S., and Dorner, F. 1998. Development of a mammalian cell (Vero) derived candidate influenza virus vaccine. *Vaccine*, 16(9-10):960-968.

Klemm, C., Boergeling, Y., Ludwig, S. and Ehrhardt, C. 2018. Immunomodulatory non-structural proteins of influenza A viruses. *Trends in microbiology*, 26(7): 624-636.

Kojaoghlanian, T., Flomenberg, P. and Horwitz, M.S. 2003. The impact of Adenovirus infection on the immunocompromised host. *Reviews in medical virology*, 13:155-171.

Koutsakos, M., Kedzierska, K. and Subbarao, K. 2019. Immune responses to avian influenza viruses. *The journal of immunology*, 202:382-391.

Kovesdi, I. and Hedley, S.J. 2010. Adenoviral producer cells. *Viruses*, 2:1681-1703.

Krauss, S., Walker, D., Pryor, S.P., Niles, L., Chenghong, L., Hinshaw, V.S. and Webster, R.G. 2004. Infuenza A viruses of migrating wild aquatic birds in North America. *Vector borne zoonotic diseases*, 4:177-189.

Krug, R.M. 1981. Priming of influenza viral RNA transcription by capped heterologous RNAs. *Current topics in microbiology and immunology*, 93:125-49.

Kubo, T., Agoh, M., Q-Mai, Le., Fukushima, K., Nishimura, H., Yamaguchi, A. and Morita, K. 2010. Development of a reverse transcription loop-mediated isothermal amplification assay for detection of pandemic (H1N1) 2009 virus as a novel molecular method for diagnosis of pandemic influenza in resource-limited settings. *Journal of clinical microbiology*, 48(3):728–735.

Kwok-Yung, Y. 2018. Another avian influenza A subtype jumping into human: this time is H7N4. *Science bulletin*, 63 (16):1025-1026.

Lai, D., Zhang, Y., Huang, Q., Yin, G., Pennerman, K.K., Liu, Z. and Guo, A. 2018. Reverse transcription loop-mediated isothermal amplification to rapidly detect rice *ragged* stunt virus. *Saudi journal of biological sciences*, 25:1577-1584.

Lamb, R.A. and Krug, R.M. 1996. Orthomyxoviridae: the viruses and their replication. In: B.N. Fieldds, D.M. Knipe, P.M. Howley, R.M Chanock, J.L Melnick, T.P Momath, B. Roizman (Eds.), Fields Virology, 3rd ed, Lippincott-Raven, Philadelphia, P.A.

Lamb, R.A. and Krug, R.M. (2001). Orthomyxoviridae: the viruses and their replication. In Knipe D.M, Howley P.M. editors. Fields Virology, vol 1. 4th Ed. Philadelphia: Lippincott Williams & Wilkins. P1487-531.

Landy, A. 1989. Dynamic, structural and regulatory aspects of lambda site-specific recombination. *Annual review of biochemistry*, 58: 913-949.

Lasswitz, L., Chandra, N., Arnberg, N. and Gerold, G. 2018. Glycomics and proteomics approaches to investigate early Adenovirus host cell interactions. *Journal of molecular biology*, 430:1863-1882.

Le Ru, A. and Jacob, D. 2010. Transfiguracion, S. Ansorge, O. Henry, and A.A. Kamen, Scalable production of influenza virus in HEK-293 cells for efficient vaccine manufacturing. *Vaccine*, 28(21):3661-3671.

Lee, C.W. and Suarez, D.L. 2004. Application of real-time RT-PCR for the quantification and competitive replication study of H5 and H7 subtype avian influenza virus. Journal of virological methods, 119:151-158.

Li, K.S., Guan, Y., Wang, J., Smith, J.D., Xu, K.M., Duan, L. and Peiris, J.S.M. 2004. Genesis of a highly pathogenic and potentially pandemic H5N1 influenza virus in eastern Asia. *Nature*, 430(6996):209-213.

Li, Y., Reddy, K., Reid, S.M., Cox, W.J., Brown, I.H., Britton, P. and Iqbal, M. 2011. Recombinant herpesvirus of turkeys as a vector-based vaccine against highly pathogenic H7N1 avian influenza and Merek's disease. *Vaccine*, 29:8257-8266.

Li, L., DeLiberto, T.J., Killian, M.L., Torchetti, M.K. and Wan, X. 2018. Evolutionary pathway for the 2017 emergence of a novel highly pathogenic avian influenza A (H7N9) virus among domestic poultry in Tennessee, United states. *Virology*, 525:32-39.

Lin, Y.P., Shaw, M., Gregory, V., Cameron, K., Lim, W., Klimov, A. and Hay, A. 2000. Avian-to-human transmission of H9N2 subtype influenza A viruses: relationship between H9N2 and H5N1 human isolates. *Proceedings of the national academy of Sciences of the United States of America*, 97:9654-9658.

Lion, T. (2014). Adenovirus infections in immunocompetent and immunocompromised patients. *Clinical microbiology reviews*, 27(3):441-462.

Liu, J., Yao, L., Zhai, F., Chen, Y., Lei, J., Bi, Z. and Zhou, J. 2018. Development and application of a triplex real-time PCR assay for the simultaneous detection of avian influenza virus subtype H5, H7 and H9. *Journal of virological methods*, 252: 49-56.

Liu, R., Han, H., Liu, F., Lv Z, Wu, K., Liu, Y. and Zhu, C. 2020. Positive rate of RT-PCR detection of SARS-CoV-2 infection in 4880 cases from one hospital in Wuhan, China, from Jan to Feb 2020. *Clinica chimica Acta*, 505:172-175.

Lone, N.A., Spackman, E. and Kapczynski, D. 2017. Immunologic evaluation of 10 different adjuvants for use in vaccines for chickens against highly pathogenic avian influenza virus. *Vaccine*, 35: 3401-3408.

Lu, B., Zhou, H., Ye, D., Kemble, G. and Jin, H. 2005. Improvement of influenza A/Fujian/411/02(H3N2) virus growth in embryonated chicken eggs by balancing the hemagglutinin and neuraminidase activities, using reverse genetics. *Journal of virology*, 79:6763-6771.

Lu, R., Wu, X., Wan, Z., Li, Y., Zuo, L., Qin, J. and Zhang, C. 2020. Development of a novel reverse transcription loop-mediated isothermal amplification method for rapid detection of SARS-CoV-2. *Virologica Sinica*, 35:344-347.

Lupiani, B. and Reddy, S.M. 2009. The history of avian influenza. *Comparative immunology, microbiology and infectious diseases*, 32:311-323.

Ma, W., Kahn, R.E. and Richt, J.A. 2009. The pig as a mixing vessel for influenza viruses: Human and veterinary implications. *Journal of molecular and genetic medicine*, 3(1):158-166.

Ma, M., Yang, X., Xia, X., Anderson, B.D., Heil, G.L., Qian, Y. and Gray, G.C. 2014. Comparison of commercial influenza A virus assays in detecting avian influenza H7N9 among poultry cloacal swabs, China. *Journal of clinical virology*, 59:242-245.

Ma, S. and Guan, J. 2018. Adenovirus-mediated gene therapy for allergy. *Iranian journal of allergy, asthma, and immunology*, 17(6):502-516.

Maan, S., Maan, N.S., Batra, K., Kumar, A., Gupta, A., Rao, P.P. and Mertens, P.P.C. 2016. Reverse transcription loop-mediated isothermal amplification assays for rapid identification of eastern and western strains of bluetongue virus in India. *Journal of virological methods*, 234:65-74.

Martin, K. and Helenius, A. 1991. Transport of incoming influenza virus nucleocapsids into the nucleus. *Journal of virology*, 65(1):232-244.

Matrosovich, M.N., Matrosovich, T.Y., Gray, T., Roberts, N.A. and Klenk, H.D. 2004. Human and avian influenza viruses target different cell types in cultures of human airway epithelium. *Proceedings of the national academy of sciences of the United States of America*, 101(13):4620-4624.

Milián, E. and Kamen, A.A. 2015. Current and emerging cell culture manufacturing technologies for influenza vaccines. *BioMed research international*, Article ID: 504831.

Miller, P.J. and Torchetti, M.K. 2014. New castle disease virus detection and differentiation from avian influenza. Animal influenza virus. *Methods in molecular biology*, 1161:235-239.

Mohan Raj, A.D. and Gregory, N.G. 1990. Investigation into the bath stunning/killing of chickens using carbon dioxide or argon-induced hypoxia. *Research in veterinary science*, 49:364-366.

Mori, Y.K., Nagamine, N., Tomita, N. and Notomi, T. 2001. Detection of loop-mediated isothermal amplification reaction by turbidity derived from magnesium pyrophosphate formation. *Biochemical and biophysical research communications*, 289:150-154.

Moser, M. and Leo, O. 2010. Key concepts in immunology. *Vaccine*, 28(3):C2-13.

Nagamine, K., Watanabe, K., Ohtsuka, K., Hase, H. and Notomi, T. 2001. Loop-mediated isothermal amplification reaction using a nondenatured template. *Clinical chemistry*, 47:1742-1743.

Nagamine, K., Hase, T. and Notomi, T. 2002. Accelerated reaction by loop-mediated isothermal amplification using loop primers. *Molecular and cellular probes*, 16: 223-229.

NCBI 3 and Blast. U.S National library of medicine. National centre for biotechnology information. https://www.ncbi.nlm.nlh.gov/tools/primer-blast. Accessed 15 October 2014.

Neumann, G., Noda, T. and Kawaoka, Y. 2009. Emergence and pandemic potential of swine-origin H1N1 influenza virus. *Nature*, 459(7249):931-939.

Ng, E.K., Cheng, P.K., Ng, A.Y., Hoang, T.L. and Lim, W.W. 2005. Influenza A H5N1 detection. *Emerging infectious diseases journal*, 11:1303-1305.

Nishiyama, K., Takeda, Y., Maeki, M., Ishida, A., Tani, H., Shigemura, K. and Tokeshi, M. 2020. Sensors and actuators: B. *Chemical*, 316:128160.

Notomi, T., Okayama, H., Masubuchi, H., Yonekawa, T., Watanabe, K., Amino, N. and Hase, T. 2000. Loop-mediated isothermal amplification of DNA. *Nucleic acids research*, 28(12):e63.

OIE (The world organization for animal health).2003. http://www.oie.int/about-us/. Accessed 09 December 2017.

OIE (The world organization for animal health).2009. Avian influenza. Chapter 2.3.4. OIE (The world organization for animal health) terrestrial manual.

OIE (The world organization for animal health). 2017a. Avian influenza: General disease information sheet. http://www.oie.int/doc/ged/D13947.PDF. Accessed 21 December 2017.

OIE (The world organization for animal health). 2017b. Terrestrial Animal Health Code.http://www.oie.int/index.php?id=169&L=0&htmfile=glossaire.htm#terme_code_terrestre. Accessed 21 December 2017.

OIE (The world organization for animal health) .2017c. OIE-Listed diseases, infections, and infestations in force in 2017. http://www.oie.int/animal-health-in-the-world/oie-listed-diseases-2017/. Accessed 09 December 2017.

Okamatsu, M., Hiono, T., Kida, H. and Sakoda, Y. 2016. Recent developments in the diagnosis of avian influenza. *The veterinary journal*, 215:82-86.

Olivier, A.J. 2006. Ecology and epidemiology of avian influenza in ostriches. In: Schudel, A., Lombard, M. (Eds.), Proceedings of the OIE/FAO international scientific conference on avian influenza. *Developmental biology (Basel)*, 124:51–57.

Palese, P., Tobita, K., Ueda, M. and Compans, R.W. 1974. Characterization of temperature sensitive influenza virus mutants defective in neuraminidase. *Virology*, 61(2):397-410.

Palese, P. and Shaw, M.L. 2007. Orthomyxoviridae: The viruses and their replication. In: Fields BN, Knipe D.M, Howley P.M, editors. FieldsVirology.5th ed.Philadelphia, USA: Wolters Kluwer Health/Lippincott Williams and Wilkins: pp 1647-1689.

Parida, MM., Santosh, S.R., Dash, P.K., Tripathi, N.K., Saxena, P., Ambuj S. and Morita, K. 2006. Development and evaluation of reverse transcription-loop-mediated isothermal amplification assay for rapid and real-time detection of Japanese encephalitis virus. *Journal of clinical microbiology*, 44:4172-4178.

Park, K. S., Lee, J., Ahn, S.S., Byun, Y.H., Seong, B. L., Baek, Y.H. and Lee, C. G. 2009. Mucosal immunity induced by Adenovirus-based H5N1 HPAI vaccine confers protection against a lethal H5N2 avian influenza virus challenge. *Virology*, 395:182-189.

Park, G.S., Ku, K., Baek, S.H., Kim, S.J., Kim, B.T., Kim, B.T. and Maeng, J.S. (2020). Development of reverse transcription-loop-mediated isothermal amplification assays targeting severe acute respiratory syndrome Coronavirus 2 (SARS-CoV-2). *Journal of molecular diagnostics*, 22:729-735.

Partridge, J. and Kieny, M.P. 2011. Global production capacity of seasonal influenza vaccine in 2011. *Vaccine*, 31(5):728-731.

Pau, M.G., Ophorst, C., Koldijk, M.H., Schouten, G., Mehtali, M. and Uytdehaag, F. 2001. The human cell line PER.C6 provides a new manufacturing system for the production of influenza vaccines. *Vaccine*, 19(17-19):2716-2721.

Pavade, G., Awada, L., Hamilton, K. and Swayne, D.E. 2011. The influence of economic indicators, Poultry density and the performance of veterinary services on the control of high-pathogenicity avian influenza in poultry. *Revenue scientifique et technique (international office of epizootics)*, 30(3):661-671.

Pavlova, S.P., Veits, J., Keil, G.M., Mettenleiter, T.C. and Fuchs, W. 2009. Protection of chickens against H5N1 highly pathogenic avian influenza virus infection by live vaccination with infectious laryngotracheitis virus recombinants expressing H5 hemagglutinin and N1 neuraminidase. *Vaccine*, 27:773-785.

Payungporn, S., Chutinimitkul, S., Chaisingh, A., Damrongwantanapokin, S., Buranathai, C., Amonsin, A. and Poovorawan, Y. 2006. Single step multiplex real-time RT-PCR for H5N1 influenza A virus detection. *Journal of virological methods*, 131:143-147.

Peiris, J.S.M., de Jong, M.D. and Guan, Y. 2007. Avian influenza virus (H5N1): A threat to human health. *Clinical microbiology reviews*, 20(20):243-267.

Peng, Y., Xie, Z., Liu, J., Pang, Y., Deng, X., Xie, Z. and Khan, M. 2011. Visual detection of H3 subtype avian influenza viruses by reverse transcription loop-mediated isothermal amplification assay. *Virology journal*, 8(337):1-10.

Peng, C., Sun, H., Li, J., Hou, G., Wang, S., Liu, S. and Jiang, W. 2018. Molecular epidemiological survey and complete genomic phylogenetic analysis of H6 subtype avian influenza viruses in poultry in China from 2011-2016. *Infection, genetics and evolution*, 65:91-95.

Pham, H.M., Nakajima, C., Ohashi, K. and Onuma, M. 2005. Loop-mediated isothermal amplification for rapid detection of Newcastle disease virus. *Journal of clinical microbiology*, 43(4):1646-1650.

Pham, P.T.V., Turan, K., Nagata, K., Kanaga, K. and Kawaguchi, A. 2018. Biochemical characterization of avian influenza viral polymerase containing PA or PB2 subunit from human influenza A virus. *Microbes and infection*, 20(6):353-359.

Ping, S., Geng, S., Ting-ting, L., Yu-shui, L., Ting, F. and Hua-nan, W. (2015). Methods to detect avian influenza virus for food safety surveillance. *Journal of integrative agriculture*, 14(11):2296-2308.

Pitt, M., Shahidur, R.K., Omar, H.C. and Millimet, D. 2003. Credit programmes for the poor and the health status of children in rural Bangladesh. *International economics review*, 44(1):87-118.

Playford, E. G. and Dwyer, D. E. 2002. Laboratory diagnosis of influenza virus infection. *Pathology*, 34:115–125.

Poon, L.L.M., Leung, C.S.W., Chan, K.H., Lee, J.H.C., Yuen, K.Y., Guan, Y. and Peiris, J.S.M. 2005. Detection of human influenza A viruses by loop-mediated isothermal amplification. *Journal of clinical microbiology*, 3(1):427–430.

Portela, A., Zurcher, T., Nieto, A. and Ortin, J. 1999. Replication of orthomyxoviruses. *Advances in virus research*, 54: 319-48.

Porto, P.S., Anjos, D., Dábilla, N., da Fonseca, S.G. and Souza, M. 2020. Immunoinformatic construction of an Adenovirus-based modular vaccine platform and its application in the design of a SARS-CoV-2 vaccine. *Infection, genetics, and evolution*, 85:104489.

Ptashne, M.A. 1992. Genetic switch: Phage (Lambda) and higher organisms. Cambridge, M.A: Cell Press.

Ptashne, M.A. 2004. A genetic switch: phage lambda revisited. 3rd ed. Cold spring harbor laboratory press.

Pu, J., Wang, S., Yin, Y., Zhang, G., Carter, R.A., Wang, J. and Webster, R.G. 2015. Evolution of the H9N2 influenza genotype that facilitated the genesis of the novel H7N9 virus. *Proceedings of the National academy of sciences of the United states of America*, 112:548-553.

Pumford, E.A., Lu, J., Spaczai, I., Prasetyo, M.E., Zheng, M.E., Zhang, H. and Kamei, D.T. 2020. Developments in integrating nucleic acid isothermal amplification and detection systems for point-of-care diagnostics. *Biosensors and Bioelectronics*, 170:112674.

Qiao, C.L., Yu, K.Z., Jiang, Y.P., Jia, Y.Q., Tian, G.B., Liu, M. and Tang, X.Y. 2003. Protection of chickens against highly lethal H5N1 and H7N1 avian influenza viruses with a recombinant fowl pox virus co-expressing H5 haemagglutinin and N1 neuraminidase genes. *Avian pathology*, 32:25-31.

Qiao, C., Tian, G., Jiang, Y., Li, Y., Shi, J., Yu, K. and Chen, H. 2006. Vaccines developed for H5 highly pathogenic avian influenza in China. *Annals of the New York academy of sciences*, 1081:182-192.

Ramdas, K., Darzi, A. and Jain, S. 2020. 'Test, re-test, re-test': using inaccurate tests to greatly increase the accuracy of COVID-19 testing*. Nature medicine*, 26(6):810-811.

Rauff, D., Strydom, C. and Abonlik, C. 2016. Evolutionary consequences of a decade of vaccination against subtype H6N2 influenza. *Virology*, 498:226-239.

Rauw, F., Palya, V., Gardin, Y., Tatar-kis, T., Dorsey, K.M., Lambrecht, B. and van den Berg, T. 2012. Efficacy of rHVT-AI vector vaccine in broilers with passive immunity against challenge with two antigenically divergent Egyptian Clade 2.2.1 HPAI H5N1 strains. *Avian diseases*, 56:913-922.

Rebel, J.M.J., Peeters, B., Fijten, H., Post, J., Cornelissen, J. and Vervelde, L. 2011. Highly pathogenic or low pathogenic avian influenza virus subtype H7N1 infection in chicken lungs: small differences in general acute responses. *Veterinary research*, 42(10).

Reddy, V.S., Natchiar, S.K., Stewart, P.L. and Nemerow, G.R. 2010. Crystal structure of human Adenovirus at 3.5 A resolution. *Science*, 329:1071-1075.

Reddy, V.S. and Nemerow, G.R. 2014. Structures and organization of Adenovirus cement proteins provide insights into the role of capsid maturation in virus entry and infection. *Proceedings of the national academy of sciences of the United States of America*, 111:11715-11720.

Rimmelzwaan, G.F., Baars, M., Claas, E.C.J. and Osterhaus, A.D.M.E. 1998. Comparison of RNA hybridization, hemagglutination assay, titration of infectious virus and immunofluorescence as methods for monitoring influenza virus replication in vitro. *Journal of virological methods*, 74(1):57-66.

Robert-Guroff, M. 2007. Replicating and non-replicating viral vectors for vaccine development. *Current opinion in biotechnology*, 18:546-556.

Robertson, J.S. 1987. Sequence analysis of the haemagglutinin of A/Taiwan/1/86, a new variant of human influenza A (H1N1) virus. *Journal of general virology*, 68:1205-1208.

Robertson, J.S., Bootman, J.S., Newman, R., Oxford, J.S., Daniels, R.S., Webster, R.G. and Schild G.C. 1987. Structural changes in the haemagglutinin which accompany egg adaptation of an influenza A (H1N1) virus. *Virology*, 160(1):31-37.

Robertson, J.S., Cook, P., Attwell, A.M. and Williams, S.P. 1995. Replicative advantage in tissue culture of egg-adapted influenza virus over tissue-culture derived virus: implications for vaccine manufacture. *Vaccine*, 13(16):1583-1588.

Russell, W.C. 2000. Update on Adenovirus and its vectors. *Journal of general virology*, 81: 2573-2604.

Rux, J.J. and Burnett, R. 1999. Adenovirus capsid proteins. In Adenoviruses: Basic biology to gene therapy (P.Seth,Ed.), pp. 5-15. Landes Bioscience, Georgetown, TX.

Saha, B., Wong, C.M. and Parks, R.J. 2014. The Adenovirus genome contributes to the structural stability of the virion. *Viruses*, 6:3563-3583.

Samji, T. 2009. Influenza A: Understanding the viral life cycle. *Yale Journal of biology and medicine*, 82:153-159.

Sanjuán, R. and Domingo-Calap, P. 2016. Mechanisms of viral mutation. *Cellular and molecular life sciences*, 73(23):4433-4448.

Sarfati-Mizrahi, D., Lozano-Dubernard, B., Soto-Priante, E., Castro-Peralta, F., Flores-Castro, R., Loza-Rubio, E. and Gay-Gutierrez, M. 2010. Protective dose of a recombinant Newcastle disease Lasota-avian influenza virus H5 vaccine against H5N2 highly pathogenic avian influenza virus and velogenic viscerotropic Newcastle disease virus in broilers with high maternal antibody levels. *Avian diseases*, 54:239-241.

Schmitz, H., Wigand, R. and Heinrich, W. 1983. Worldwide epidemiology of human Adenovirus infections. *American journal of epidemiology*, 117:455-466.

Schrenzel, M., Oaks, J.L., Rotstein, D., Maalouf, G., Snook, E., Sandfort, C. and Rideot, B. 2005. Characterization of a new species of Adenovirus in falcons. *Journal of clinical microbiology*, 43:3402-3413.

Scott, A.B., Toribio, J.-A., Singh, M., Groves, P., Barnes, B., Glass, K. and Hernandez-Jover, M. (2018a). Low pathogenic avian influenza exposure risk assessment in Australian commercial chicken farms. *Frontiers in veterinary science*, 5(68).

Scott, A. B., Toribio, J.-A.L.M. L., Singh, M., Groves, P., Barnes, B., Glass, K. and Hernandez-Jover, M. (2018b). Low- and high-pathogenic avian influenza H5 and H7 spread risk assessment within and between Australian commercial chicken farms. *Frontiers in veterinary science*, 5 (63).

Scott, A., Hernandez-Jover, M., Groves, P. and Toribio, J. 2020. An overview of avian influenza in the context of the Australian commercial poultry industry. *One Health*, 10:100139.

Senne, D.A., Suarez, D.L., Stallknecht, D.E., Pedersen, J.C. and Panigrahy, B. 2006. Ecology and epidemiology of avian influenza in North and South America. In: Schudel, A., Lombard, M. (Eds.), Proceedings of the OIE/FAO International Scientific Conference on Avian Influenza. *Developments in Biologicals (Basel)*, 124:37–43.

Shabat, M.B., Meir, R., Haddes, R., Lapin, E., Shkoda, I., Raibstein, I. and Davidson, I. 2010. Development of a real-time Taqman RT-PCR assay for the detection of H9N2 avian influenza viruses. *Journal of virological methods*, 168:72-77.

Shapiro, G.I. and Krug, R.M. 1988. Influenza virus RNA replication *in vitro*: synthesis of viral template RNAs and virion RNAs in the absence of an added primer. *Journal of virology*, 62(7):2285-2290.

Sharma, V., Chaudhry, D. and Kaushik, S. 2018. Evaluation of clinical applicability of reverse transcription-loop-mediated isothermal amplification assay for detection and subtyping of influenza A viruses. *Journal of virological methods*, 253:18-25.

Shekaili, T.A.I., Clough, H., Ganapathy, K. and Baylis, M. 2015. Sero-surveilance and risk factors for avian influenza and Newcastle disease virus in backyard poultry in Oman. *Preventive veterinary medicine*, 122(1-2):145-153.

Shen, M., Zhou, Y., Ye, J., AL-maskri, A.A., Kang, Y., Zeng, S. and Cai, S. (2020). Recent advances and perspectives of nucleic acid detection for Coronavirus. *Journal of pharmaceutical Analysis*, 10:97-101.

Shenk, T. 1996. Adenoviridae: The viruses and their replication. In virology. B.N.Fields, D.M.Knipe, and P.M Howley, eds. (Lippin-cott-Raven, New York): 2111-2148.

Sheridan, C. 2020. Fast, portable tests come online to curb Coronavirus pandemic. *Nature Biotechnology*, 38(5): 515-518.

Shi, L., Yu, X., Yao, W., Yu, B., He, L., Gao, Y. and Wang, X. 2019. Development of a reverse-transcription-loop-mediated isothermal amplification assay to detect avian influenza viruses in clinical specimens. *Journal of integrative agriculture*, 18(7):1428-1435.

Sieczkarski, S. B. and Whittaker, G. R. 2005. Viral entry. *Current topics in microbiology and immunology*, 285:1-23.

Silva, A.C., Peixoto, C., Lucas, T., Küppers, C., Cruz, P.E., Alves, P.M. and Kochanek, S. 2010. Adenovirus vector production and purification. *Current gene therapy*, 10(6):437-457.

Silva, A.C., Teixeira, A.P. and Alves, P.M. 2016. Impact of Adenovirus infection in host cell metabolism evaluated by H-NMR spectroscopy. *Journal of biotechnology*, 231:16-23.

Singh, S., Toro, H., Tang, D-C., Briles, W.E., Yates, L.M., Kopulos, R.T. and Collisson, E.W. 2010. Non-replicating Adenovirus vectors expressing avian influenza virus hemagglutinin and nucleocapsid proteins induce chicken specific effector, memory and effector memory $CD8^+$ T lymphocytes. *Virology*, 405:62-69.

Skehel, J.J. and Wiley, D.C. 2000. Receptor binding and membrane fusion in virus entry: the influenza hemagglutinin. *Annual review of biochemistry*, 69:531-569.

Sobel, L.A., Weissman, D.B., Greenbaum, B., Ghedin, E. and Koelle, K. 2017. Transmission bottleneck size estimation from pathogen deep-sequencing data, with an application to human influenza A virus. *Journal of virology*, 91:e00171-17.

Song, H., Bae, Y., Park, S., Kwon, H., Lee, H. and Joh, S. 2018. Loop-mediated isothermal amplification assay for detection of four immunosuppressive viruses in chicken. *Journal of virological methods*, 256: 6-11.

Song, C.L., Liao, Z.H., Shen, Y., Wang, H., Lin, W.C., Li, H. and Xie, Q.M. 2020. Assessing the efficacy of a recombinant H9N2 avian influenza virus-inactivated vaccine. *Poultry science*, 99:4334-4342.

South African ostrich business chamber. 2011. Ostrich meat export suspension. http://www.ostrichsa.co.za/ostriches.php?action=get_article&id=124. Accessed 28 February 2013.

Spackman, E., Senne, D.A., Myers, T.J., Bulaga, L.L., Garber, L.P., Perdue, M.L. and Suarez, D.L. 2002. Development of a real-time reverse transcriptase PCR assay for type A influenza virus and the avian H5 and H7 hemagglutinin subtypes. *Journal of clinical microbiology*, 40(9):3256-3260.

Stegmann, T. 2000. Membrane fusion mechanisms: The influenza hemagglutinin paradigm and its implications for intracellular fusion. *Traffic*, 1(8):598-604.

Stingone, J.A. and Wing, S. 2011. Poultry litter incineration as a source of energy: Reviewing the potential for impacts on environmental health and Justice. *New solutions*, 21(1): 27-42.

Stöhr, K. 2013. “Influenza vaccine production” in Textbook of influenza, pp 352-370, John Wiley and Sons.

Suarez, D.L. 2012. DIVA vaccination strategies for avian influenza virus. *Avian diseases*, 56:836-844.

Suarez, D.L. and Partin-Jackwood, M.J. 2017. Recombinant viral-vectored vaccines for the control of avian influenza in poultry. *Veterinary microbiology*, 206:144-151.

Sutton, T.C. 2018. The pandemic threat of emerging H5 and H7 avian influenza viruses. *Viruses*, 10(461).

Swayne, D.E. and Suarez, D.L. 2000. Highly pathogenic avian influenza. *Revenue scientifique et technique (International office of epizootics)*, 19:463-482.

Swayne, D.E. 2001. Avian influenza vaccine use during 2001. In: Proceedings of the 10th annual meeting of the U.S Animal Health Association. USAHA, Richmond, Virginia, USA, 469-471.

Swayne, D.E. 2003. Vaccines for list A poultry diseases, emphasis on avian influenza. *Developments in biologicals (Base 1)*, 114:201-212.

Swayne, D.E. and Halvorson, D.A. 2003. Influenza. In: Saif Y.M, Barnes H.J, Glisson J.R *et al*, eds. Disease of poultry 11th Edition. Iowa state university press, Ames, IA, 135-160.

Swayne, D.E. 2004. Application of new vaccine technologies for the control of transboundary diseases. *Developmental biology*, 119:219-228.

Swayne, D.E. and Kapczynski, D. 2008. Strategies and challenges for eliciting immunity against avian influenza virus in birds. *Immunological reviews*, 225: 314-331.

Swayne, D.E., Pavade, G., Hamilton, K., Vallat, B. and Miyagishima, K. 2011. Assessment of national strategies for control of high-pathogenicity avian influenza and low pathogenicity notifiable avian influenza and in poultry, with emphasis on vaccines and vaccination. *Revue scientifique et technique (Office international des epizooties)*, 30:839-870.

Tahir, M.F., Abbas, M.A., Ghafoor, T., Dil, S., Shahid, M.A., Bullo, M.M.H. and Naseem, M.T. 2020. Seroprevalence and risk factors of avian influenza H9 virus among poultry professionals in Rawalpindi, Pakistan. *Journal of infection and public health*, 13: 414-417.

Takizawa, T., Matsukawa, S., Higuchi, Y., Nakamura, S., Nakanishi, Y. and Fuhuda, R. 1993. Induction of programmed cell death (apoptosis) by influenza virus infection in tissue culture cells. *Journal of general virology*, 74:2347-2355.

Tatsis, N. and Ertl, H.C.J. 2004. Adenoviruses as vaccine vectors. *Molecular therapy*, 10(4):616-629.

Terasako, K., Oshima, K., Wada, H., Ishihara, Y., Kawamura, K. and Sakamoto, K. 2012. Fulminant hepatic failure caused by Adenovirus infection mimicking peliosis hepatitis on abdominal computed tomography images after allogeneic hematopoietic stem cell transplantation. *International medicine*, 51:405-411.

The Poultry Site. 2007. Depopulation methods for a commercial layer flock: Part 1 and 2. http://www.thepoultrysite.com/articles/843/depopulation-methods-for-a-commercial-layer-flock-part-1-and-2/. Accessed 21 December 2017.

The Poultry Site. 2017. Avian flu guide. http://www.thepoultrysite.com/bird-flu/bird-flu-news.php?country=za. Accessed 12 December 2018.

To, K.K-W., Tsang, O.T-Y., Yip, C.C-Y., Chan, K-H., Wu, T.C., Chan, J.M-C. and Yuen, K-Y. 2020. Consistent detection of 2019 novel Coronavirus in saliva. *Clinical infectious diseases*, 71(15):841-843.

Tomita, N., Mori, Y., Kanda, H. and Notomi, T. 2008. Loop-mediated isothermal amplification (LAMP) of gene sequences and simple visual detection of products. *Nature Protocols*, 3(5):877-882.

Tomlinson, J.A., Dickinson, M.J. and Boonham, N. 2010. Detection of *Botrytis cinerea* by loop-mediated isothermal amplification. *Letters in applied microbiology*, 51:650-657.

Toro, H. and Tang, D.C. 2009. Protection of chickens against avian influenza with nonreplicating Adenovirus-vectored vaccine. *Poultry science*, 88:867-871.

Ura, T., Okuda, K. and Shimada, M. 2014. Developments in viral vector-based vaccines. *Vaccines*, 2:624-641.

Vemula, S.V. and Mittal, S.K. 2010. Production of Adenovirus vectors and their use as a delivery system for influenza vaccines. *Expert opinion on biological therapy*, 10:1469-1487.

Vemula, S.V., Zhao, J., Liu, J., Wang, X., Biswas, S., Hewlett, I. 2016. Current approaches for diagnosis of influenza virus infections in humans. *Viruses*, 8 (96).

Virginia Cooperate Extension. 2009. Publications and Educational resources. Composting Dead Poultry. http://pubs.ext.vt.edu/442/442-037/442-037.html. Accessed 21 December 2017.

Voeten, J.T.M., Brands, R., Palache, A.M., van Scharrenburg, G.J., Rimmelzwaan, G.F., Osterhaus, A.D. and Claas, E.C. 1999. Characterization of high-growth reassortant influenza A viruses generated in MDCK cells cultured in serum-free medium. *Vaccine*, 17(15-16):1942-1950.

Vogels, R., Zuijdgeest, D., Van Rijnsoever, R., Hartkoom, E., Damen, I., de Bethune, M.P. and Havenga, M. 2003. Replication-deficient human Adenovirus type 35 vectors for gene transfer and vaccination: efficient human cell infection and bypass of pre-existing Adenovirus immunity. *Journal of virology*, 77:8263-8271.

Walhout, A.J., Temple, G.F., Brasch, M.A., Hartley, J.L. and Lorson, M.A. 2000. GATEWAY recombinational cloning: Application to the cloning of large numbers of open reading frames or ORFeomes. *Methods in enzymology*, 328:575-592.

Walker, D., Gregory, W.F., Turnbull, D., Rocchi, M., Meredith, A.L., Philbey, A.W. and Sharp, C.P. 2017. Novel Adenoviruses detected in British mustelids, including a unique AviAdenovirus in the tissues of pine martens (Martes martes). *Journal of medical microbiology*, 66:1177-1182.

Wang, I.I. and Huang, I.I. 2000. Adenovirus technology for gene manipulation and functional studies. *Drug discovery*, 5:10-16.

Webster, R.G., Bean, W.J., Gorman, O.T., Chambers, T.M. and Kawaoka, Y. 1992. Evolution and ecology of influenza A viruses. *Microbiological reviews*, 56:152-179.

Webster, R.G. and Govorkova, E.A. 2014. Continuing challenges in influenza. *Annals of the New York academy of sciences*, 1323(1):115-139.

Weldemariam, T. 2016. A review on zoonosis and avian influenza (Bird flu): A literature review. *The journal of zoology studies*, 3(2):07-23.

Wellehan, J.F., Johnson, A.J., Harrach, B., Benko, M., Pessier, P., Johnson, C.M. and Jacobson, E.R. 2004. Detection and analysis of six lizard Adenoviruses by consensus primer PCR provides further evidence of a reptilian origin for the Adenoviruses. *Journal of virology*, 78(23):13366-13369.

Widjaja, L., Krauss, SL., Webby, RJ., Xie, T. and Webster, RG. 2004. Matrix gene of influenza A viruses isolated from wild aquatic birds: ecology and emergence of influenza A viruses. *Journal of virology*, 78:8771-9.

Wilson-Welder, J.H., Torres, M.P., Kipper, M.J., Mallapragada, S.K., Wannemuehler, M.J. and Narasimhan, B. 2009. Vaccine adjuvants: current challenges and future approaches. *Journal of pharmaceutical sciences*, 98:1278-1316.

Wivel, N.A. 1999. Adenovirus vectors. In: The development of human gene therapy, T. Friedmann, ed. (Cold Spring Harbor, NY: Cold Spring Harbor Laboratory Press), pp 87-110.

Wong, S.S. and Webby, R.J. 2013. Traditional and new influenza vaccines. *Clinical microbiology reviews*, 26(3):476-492.

Woolcock, P.R. and Cardona, C.J. 2005. Commercial immunoassay kits for the detection of influenza virus Type A: Evaluation of their use with poultry. *Avian Disease*, 49(4):477-481.

Xie, J., Liu, G., Tian, Z. and Luo, J. 2013. Development of loop-mediated isothermal amplification (LAMP) for detection of *Theileria equi*. *Acta tropica*, 127:245-250.

Xu, JT., Zhang, ZM., Yin, YB., Cui, SJ., Xu, SZ., Guo, YY. and Han, LM. 2009. Development of reverse-transcription loop-mediated isothermal amplification for the detection of infectious bursal disease virus. *Journal of virological methods*, 162:267–271.

Xue-Cheng, T., Shan-Shan, W., Feng, X., Xing, W., Tian-Min, X. and Wen-Hong, Z. 2018. First human infection by a novel avian influenza A (H7N4) virus. *Journal of infection*, 77(3):249-257.

Yan, C., Cui, J., Huang, L., Du, B., Chen, L., Xue, G. and Yuan, J. 2020. Rapid and visual detection of 2019 novel Coronavirus (SARS-CoV-2) by a reverse transcription loop-mediated isothermal amplification assay. *Clinical Microbiology and infection*, 26(6):773-779.

Youil, R., Su, Q., Toner, T.J., Szymkowiak, C., Kwan, W.S., Rubin, B. and Distefano, D. 2004. Comparative study of influenza virus replication in Vero and MDCK cell lines. *Journal of virological methods*, 120(1):23-31.

Yu, Y., Zhang, X., Zhao, B., Sun, Y., Zhang, X., Bai, T. and Qin, K. 2017. A sandwich ELISA for the detection of neuraminidase of avian influenza A (H7N9) virus. *Journal of virological methods*, 247:58-60.

Yu, L., Wu, S., Hao, X., Dong, X., Mao, L., Pelechano, V. and Yin, X. 2020. Rapid colorimetric detection of Covid-19 Coronavirus using a reverse transcriptional loop-mediated isothermal amplification (RT-LAMP) diagnostic platform. *Clinical Chemistry*, 66(7):975-977.

Zeng, F., Cong, F., Liu, X., Lian, Y., Wu, M., Xiao, L. and Luo, M. 2018. Development of a real time loop-mediated isothermal amplification method for detection of Senecavirus. *Journal of virological methods*, 261:98-103.

Zepp, F. 2010. Principles of vaccine design-Lessons from nature. *Vaccine*, 28(3):C14-24.

Zhang, Q., Shi, J., Deng, G., Guo, J., Zeng, X., He, X. and Liu, J. 2013. H7N9 influenza viruses are transmissible in ferrets by respiratory droplet. *Science*, 341:410-414.

Zhang, W. and Ehrhardt, A. 2017. Getting genetic access to natural Adenovirus genomes to explore vector diversity. *Virus genes*, 53:675-683.

Zhang, R., Yao, D., Chen, J., Ye, W., Ou, X., Chen, T. and Sun, B. (2018). Development and evaluation of a real-time RT-PCR assay for detection of a novel avian influenza A (H5N6) virus. *Journal of virological methods*, 257:79-84.

Zhang, Y., Odiwuor, N., Xiong, J., Sun, L., Nyaruaba, R.O., Wei, H. and Tanner, N.A. 2020. Rapid molecular detection of SARS-CoV-2 (COVID-19) virus RNA using colorimetric LAMP. *medRxiv*, doi: https://doi.org/10.1101/2020.02.26.20028373.

Zhigao, B. 2007. Field trials with chimera vaccines. OIE/FAO conference on vaccination: a tool for the control of avian influenza. Presented 22 March 2007, Verona, Italy.

Zhu, W., Dong, J., Zhang, Y., Liu, J., Shu, Y. and Wang, D. 2018. A gene constellation in avian influenza A (H7N9) viruses may have facilitated the fifth wave outbreak in china. *Cell reports*, 23:909-917.

Zhu, X., Wang, X., Han, L., Chen, T., Wang, L., Li, H. and Wang, Y. 2020. Reverse-transcription loop-mediated isothermal amplification combined with nanoparticles-based biosensor for diagnosis of COVID-19. *Biosensors and Bioelectronics*, doi: 10.1016/j.bios.2020.112437.